Portfolio of Evidence

Group 8: Development of WUSAT-4 CubeSat Mission Phase 3

Names and IDs

Natasha Galpayage Dona (2003126), Nilavan Thipaharan (2030293), Avani Sawe (2064758), Alia Meek (2106850), Josh Shilling (2107742), Aman Batra (2119325), Iniyavan Guhan Kavitha (2110413), Devansh Barman (2149830)

Supervisor: Dr. William Crofts

School of Engineering

University of Warwick

Abstract

The WUSAT-4 project represents a multidisciplinary engineering initiative to develop a 3U CubeSat platform capable of supporting biological experimentation in space. This portfolio documents the progression of the satellite design from preliminary definition (Phase B) toward detailed development (Phase C) according to European Cooperation for Space Standardization (ECSS) methodology. Building upon previous conceptual work, our team implemented a concurrent engineering framework to advance multiple subsystems simultaneously while maintaining system-level integration. The primary objective focused on creating a robust platform to house, operate, and retrieve data from the Fluorescent Deep Space Petri Pod (FDSPP) biological payload, which contains nematode worms for studying physiological effects of microgravity. Comprehensive structural analysis yielded a chassis design exceeding frequency requirements while maintaining strict mass budgets. Thermal simulations validated operational temperature ranges across all mission phases, with proposed passive thermal control strategies to mitigate temperature extremes. Power system analysis confirmed sufficient generation capacity across various orbital scenarios, and the communication system was designed to ensure reliable data transmission. Industry collaborations with the European Space Agency, Airbus, and Space Park Leicester provided critical guidance throughout development. The project successfully established a preliminary design substantiated by rigorous simulation and analysis, with component selection and physical prototyping initiated. This work establishes a technical foundation for subsequent iterations to complete detailed design specifications, conduct physical testing, and progress toward flight readiness.

Keywords: CubeSat, Concurrent Engineering, WUSAT, ESA

Acknowledgements

We thank Dr. William E. Crofts for his invaluable guidance, Julia Hunter-Anderson for her technical expertise, ESA and Airbus for sponsorship and knowledge, ESATAN for software support, our other sponsors for their contributions, and former WUSAT students for sharing their insights.

Abbreviations

Assembly, Integration and Verification	AIV
Attitude Determination Control System	ADCS
Beginning of Life	BOL
Centre of Mass	COM
Commercial off-the-shelf	COTS
Concept of Operations	CONOPS
Consultative Committee for Space Data Systems	CCSDS
CubeSat Design Specification	CDS
Discrete Cosine Transform	DCT
Electrical Power System	EPS
End of Life	EOL
European Cooperation for Space Standardization	ECSS
European Space Agency	ESA
Failure Modes and Effects Analysis	FMEA
Fault detection, isolation, and recovery	FDIR
Field Of View	FOV
Finite Element Method	FEM
Finite State Machine	FSM
Fluorescent Deep Space Petri-Pod	FDSPP
Fluorinated Ethylene Propylene	FEP
Fly Your Satellite	FYS
Gaussian-Frequency-Shift-Keying	GFSK
Gaussian-Minimum-Shift-Keying	GMSK
Integrated Development Environment	IDE
International Standards Organization	ISO
Internet Protocol	IP
Inter-Integrated Circuit	I2C
Joint Photographic Experts Group	JPEG
Low Earth Orbit	LEO
Maximum Power Point	MPP
Maximum Power Point Tracking	MPPT
Microcontroller Unit	MCU
Multi-Layered Insulation	MLI
On-Board Data Handling	OBDH
On-Off Keying	OOK
Open Systems Interconnection	OSI
Operational Control Field	OCF
Perturb and Observe	P&O
Photo Voltaic	PV
Portable Network Graphics	PNG

Power Conditioning and Distribution Unit	PCDU
Preliminary Design Review	PDR
Printed Circuit Board	PCB
Qualification Model	QM
Radio Frequency	RF
Random Access Memory	RAM
Real-Time Clock	RTC
Reliable User Datagram Protocol	RUDP
Remote Control Unit	RTU
Round-trip Time	RTT
School of Engineering	SoE
State of Charge	SoC
Single Point of Failure	SPOF
Space Avionics Open Interface Architecture	SAVIOR
Space Park Leicester	SPL
Structures	STR
Technology Readiness Level	TRL
Telemetry	TM
Total Ionisation Dose	TID
Transmission Control Protocol	TCP
Two-Line-Element	TLE
Ultra- High Frequency	UHF
University of Exeter	UoE
User Datagram Protocol	UDP
Very High Frequency	VHF
Warwick University Satellite Application Protocol	WUSAPP
Warwick University Satellite Team	WUSAT
WUSAT-4	W4
Half Unit (50 x 100 x 100mm)	0.5U
One Unit (100 x 100 x 100mm)	1U
Three Unit (300 x 100 x 100mm)	3U

Contents

List of Figures

List of Tables

1 Introduction

The WUSAT-4 project represents a significant leap in the University of Warwick School of Engineering's commitment to advancing space technology through CubeSat development. This initiative aims to demonstrate the capabilities of a 3U CubeSat platform in supporting research in Low Earth Orbit (LEO), specifically focusing on the Fluorescent Deep Space Petri Pod (FDSPP) payload. This payload, developed in collaboration with the University of Exeter and Space Park Leicester, contains nematode worms (Caenorhabditis elegans) to study the physiological and molecular responses to microgravity and space radiation. Such research is pivotal for developing countermeasures for long-duration human spaceflight, providing insights into the effects of space environments on biological systems.

This portfolio documents the technical journey in transitioning the WUSAT-4 project from Phase B (Preliminary Definition) towards Phase C (Detailed Definition/Development) according to the European Cooperation for Space Standardization (ECSS) methodology. Our work builds upon the foundational efforts of previous cohorts, focusing on refining the satellite's design through rigorous simulation, analysis, and component selection. Employing a concurrent engineering framework, we have advanced multiple subsystems simultaneously, ensuring system-level integration and adaptability to continuous developmental changes.

2 Project Overview

WUSAT-4 aims to be a technical demonstration of a CubeSat's ability to deliver, maintain, and operate the Fluorescent Deep Space Petri Pod (FDSPP) biological payload in Low Earth Orbit.

The main outcome of the WUSAT-4 mission is that team members complete an in-depth experience of satellite design to meet a set of payload requirements, and if possible, we can achieve the technical objectives of operating FDSPP in LEO and implementing an appropriate communications system to capture and return data images from FDSPP to the ground. Future applications could include the use of technology and procedures developed by WUSAT-4 in future FDSPP 'full experiment' missions, as well as the possibility of future WUSAT missions providing an in-orbit test/demonstration for other payloads.

2.1 Project Aim and Scope

The WUSAT-4 project as a while covers the following aims for the project:

- Deliver a secure, space-standard CubeSat Vehicle capable of securing, protecting, and interfacing with the payload, verifying each of these
- Ensure the communications infrastructure is in place to extract, process, and transmit the required data to and from the satellite to the client requirements (currently 1 image within 6 orbital periods)
- Develop a suitable ground station to receive and transmit telemetry and telecommands
- Assist in securing a launch vehicle and window to deliver the CubeSat to Low Earth Orbit (Later on)

2.2 Subsystems

WUSAT teams typically comprise eight 4th Yr MEng students of mixed engineering discipline to meet the requirements of the mission at each stage. The teams also include other students who have expertise in e.g. Ground Station or specific requirements of the payload.

2.3 Payload Overview

The full engineering details and documentation of the FDSPP can be found in the Teams Portfolio under FDSPP documentation.

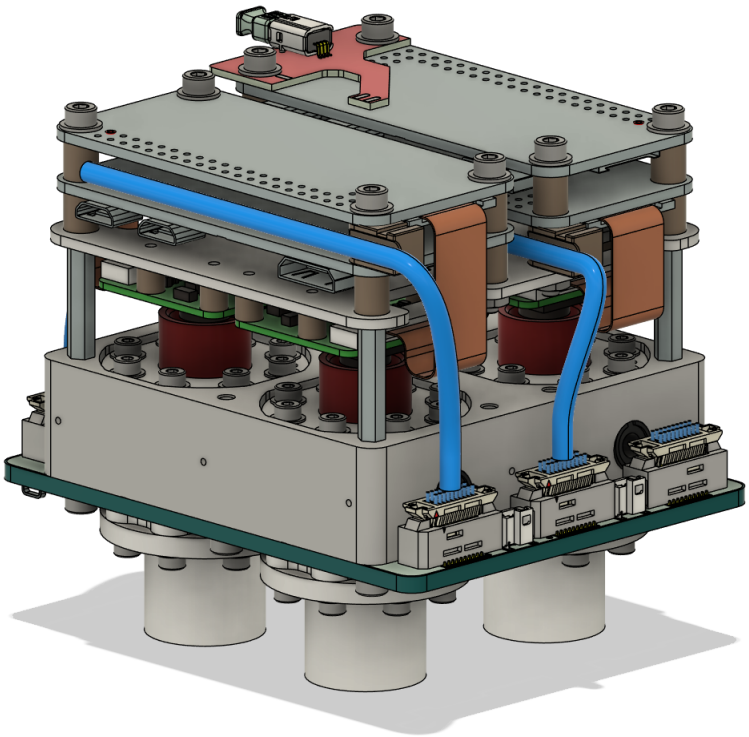

Figure 2.1: FDSPP Primary Pad Assembly

The FDSPP configuration built for WUSAT-4 is a reduced configuration of the full FDSPP, which is built to interface with the International Space Station and perform the experiment with the full capabilities of the platform. The configuration used for this project will be designed to contain and provide limited life support for the nematode worms by enclosing them in a volume of air, providing food and water from an Agar mixture, and maintaining the temperature of the immediate environment through on-board heaters. Observations of the experiment will be conducted through image and video captures with on-board cameras, LEDs, and by fluorescence induced with a 488nm LASER.

2.4 Link to Teams Portfolio

Click here to go to the Portfolio

3 Industry Collaboration

WUSAT-4 is an ambitious student project interacting with the space industry – which has extremely high standards of engineering, with stringent requirements and compliances that need to be met. Many of these are beyond the level practised through standard engineering courses. As such, an effort is typically in this project to educate the team about the industry through various courses and collaborations. The most significant of these are highlighted in this section.

3.1 European Space Agency (ESA)

In this year of the project, 2 ESA courses were attended, the Concurrent Engineering Workshop by 1 member, and the "Fly Your Satellite!" Design Booster 2 course by 5 members of the team, and 2 members of Warwick Aerospace Society, who were taking the lead in developing the ground station for the project.

3.1.1 Concurrent Engineering Workshop (CEW)

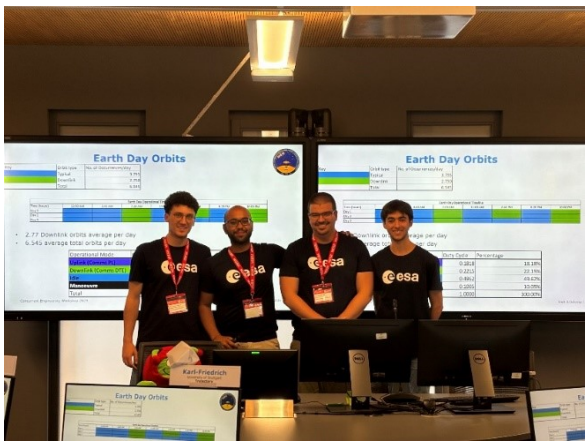

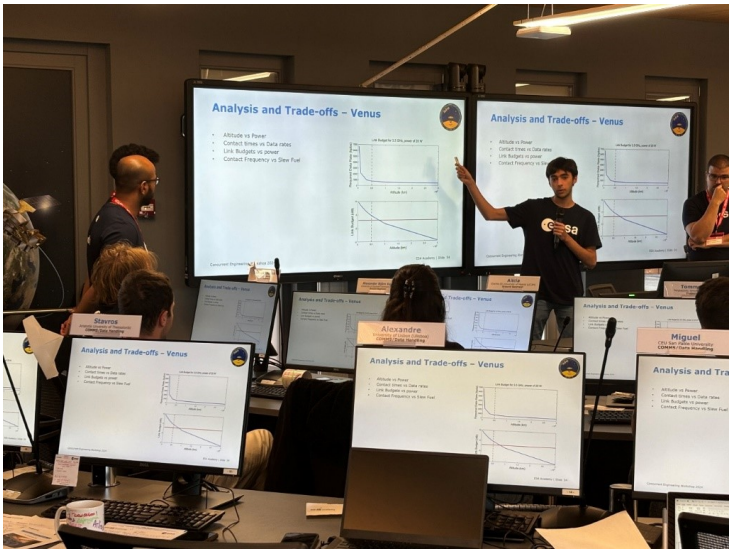

Figure 3.2: Concurrent Engineering Workshop (CEW)

This workshop saw the attendees complete Phase 0 of a proposed space mission over the course of a week at the ESEC Galaxia facility in Libin, Belgium. The exercise was focused on the preliminary definition of a mission to measure and transmit data from Venus to Earth. The key benefits from this were developing familiarity of the space industry, including terminology, regulations, standards, and individual connections with other students in the sector.

The largest takeaway was an understanding of the concept of "Concurrent Engineering", and practises to apply it. Concurrent Engineering is a specific management methodology which facilitates the rapidly changing nature of an early engineering project, beyond the typical requirements of regular communication and meetings.

This was done in this mission using the CDP4-COMET software, which was a spreadsheet interface tool which allowed tracking, uploading, and extracting of Microsoft Excel data through a GUI. Every component that was to be included in the mission would be added to the master spreadsheet, with the subsystem it belongs to. Individual sub-teams could then "subscribe" to components relevant to them, or "own" components which were selected by them.

For example, the Configuration sub-team (responsible for physical component placement in the orbiter) would "subscribe" to the space-side antenna, extracting its mass and dimensions, but the Communications sub-team would "own" the antenna, meaning they could change any or all of the parameters when needed.

The result was as composite database of all components in the system, as well as seamless interaction between the sub-teams in terms of updating changes – all relevant members would be notified of changes in real time and could express if any limitations or constraints were exceeded.

It must be noted that this is most effective in the earlier stages of an Engineering project, where refinement and trade-offs are regularly being made, and component selection is actively occurring. Applying concurrent engineering techniques to WUSAT-4 enabled a higher level of system analysis very early into the project, even allowing the team to verify the potential for an extra payload despite the premature stage of the project. Section 6 shows how this methodology was incorporated into the project.

3.1.2 Fly Your Satellite! Design Booster 2 (FYSDB2)

In October, the team applied and was selected for the ESA FYSDB2 scheme. Five of us, as well as our contacts within Warwick Aerospace, attended the event in Noordwijk in November.

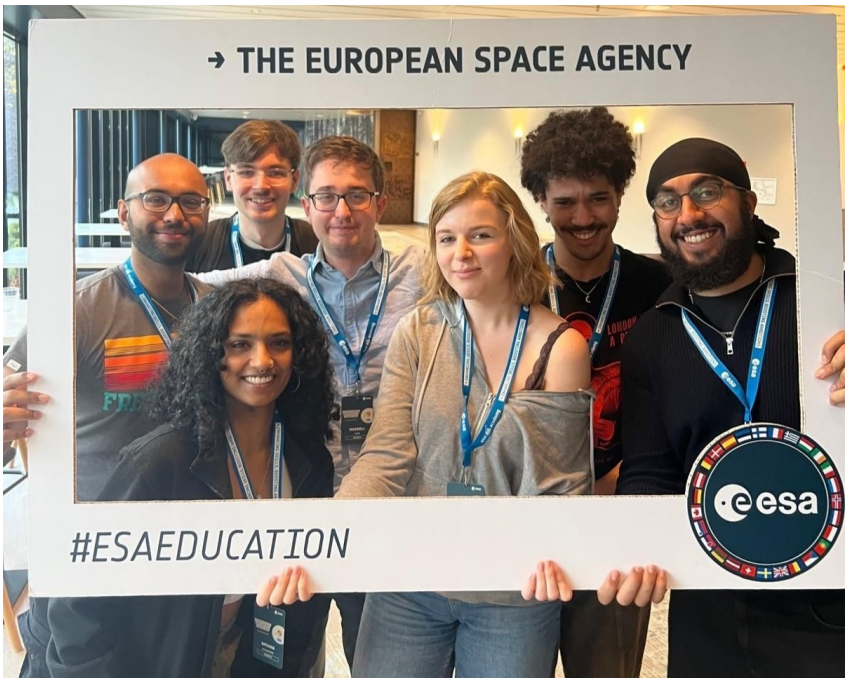

Figure 3.3: Team at Fly You Satellite! Design Booster in Noordwijk, Netherlands

The event was incredibly insightful, with sessions covering topics including how ESA mitigates space debris, the legal aspects of our mission, and the design and verification of each of our subsystems. The team realised early-on that the design of WUSAT-4 needed significant modification. For example, it was previously decided that any kind of Attitude and Orbit Control Systems (AOCS) would not be present within the CubeSat, owing to space concerns. After the AOCS lecture, the team realised that this would severely impact power generation and communications, as the satellite would be continuously spinning. As a result, research into passive AOCS using magnetorquers began – see 7.2.1 for the discussion on this.

After the event, the team has continued to draw on what was learnt over the week. For example, the spreadsheets shown in 2.1.4, which the team uses to determine mission feasibility, drew from those used by ESA in one of the interactive sessions. A document detailing the project's progress, and what was to be achieved this year was also produced as part of the application process – see the Teams Portfolio, under .

Though we were overall unsuccessful in gaining a spot on the full FYS scheme, the team remains immensely grateful to ESA for the opportunity, and the insight and feedback gained from the workshop and selection process.

3.2 Airbus Defence and Space

Throughout the course of this project, the group received valuable aid from Airbus. In addition to their sponsorship, Airbus attended many of our progress meetings and imparted their expert opinions, which greatly influenced and benefitted the design process of the

CubeSat. Additionally, the group was invited to attend their CubeSat day in Stevenage on the 5th of March 2025, where an overview of the design and mission was presented to other groups. The visit also consisted of talks from industry professionals regarding careers and technical developments, a site tour, and a networking session.

3.3 Space Park Leicester and University of Exeter

WUSAT-4 is a 3U CubeSat designed to carry a Fluorescent Deep Space Petri Pod (FDSPP) experiment as its payload. The experiment is the work of Prof. Tim Etheridge (University of Exeter) and the FDSPP module is designed and manufactured by Space Park Leicester (member of our Midlands Innovation Space Group). The payload itself is a self-sustaining 1U housing to hold a petri dish containing nematode worms (Caenorhabditis elegans). The health of the nematode worms will be monitored through images taken by an in-built camera, laser induced fluorescence, and video capture, which are then transmitted down to earth. The experimental subject matter, the non-parasitic, multicellular nematode worm, C. elegans, have 83 percent of human homologues genes, making a good representation of human physiology. Hence, the similar adverse physiological and molecular response of humans and C. elegans to microgravity and Space radiation is of key interest in the development of future countermeasures for long-duration human spaceflight. The contribution of WUSAT-4 to the development of a full specification FDSPP experimental flight would eventually include end-data users:

- ESA
- NASA
- Any other Space provider, researcher, developer interested in developing countermeasures against the adverse effects of long-term human spaceflight.

3.4 XCAM

XCAM has been a partner WUSAT for many years with flight heritage of their C3D imaging system used in WUSAT-3. WUSAT-4 aims to maintain this relationship by implementing a camera system payload into the mission to take promotional images during orbit.

3.5 24/25 New Sponsors

WUSAT received the backing of four new sponsors this academic year: Altium, Ansys, Dassault Systems, and Siemens. It was necessary to access the industrial software offered by these companies to ensure WUSAT's tests and simulations were of the highest standard. The benefits of the sponsors can be summarized as follows:

- **Altium** is a PCB design software that would allow the OBDH team to design, prototype, and optimize the on-board data and power systems.

- **Ansys** provides access to simulation software that is useful for mechanical, especially thermal, subsystems and material analyses.
- **Dassault Systems** has equipped WUSAT with their 3DEXPERIENCE platform that can be used as a unified tool for project mapping, allowing concurrent collaboration between all subsytems. This is extensively used in industry.
- **Siemens** endowed WUSAT with several software packages for the mechanical subteam, including capabilities like field element analysis, 3D modelling, and thermal design.

4 Previous Work Overview

4.1 Phase Definitions

WUSAT-4 follows the Space Systems Methodology Phases, used in industry by ESA. This can be defined as follows:

Phase	Summary	Description
0	Mission Definition	Defining targets, constraints, and capabilities of the mission
A	Feasibility Study	Calculations and basic simulations to verify if the mission is feasible
B	Preliminary Definition/Design Phase	Simulations and Analysis performed to begin modelling the mission and narrowing component requirements
C	Detailed Definition/Development	Component Selection from analysis. Development of testing models ready for verification.
D	Qualification and Production	Testing of models against verification plans. If it passes the Critical Design Review, production of final Flight Model after testing process.
E	Utilisation/Operation	Conducting the mission itself in space
F	Disposal	End-of-Life processes of the mission

Table 4.1: ESA Space System Methodology Phases

4.2 Progress From Last Year

An overview of the stages of each subsystem from last year can be seen below:

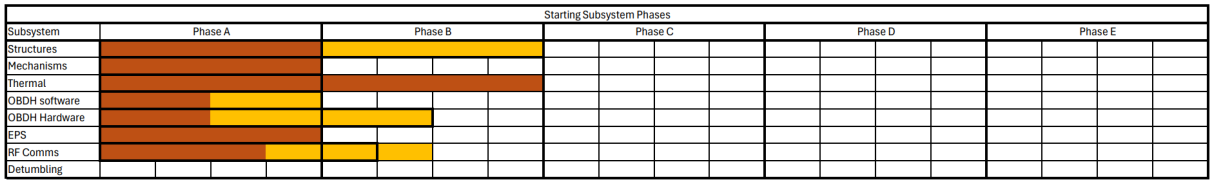

Figure 4.1: Progress made by each subsystem at the start of the 24/25 academic year. Orange represents ESA standard, yellow represents work which had to be refined.

The development stages are broken into two colours due to the requirements of the work produced. As mentioned in the narrative, after attending the FYSDB2 workshop, we

realised that there were strict standards that needed to be developed to for a mission that will fly to space. After reviewing the work from last year, it was clear that some would need to be redone to comply with space standards. These parts are highlighted in yellow in Figure 4.1. The work for each individual sub-systems is summarised in their relevant sections.

5 Mission Analysis

5.1 Concept of Operations

The Concept of Operations (ConOps) of a space mission defines the phases and modes that the system will go through. The "system" is defined as the satellite, and all the facilitating architecture that comprises of the space mission, such as:

- Ground Station
- Satellite
- Launch Vehicle

And any other technology used. A phase is defined as synchronous (time-defined) stage of the mission, which flow in chronological order. A mode is defined as an asynchronous state of the system, which can be stepped into and out of using software and commands as needed. The phases and modes for the mission, as defined at the time of this document, are below.

5.2 Mission Phases

1. **Pre-launch Phase**
   (a) Battery charging
   (b) Initialisation of control software and timers for, e.g., post-deployment sleep mode, etc.
2. **Launch Phase**
   (a) All subsystems powered off.
   (b) On-board computer (OBC) in sleep mode pending triggering of 30-minute and 45-minute post-deployment activities.
3. **De-tumbling Phase**
   (a) Passive magnetorquer coils embedded into PCBs are being considered to de-tumble the spacecraft after launch.
4. **Early-Orbit Phase**
   (a) 30-minute post-deployment – Antenna deployed
   (b) 45-minute post-deployment – OBDH, Communications, EPS, FDSPP subsystems turned on.
   (c) Heartbeat signal begins transmission (Risks associated with this will be mitigated by a command-loss timer in the OBDH that triggers a recovery routine if connection with a ground station is not established after a specified period).

(d) Internal temperature, battery level and solar panel temperature readings recorded and transmitted to the ground station.

5. **Operational Phase [up to 6 months]**

   (a) Science operations conducted according to the defined **modes**, facilitating FD-SPP experimentation.

6. **End of Life Phase**

   (a) Non-Critical systems shut down, allowing the satellite to de-orbit and burn up on atmospheric re-entry

5.2.1 Mission Modes

- **Nominal Mode**
  - This mode relies on a timer to initiate a signal. This will take a photo of the Petri Pod, and the photo will be processed using the OBDH and OBSW and stored to transmit. Housekeeping data will be collected as normal, and the FDSPP will be drawing maintenance power.
- **Transmit Mode**
  - The Transmit mode is defined as when the CubeSat is within the communication window of the ground station AND is actively transmitting. This will be initiated by the tracking ground station, which will send a start signal after confirming link closure using a handshake. Due to the power restrictions, transmit phase will not be entered during eclipse periods.
- **Eclipse Mode**
  - The Eclipse mode is defined as when the CubeSat is in solar eclipse. This will be initiated by the sensors on the OBDH after the incoming power from the solar panels falls to 0W (value to be revised based on power budgets and SOC) Only critical housekeeping data is generated, with most equipment in low power mode to not draw too much energy from the battery. The FDSPP will draw increased power to maintain environmental conditions, but this needs to be confirmed with the payload client.
- **Safe Mode**
  - If the EPS battery level depletes below a specific value (¡40%), the satellite will enter safe mode. No payload data will be processed or transmitted; only housekeeping data will be transmitted to the ground station to understand why safe mode has been entered. Power generation will be prioritised such that the battery level can be returned to normal operating levels (¿60%) and the system

will then return to normal operational mode. It is assumed that this will only happen once rather than continuously if the satellite remains in Safe Mode for multiple orbits.

- **Survival Mode**
  - In the event of an emergency, failure of mission critical components or operational limits being exceeded (TBD), the satellite will enter Survival Mode. In this mode only the EPS and the OBDH should be turned on to conserve power, and if necessary, the OBDH could be rebooted to try to resolve any software related issues. If recovery is possible, the satellite should return to normal operation via Safe Mode to ensure power generation is prioritised. If this is not possible, the satellite should terminate operations and enter End of Life mode.
- **End of Life Mode**
  - This mode is used to end operation of the CubeSat. All on-board systems will be shut down and the satellite will proceed to de-orbit naturally, burning up in the atmosphere.

The state diagram to visualise this can be represented below:

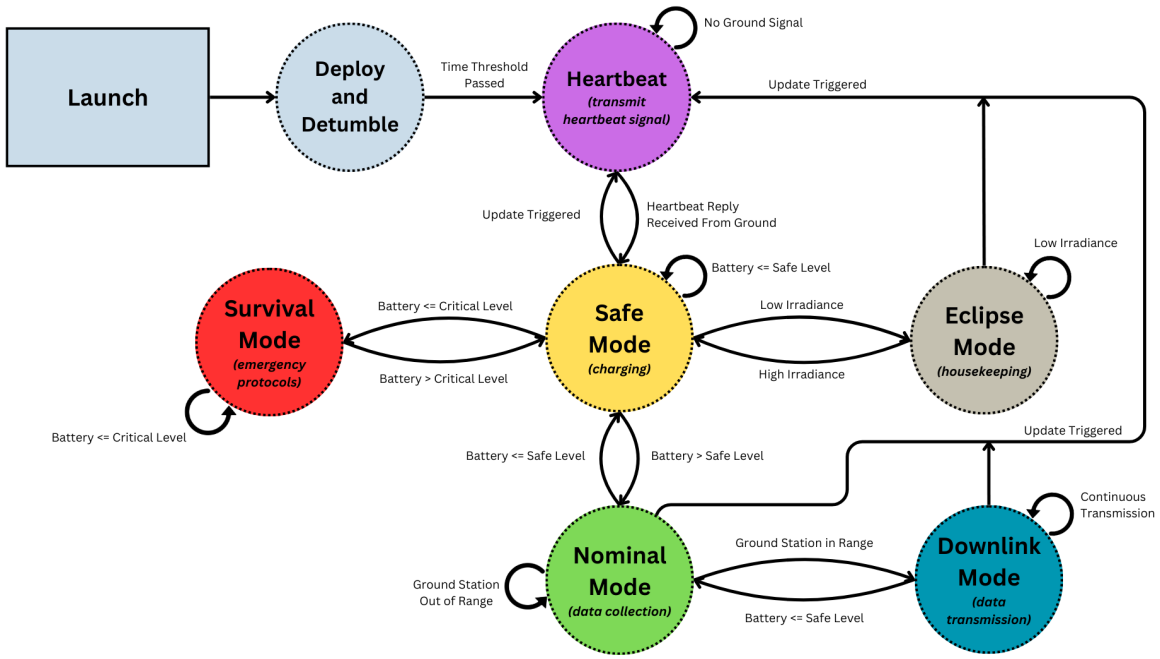

Figure 5.1: WUSAT-4 CONOPS

5.3 Closing Remarks and Open Points

This year, the Mission Analysis has been developed from scratch with what aims to be a cohesive model that can be updated and used in the next iterations of the project. The application of Concurrent Engineering practices aims to help the project run interactively,

ensuring the sub-teams work synchronously. Due to the stage of the project, and the redefinitions it went through as referenced in the Design Narrative document, certain aspects were not defined, and open points are left. Suggestions of points to work on are:

- Work with individual sub-systems to investigate legal requirements of the CubeSat project
  - Space projects have many legal obligations to fulfil, and due to the age of the project these have not been fully explored. Since testing is likely to begin over the next year, it is encouraged to investigate insurance, compliances, and any other legal issues that may arise.
- Check to see if collision probability is required
  - Low Earth Orbit is one of the most populated areas in space. Part of the legal requirements may need verification of collision probabilities, or at the very least, justification as to why this is not needed.
- Estimate times for each ConOps phase, using heritage flight data
  - The amount of time spent in each phase will also affect power and thermal budgets.

6 Concurrent Engineering

6.1 Overview

Using the skills gained from the ESA course in 3.1.1, a re-evaluation of the project was undertaken, with concurrent engineering practises applied. The main aims for this were:

- Provide a consistent, coherent document that encompasses all technical design parameters for the CubeSat
- Monitor and update the impact on the entire system when each component is changed
- Assist in the application and evaluation of design margins, and redundancies present in the system

CDP4-COMET is an ESA standard software; however, it is not cloud-enabled. This would limit the access to the documentation for team-members without laptops. It would also be difficult for future teams to continue using the software should they not have the opportunity to take the course. Instead, a composite Microsoft Excel sheet was developed, ensuring everyone had access, and reducing the learning curve for future teams.

6.2 Workflow

This spreadsheet compiles all of the components in the satellite and contains the relevant parameters to perform system-level analysis but omits sub-system specific information. For example, component operating temperature ranges would be included, but their thermal masses would not – these would be accessed using the datasheet link provided. The full interactive spreadsheet can be found in via the link in 2.4 under Engineering >System Budgets. The tool is intended to be used in the next iterations of the project, and as such an overview will be provided in this section.

Orange entry fields are intended to be inputs from the users of the spreadsheet. Purple entry fields will auto-calculate based on the provided information.

6.2.1 System Level Sheets

The first sheets comprise of the Mission Analysis data, and a composite list of all the components in the satellite. Figure 6.1 shows an early configuration of this, with data from section 2 filled in. The relevant factors for system analysis are calculated in the purple fields as mentioned.

Orbital Information	
Altitude (km)	408
Eccentricity	0.000021
Orbit Period (mins)	90
Eclipse time (mins)	30
Eclipse Frequency (Orbits)	1
Solar Incidence Ratio	0.666667
Contact Time (mins)	4
Contact Frequency (Orbits)	1

CONOPS	
Phase	Ratio per orbit (AVG)
Nominal	0.611222222
Downlink	0.044444444
Eclipse	0.333333333
Safe	0.01
Survival	0.001
Total	1

Figure 6.1: Mission Analysis data

Logically, safe and survival mode will not be a regular, defined length of time when entered. However, an estimate was made from the portion of the entire mission length (∼6 months) that would be spent in these modes, and arbitrary values chosen from this. Over a large number of simulation cycles, it would give a starting point to estimate power consumption – but further simulations would be needed with more accurate data in the future.

Component	Subsystem	Datasheet	TRL	Mass (kg)	Width (m)	Length (m)	Height (m)	Idle Power (W)	Nominal Power (W)	Max Power (W)	Min temperature (C)	Max temperature (C)
Endurosat UHF Antenna	TTC	https://ww	8	0.085	0.098	0..098	0.01225	0.005	1.25	3.5	-40	125
Endurosat 1U Transceiver	TTC	https://ww	8	0.095	0.089	0.095	0.023	0.005	1	1	-40	80
FDSPP module	OBDH	https://live	1	0.164	0.0968	0.0968	0.042	0.8	3.29	4.2	-40	85
ISIS iEPS A	EPS	https://ww	8	0.184	0.092	0.096	0.0113	0.09	0	0	-40	70
LM65645-Q1	EPS	https://ww	8	0.05	0.0036	0.0026	0.001	0.0000109			-40	125
On Board Computer	OBDH	https://ww	1	0.2	0.096	0.09	0.0124	0.1	0.4	1	-40	125
Arducam Camera	OBDH											
DHV 1U (Z-axis) Solar Panels	EPS	https://live	8		82.8	97.8	1.6				-50	125
DHV 3U (Type-1) Solar Panels	EPS	https://live	8		82.8	32.6	1.6				-50	125
			8									

Figure 6.2: Composite Component List

Figure 6.2 shows the main components list of the spreadsheet, with further columns omitted for readability (full details can be seen in the file itself). After the mission definition is selected, this sheet is updated to current standards, and is kept as a 'live' document, updating parameters as they change.

6.2.2 Sub-system sheets

From these main sheets, various sub-system sheets will extract and update relevant data at varying levels of complexity. An example of this is the mass budget:

Component	Subsystem	Datasheet	TRL	Mass (kg)	Width (m)	Length (m)	Height (m)	Idle Power (W)	Nominal Power (W)	Max Power (W)	Min temperature (C)	Max temperature (C)
Endurosat UHF Antenna	TTC	https://ww	8	0.085	0.098	0..098	0.01225	0.005	1.25	3.5	-40	125
Endurosat 1U Transceiver	TTC	https://ww	8	0.095	0.089	0.095	0.023	0.005	1	1	-40	80
FDSPP module	OBDH	https://liv	1	0.164	0.0968	0.0968	0.042	0.8	3.29	4.2	-40	85
ISIS iEPS A	EPS	https://ww	8	0.184	0.092	0.096	0.0113	0.09	0	0	-40	70
LM65645-Q1	EPS	https://ww	8	0.05	0.0036	0.0026	0.001	0.0000109			-40	125
On Board Computer	OBDH	https://ww	1	0.2	0.096	0.09	0.0124	0.1	0.4	1	-40	125
Arducam Camera	OBDH											
DHV 1U (2-axis) Solar Panels	EPS	https://live	8		82.8	97.8	1.6				-50	125
DHV 3U (Type-1) Solar Panels	EPS	https://live	8		82.8	32.6	1.6				-50	125
			8									

Characteristics						Margin policy		Total	
Component	Subsystem	TRL	Mass (kg)	Margin	Gross Mass (kg)	TRL	Margin	Mass (kg)	Gross Mass (kg)
						1	30%	0.778	0.9361
Endurosat UHF Antenna	TTC	8	0.085	0.1	0.0935	5	25%		
Endurosat 1U Transceiver	TTC	8	0.095	0.1	0.1045	6	20%		
FDSPP module	OBDH	1	0.164	0.3	0.2132	7	15%		
ISIS iEPS A	EPS	8	0.184	0.1	0.2024	8	10%		
LM65645-Q1	EPS	5	0.05	0.25	0.0625	9	5%		
On Board Computer	OBDH	1	0.2	0.3	0.26				

Figure 6.3: Mass Budget

The green box shows the component identifiers automatically extracted by the datasheet, and the red box shows the relevant parameters associated to the component. The right of the mass budget sheet contains the relevant margin to apply for each component, based on the TRL (Technology Readiness Level) as advised by ESA.

This same theory is applied to the configuration budget (which measures the volume and height of space remaining in the CubeSat) and thermal budget (which collates the operating temperatures of the components).

The Link Budget sheet contains parameters used to calculate attenuation and transmission losses, which can then be input to MATLAB to simulate this. The Data Budget spreadsheet is composed of the various sensors and their bit-depths, which are summed, and used to calculate a required data rate based on the information from the Mission Analysis sheet, and applied margins.

Housekeeping Data tracking				
Component	Amount	Frequency (No of senses per second	Bit depth (bits	Data generated per second
Voltage and current sensor: INA219	25	1879.699248	12	563909.7744
GPS: STMicroelectronics Teseo-LIV3F	12	10	512	61440
DS18B20 temperature sensor (for payload)	10	10.66666667	9	960
LM75 temperature sensor (for OBDH, Comms, EPS)	20	10	9	1800
				0
				0
				0
				0
				0
				0

Data Generation	
Data Source	Data generated per orbit (bits)
Housekeeping	471082.3308
Margin	20%
Total	565298.797
Contact time (mins)	4
Header Length (Bytes)	20
Packet Length (Bytes)	65536
Image Size (Bytes)	15728640
Compression Ratio	10
No. Packets Required	33
Data rate required (kbps)	8.8

Figure 6.4: Data Budget

The power budget sheet is the most involved and has been developed to calculate preliminary battery cycling simulations.

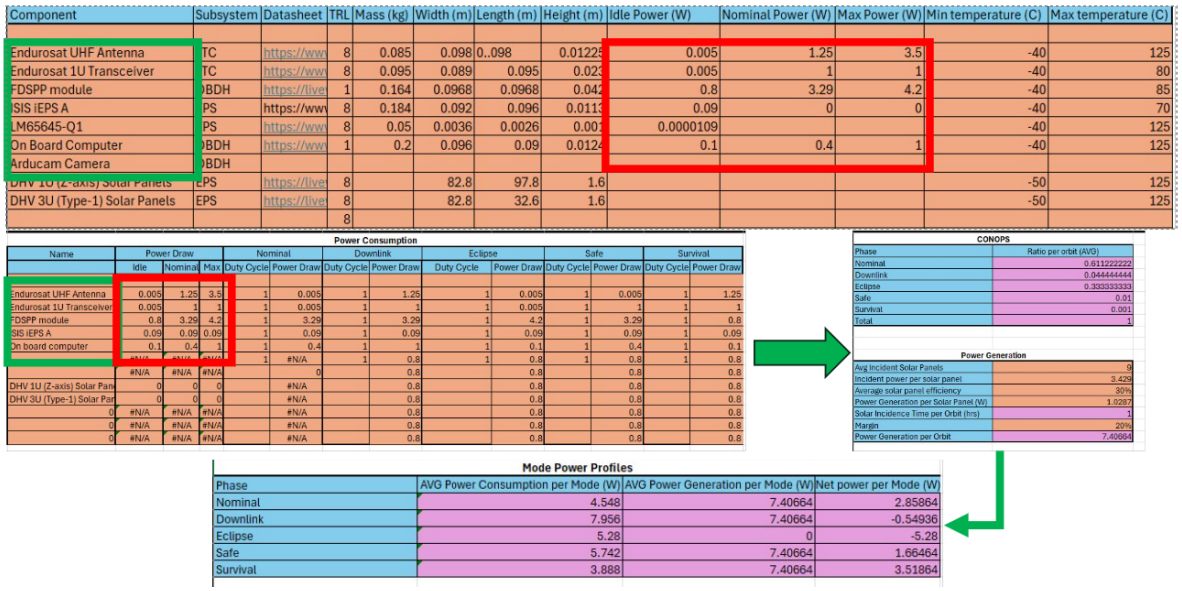

Component	Subsystem	Datasheet	TRL	Mass (kg)	Width (m)	Length (m)	Height (m)	Idle Power (W)	Nominal Power (W)	Max Power (W)	Min temperature (C)	Max temperature (C)
Endurosat UHF Antenna	TC	https://ww	8	0.085	0.098	0..098	0.0122	0.005	1.25	3.5	-40	125
Endurosat 1U Transceiver	TC	https://ww	8	0.095	0.089	0.095	0.023	0.005	1	1	-40	80
FDSPP module	BDH	https://live	1	0.164	0.0968	0.0968	0.042	0.8	3.29	4.2	-40	85
SIS iEPS A	PS	https://ww	8	0.184	0.092	0.096	0.011	0.09	0	0	-40	70
LM65645-Q1	PS	https://ww	8	0.05	0.0036	0.0026	0.001	0.0000109			-40	125
On Board Computer	BDH	https://ww	1	0.2	0.096	0.09	0.0124	0.1	0.4	1	-40	125
Arducam Camera	BDH											
DHV 1U (Z-axis) Solar Panels	EPS	https://live	8		82.8	97.8	1.6				-50	125
DHV 3U (Type-1) Solar Panels	EPS	https://live	8		82.8	32.6	1.6				-50	125
			8									

Power Consumption

Name	Power Draw			Nominal		Downlink		Eclipse		Safe		Survival	
	Idle	Nominal	Max	Duty Cycle	Power Draw	Duty Cycle	Power Draw	Duty Cycle	Power Draw	Duty Cycle	Power Draw	Duty Cycle	Power Draw
Endurosat UHF Antenna	0.005	1.25	3.5	1	0.005	1	1.25	1	0.005	1	0.005	1	1.25
Endurosat 1U Transceiver	0.005	1	1	1	0.005	1	1	1	0.005	1	1	1	1
FDSPP module	0.8	3.29	4.2	1	3.29	1	3.29	1	4.2	1	3.29	1	0.8
SIS iEPS A	0.09	0.09	0.09	1	0.09	1	0.09	1	0.09	1	0.09	1	0.09
On board computer	0.1	0.4	1	1	0.4	1	1	1	0.1	1	0.4	1	0.1
	#N/A	#N/A	#N/A	1	#N/A	1	0.8	1	0.8	1	0.8	1	0.8
	#N/A	#N/A	#N/A		0		0.8		0.8		0.8		0.8
DHV 1U (Z-axis) Solar Pan	0	0	0		#N/A		0.8		0.8		0.8		0.8
DHV 3U (Type-1) Solar Pan	0	0	0		#N/A		0.8		0.8		0.8		0.8
0	#N/A	#N/A	#N/A		#N/A		0.8		0.8		0.8		0.8
0	#N/A	#N/A	#N/A		#N/A		0.8		0.8		0.8		0.8
0	#N/A	#N/A	#N/A		#N/A		0.8		0.8		0.8		0.8

CONOPS

Phase	Ratio per orbit (AVG)
Nominal	0.611222222
Downlink	0.044444444
Eclipse	0.333333333
Safe	0.01
Survival	0.001
Total	1

Power Generation

Avg Incident Solar Panels	9
Incident power per solar panel	3.429
Average solar panel efficiency	30%
Power Generation per Solar Panel (W)	1.0287
Solar Incidence Time per Orbit (hrs)	1
Margin	20%
Power Generation per Orbit	7.40664

Mode Power Profiles

Phase	AVG Power Consumption per Mode (W)	AVG Power Generation per Mode (W)	Net power per Mode (W)
Nominal	4.548	7.40664	2.85864
Downlink	7.956	7.40664	-0.54936
Eclipse	5.28	0	-5.28
Safe	5.742	7.40664	1.66464
Survival	3.888	7.40664	3.51864

Figure 6.5: Power Budget

As before, the green and red boxes show the identifiers and parameters respectively being extracted automatically. The power consumption sheet is then filled out by the user, detailing duty cycles and power consumption. The sheet then combines this information with the Mission Analysis data and develops a net power consumption for each mode (as defined in Section 5.2.1). This was done for three scenarios and plotted to assess capabilities of the CubeSat. This is shown in further detail in Section 11.

6.3 Closing Remarks and Open Points

The concurrent engineering spreadsheet provides a method to ensure cohesive interaction between the various sub-systems. The first iteration proved useful for early mission analysis, but further improvements can be made, ideally by the systems engineer.

- Format data in a relevant manner for each sub-team's simulations
  - Certain sub-teams will use the spreadsheet variables as inputs to, or outputs from their simulations. Depending on the software, each sub-sheet can be modified to accommodate this.
- Craft any more budgets required
  - De-tumbling and trajectory were only fully developed this year, and there may be other budgets to consider. These should be reflected in the spreadsheet aas it constantly evolves with the project.
- Create a summary 'capabilities' sheet
  - A summary sheet to collate all of the CubeSat's features (available space, available data, available power etc) could help assess feasibilty of any project going forward, so should be created when possible.

7 Orbital Analysis

7.1 Trajectory

7.1.1 Analysis

The trajectory analysis of a space mission is heavily dependent on the selected launch vehicle. A launch vehicle has not been defined yet, but the mission will be conducted in Low-Earth-Orbit (LEO). As such, a trajectory study has been performed using orbital parameters extracted from the ISS ZARYA module, which orbits in LEO [11].

The TLE (Two-Line Element) file was extracted and used in conjunction with MATLAB's Satellite Communications Toolbox to create a satellite scenario in MATLAB. It should be noted that the goal is to develop TLE parameters specific to WUSAT based on its launcher, but for now the ZARYA data is used to show the working method for trajectory analysis.

The scenario requires a start date to begin analysis. An arbitrary date of June 2nd, 2026 was chosen to begin the analysis.

A ground station can also be added using co-ordinates, and this has been placed at the University of Warwick, since the goal is for Warwick Aerospace Society to develop the ground station before launch. Using these parameters, the orbit can be visualised:

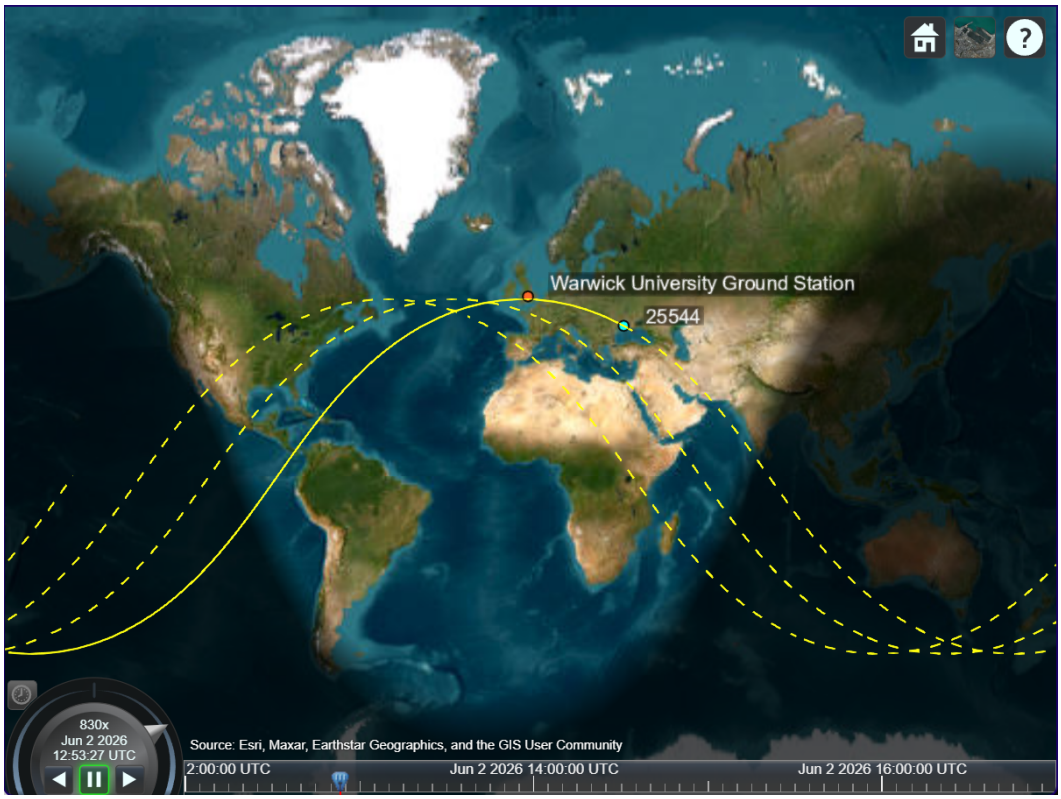

Figure 7.1: 3D orbit visualisation

The blue line represents the satellite itself, and the dotted yellow line represents the "ground trace" of the satellite, i.e. its position projected onto the Earth's surface.

This ground trace provides essential data to analyse the link budget and access times of the satellite itself. This can be plotted on a 2D map to assist link analysis and path tracking:

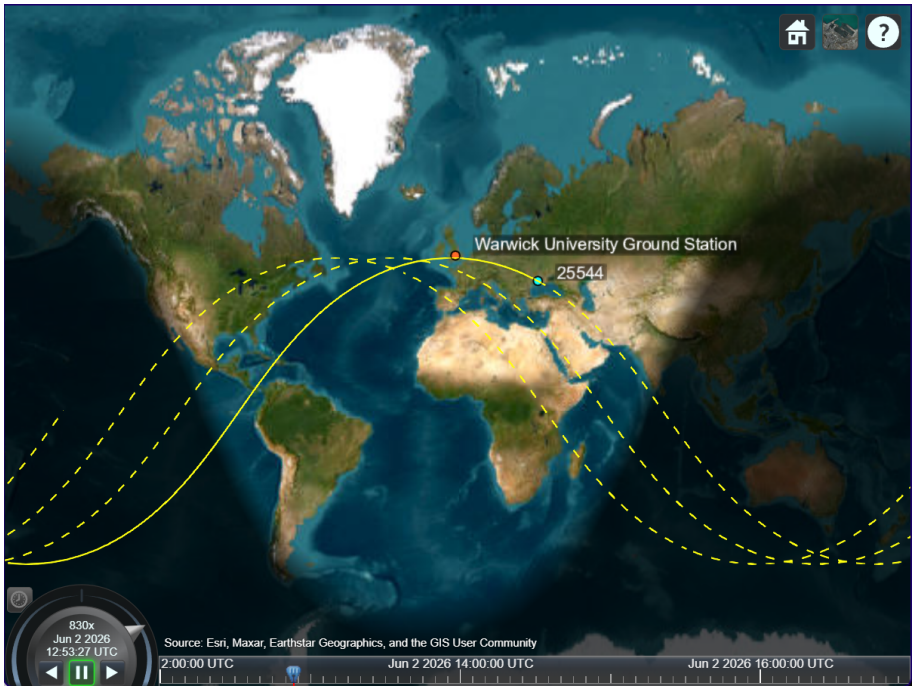

Figure 7.2: 2D ground trace visualisation

The visualiser is able to show the movement of the satellite across time, as shown through the solid line following the "25544" object (ISS ZARYA Designator). This visualisation can later be used by the RF sub-system to plot the field-of-view (FOV) of the ground station, and extract access times for a sample calculation, through application of the link budget. Due to factors explained in the project management overview, the RF engineer had to overtake the systems roles, and wasn't able to finalise and simulate the link budget. However, Warwick Aerospace determined a preliminary value of 157° for their FOV. Using this, the average contact time of 6 minutes was calculated, and the following ConOps times were deduced:

Phase	Ratio per orbit (AVG)	Time per orbit (mins)
Nominal	0.59	55.01
Downlink	0.07	6.00
Eclipse	0.33	30.00
Safe	0.01	0.90
Survival	0.00	0.09
Total	1.00	90.00

Table 7.1: Duty cycle and times of mission modes

These values will be used throughout the paper to determine various capabilites of the mission.

7.1.2 Next Steps

- Investigate possible Launchers and define a TLE file for WUSAT specifically, through simulations of launch and heritage flights.
- Perform Orbital decay simulations to verify that the mission complies with ESA Space Debris legislation, De-orbiting within 5 years.

7.2 Detumbling

7.2.1 Analysis

Another important consideration for the satellite orbit is de-tumbling. This refers to the satellite stabilising both after ejection from the launch vehicle, and across its orbit. Typically, this is done through an Attitude and Orientation Control System (AOCS) composed of reaction wheels and active computations of the satellite's orientation. However, due to mechanical constraints and the space required for reaction wheels, this is unlikely to be possible for this mission. Nevertheless, a stable orbit and orientation remains necessary to facilitate ground communications and mission lifetime analysis. Preliminary analysis suggests that *magnetorquers* could effectively reduce the angular velocity with a lower physical footprint [12]. Magnetorquers are de-tumbling devies consisting of copper coils, typically embedded in PCBs, used to produce magnetic fields which will slow down the angular velocity of the CubeSat. Active de-tumbling uses magnetometers to sense a magnetic field, which is fed to a controller. This controller then calculates the required torque response, and the magnetic field that can cause this, through the 'B-dot' mode [13]. It then outputs the required currents to generate this magnetic field to the magnetorquers, which are copper coils across the satellite. Preliminary analysis using a MATLAB CubeSat De-tumbling Github repository [14] and the orbital parameters calculated produced the following:

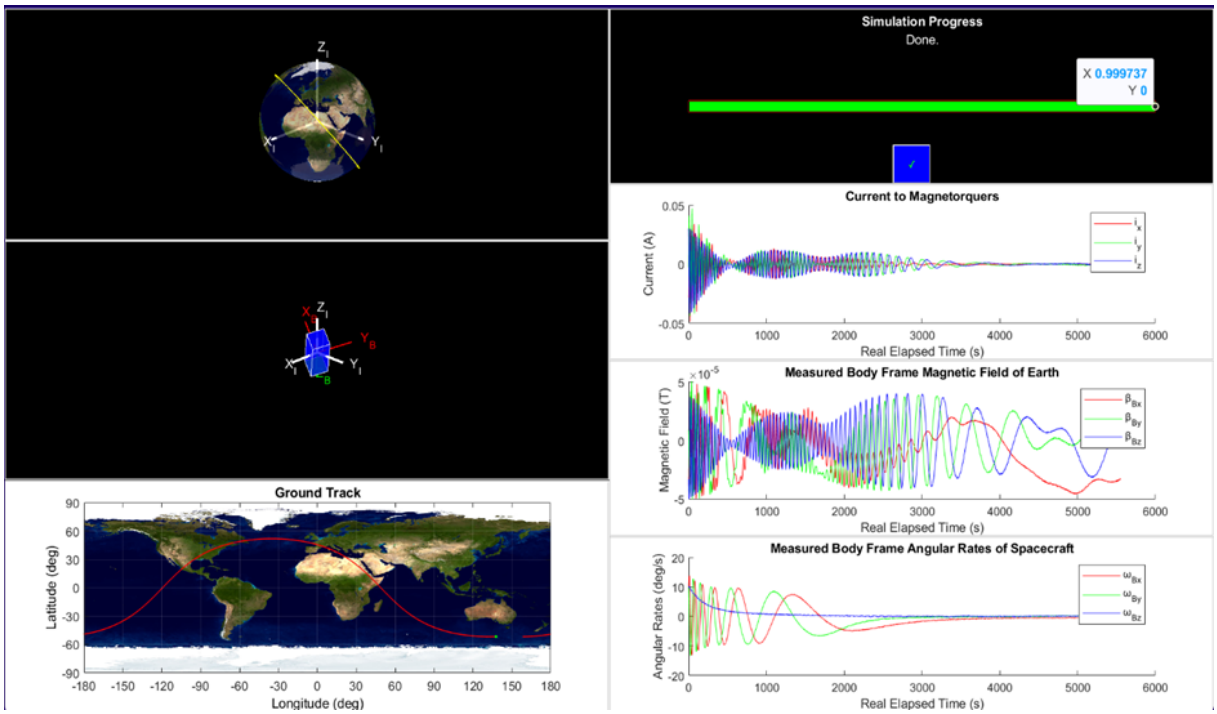

Figure 7.3: De-tumbling Simulation Viewer

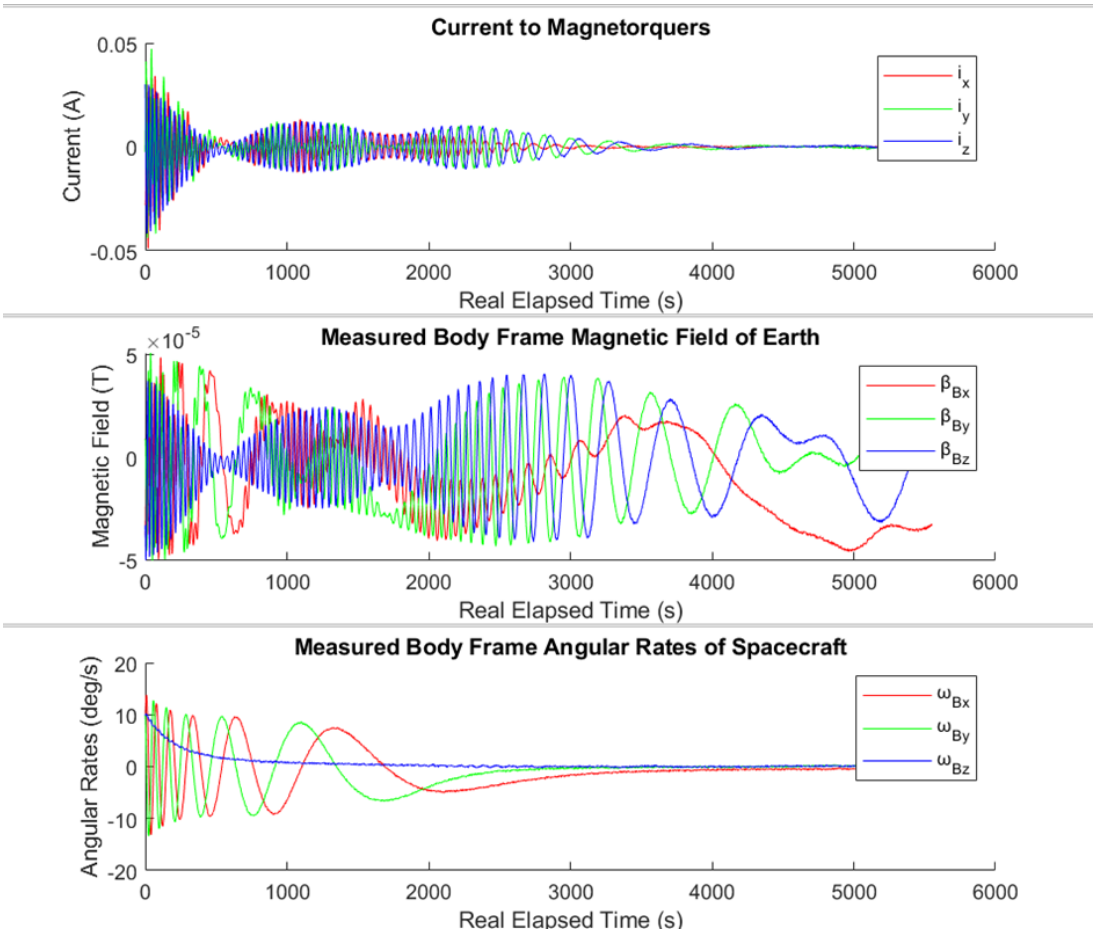

Figure 7.4: De-tumbling Simulation Outputs

The simulation outputs show that the magnetorquers exhibit a peak current draw of 50mA, with consistent draw of 20mA until stabilisation is achieved. With the current parameters, this is at approximately 2000 seconds, or 33 minutes. To optimise the current draw against the settling time, the controller parameters can be altered in the simulation. However, close attention should be given to the power budget, to ensure that the satellite can accommodate the detumbling. It should be noted that nominal operations should not begin until stabilisation is achieved. A paper also explored the effects of positioning and coil count in the magnetorquers damping effectiveness [12].

7.2.2 Closing Remarks and Next Steps

De-tumbling was neglected in previous years and, as such, is in a very early stage of development. It is recommended that this section, and the rest of the orbital sub-system is prioritised to ensure it is in line with the other sub-systems of the project. The tools available have been explored, but accurate analysis and simulation needs to be undertaken. The recommended next steps are:

- Explore the de-tumbling simulation using GitHub and the MATLAB file, and create an accurate model for simulation of the mission through the relevant parameters
- Communicate with EPS, Thermal, and OBDH sub-systems to optimise the controller requirements, current draw, and settling time based on budgets
- From the output of the optimisation, select or design magnetorquers and a relevant B-dot controller sufficient for the mission

8 Structures

8.1 Introduction

This section documents the structural engineering development of WUSAT-4's 3U CubeSat platform, focusing on the integration of a 1U FDSPP payload while adhering to ECSS standards and CubeSat Design Specification Rev 14. [15] Through design iterations validated by ABAQUS FEA, the team achieved a 410.98 Hz first natural frequency (315% above ECSS minimum) while maintaining a strict structural mass budget allocation.

8.2 Review of 23/24 Progress

Assessment of suitability for a 2U CubeSat size housing a 0.5U payload was carried out as well as additional investigation including thermal modelling on ESATAN and ABAQUS Tosca studies for a 3U CubeSat size with a 1U payload housing the FDSPP payload.

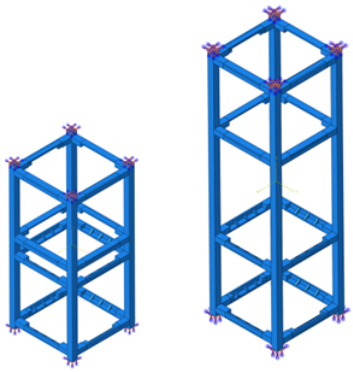

Figure 8.1: 2023/24 2U (left) and 3U (right) simulation boundary conditions and locations

The 3U CubeSat structure First Natural Frequency was found to be 406.41 Hz through ABAQUS simulations, moving from a 2U to 3U structure yielded a 36% reduction in first natural frequency. This and various other factors led to the decision to change to a 3U CubeSat housing a 1U payload. Subsequently, 3U Chassis designs and further ABAQUS studies were carried out as shown in the figures below.

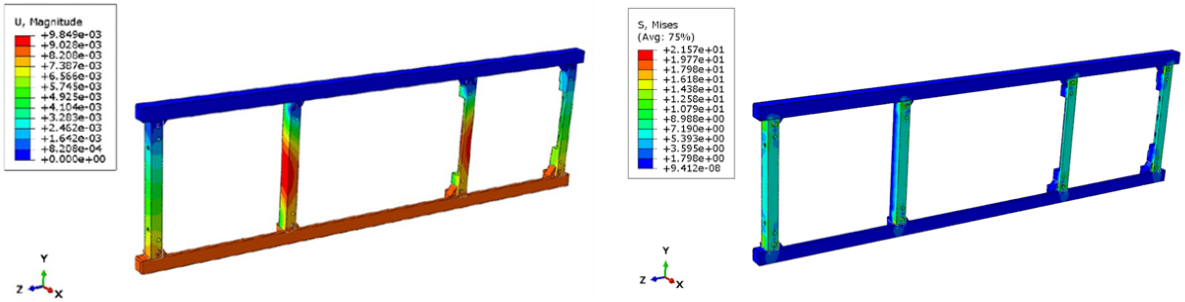

(a) $y = x$ **(b)** $y = 3\sin x$

Figure 8.2: 3U Rail deflection (left) and stress (right) results with lateral loading condition and non-linear contact

In these simulation results, the maximum stresses are experienced on the cross-members, with the maximum stress and maximum deflection well within the constraints of the material. A full final configuration of the chassis design is shown in the figure below however no viable manufacturing or assembly plan was made. An overview of material choices for the structure was assessed, using ESA requirements and advice of workshop technicians, the decision to use a combination of Al-6082 for the 3U rail elements, due to its anodising success, and Al-7075 for the other structural components.

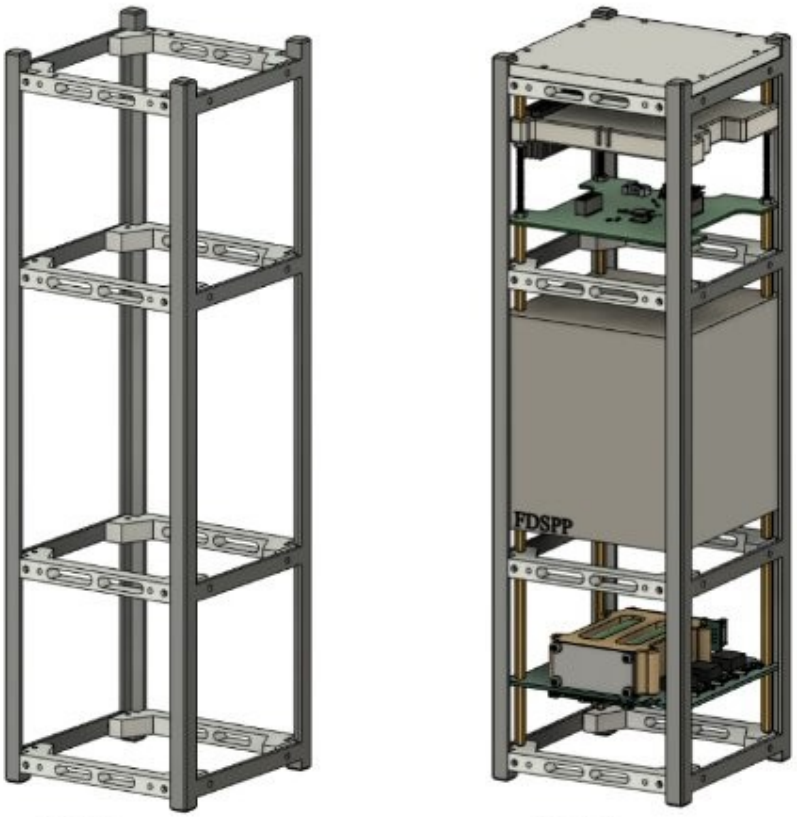

(a) Without components (b) With components

Figure 8.3: 2023/24 WUSAT-4 3U CubeSat chassis design

Two mounting concepts to determine how internal subsystems and devices are secured were developed. These are to be further evaluated and validated for implementation. ABAQUS analyses for the designs were used to validate and iterate design decisions. From a structural perspective, the move towards Phase C would see large amounts of iterative design and prototyping to validate and improve upon the established preliminary design. [2]

8.3 Requirements

W4-STR-10 The design shall meet the European Cooperation for Space Standardization (ECSS) guidelines for materials and assembly.

W4-STR-20 The structure shall conform to the CubeSat Design Specification Rev. 13 for 3U form factor.

W4-STR-30 The structural subsystem shall contribute no more than 20% of the total satellite mass budget to ensure compliance with overall weight limitations.

W4-STR-40 The satellite structure shall withstand all mechanical loads experienced during launch, including vibrations, shocks, and static loads, without permanent deformation or failure.

- **W4-STR-41** The structure shall maintain its integrity under lateral and vertical loading conditions as per launch provider specifications.
- **W4-STR-42** The natural frequencies of the structure shall be higher than the defined threshold to avoid resonance during launch (e.g., first mode frequency > 100 Hz).

W4-STR-50 The tests will simulate sinusoidal and random excitations of the launch environment as well as all other vibrations, shocks, and thermal loads in the 'worst case' test definition.

W4-STR-60 The materials used in the structure shall operate within a temperature range defined by the mission.

- **W4-STR-61** The structure shall facilitate thermal control by incorporating provisions for radiative and conductive heat dissipation mechanisms.

W4-STR-70 The structure shall accommodate the mounting of all subsystems, ensuring accessibility for integration, testing, and maintenance.

- **W4-STR-71** All mounting points shall be designed to prevent misalignment during assembly and operation with no SPOF.
- **W4-STR-72** The design shall allow for easy assembly and disassembly of subsystems for integration and testing purposes.

W4-STR-80 The structure shall remain functional throughout the mission duration, including exposure to the space environment (vacuum, radiation, and thermal cycling).

- **W4-STR-81** The structure shall maintain alignment throughout the mission duration, including exposure to the space environment (vacuum, radiation, and thermal cycling).

W4-STR-82 Structural connections shall include secondary fasteners or locking mechanisms to ensure reliability under extreme conditions.

W4-STR-90 The structure shall support the deployment of antennas and any external mechanisms without obstructing other subsystems.

W4-STR-100 The structure shall be properly finished/anodized to ensure no metal-to-metal contact points.

W4-STR-110 The structure shall be manufacturable using standard machining and finishing processes to minimise production time and costs.

8.4 Preliminary Technical Work

8.4.1 Materials Selection

Following the review of potential materials that would meet the CubeSat specification, the decision was made to use Al-6082 for the rails and the structural components, due to its anodising potential and flight proven durability. The SoE workshop staff reported success with anodising this material — a process deemed crucial by ESA FYS requirement 4.1.22. Al-6082 Material Data from GRANTA Edupack [16]:

- Young‘s Modulus = 72000 MPa
- Poisson‘s Ratio = 0.33
- Density, $\rho = 2.7E-09$ tonne/mm^3

8.4.2 Fastener Selection

Based on component data sheets, the solar panels, antenna, EPS, and transceiver all utilise M3 fasteners. To ensure simplicity and ease of assembly and manufacture, the decision was made to use M3 fasteners for the entire CubeSat.
A decision on material type has not yet been made, but ECSS will be used as a tool for guidance on steel, stainless steel or titanium fastener material based on supplier research. Flat head socket screws will be implemented throughout, except for the fasteners on the exterior faces of the CubeSat (e.g. for the solar panels). It is also noted that a thread locker (Loctite) will be necessary for all structural fasteners, or those used for the structure, to prevent them from slipping under the intense vibrations to be experienced during launch.

8.4.3 Assessment of 3U Structure

Many of the chassis crossmember designs done in 2023/24 were not viable for CNC machining and do not meet the ESA AIV requirements; therefore, the decision was made for our team to produce a new chassis design appropriate for prototyping and the qualification model, ensuring the 3U structure does not have any SPOF. Taking inspiration from

previous iterations to design a new chassis from the ground-up, adhering to all CubeSat standards from ESA and Cal Poly CubeSat Design Specification Rev 14. [15]
ABAQUS workflows for:

1. First natural frequency prediction.
2. Stress distribution under 6g/11g loads.

Boundary Conditions:

1. Fixed base (launch vehicle interface).
2. Non-linear contact modelling for rail joints.

8.5 Methodology and Design

A decision was made to adopt a rail and cross-member based CubeSat structure rather than a panel-based structure. The rails and cross-members were developed in parallel, given the intrinsic dependency of the design of each component on the other.

8.5.1 Iterative Design

The structural design process for the WUSAT-4 CubeSat followed an iterative approach to balance performance, manufacturability, and compliance with ECSS/CubeSat standards. Key drivers included:

1. CNC machining constraints.
2. Chassis AIV, designed for assembly and ease of mounting.
3. Natural frequency optimization (target >130 Hz).
4. Mass reduction to meet 20% total budget requirement (W4-STR-30).

Some key iterations are shown in the figure below. The application of AQAQUS simulations drove the decisions behind mass reduction and overall final chassis design.

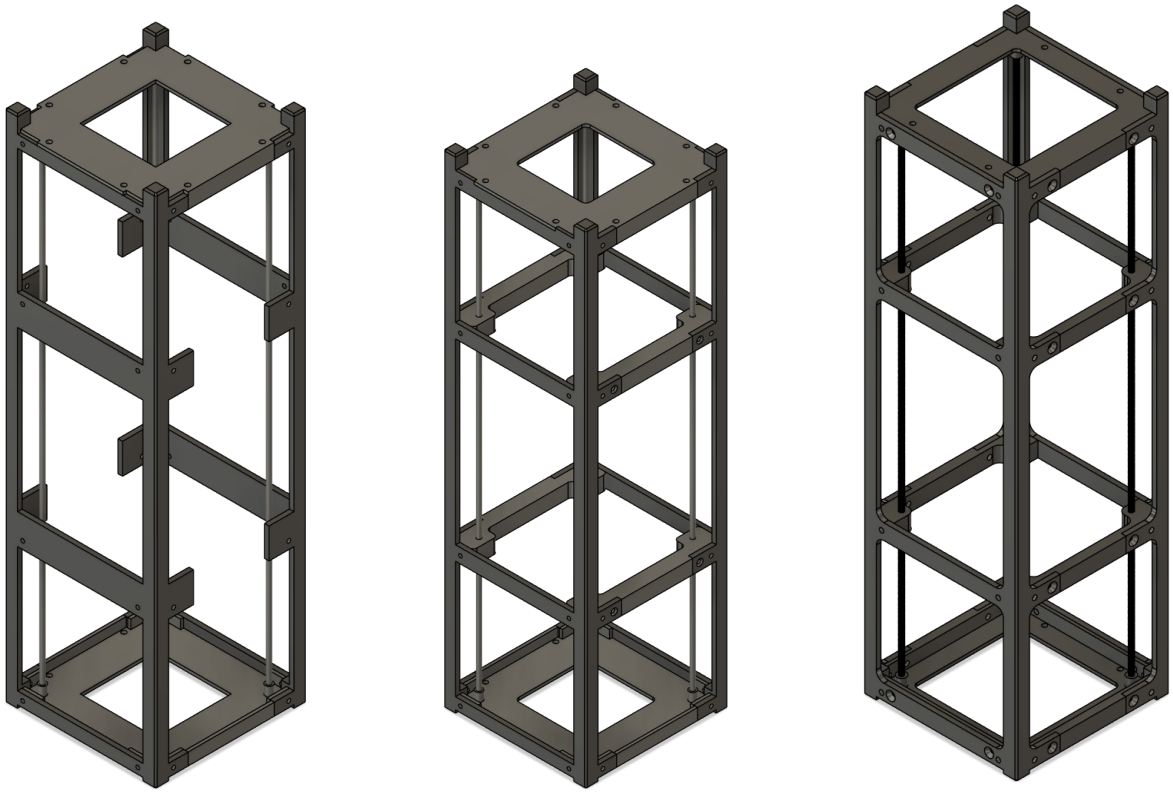

Figure 8.4: Examples of Chassis Iterations

This iterative process ultimately delivered a 3U chassis exceeding all frequency requirements (410Hz first mode) while maintaining 2L functional volume and less than 450g total structural mass.

8.5.2 ABAQUS Simulations

The structural performance of the chassis under launch conditions was deduced through Finite Element Analysis (FEA) using ABAQUS. For the sake of simplicity, the chassis and the rails are modelled as one body with no joints, ensuring that the mesh stays within the node limit of the educational license of ABAQUS. The analysis focuses on the Von Mises stress distribution across the chassis, the displacement due to stress, and the acquisition of the smallest natural frequency of the chassis to ensure that it will withstand vibrational frequencies during launch.

To ensure that the chassis will withstand any vibrations during launch, which are estimated to be at a maximum frequency of 150Hz, the first mode's natural frequency must be greater than 130Hz by a reasonable margin. The first mode was found to be a natural frequency of 410.98Hz, which is much higher than the required tolerance of 130Hz, thus the chassis will withstand the vibrational forces during launch.

When simulating the launch conditions, the minimum expected load and absolute maxi-

mum expected load were simulated as it can be assumed that the chassis can withstand the load between these two scenarios. The launch load is assumed to purely be due to acceleration due to gravity, thus acting in the Z-axis. The minimum acceleration load is assumed to be 6g, with the absolute maximum load being assumed to be 11g in the Z-axis and 6g in both the X-axis and Y-axis [17]. The results are deemed acceptable should the maximum stresses fall being the yield strength Al-6082 (228MPa).

Minimum Launch Load

Figure 8.6 represents the Von Mises stress distribution across the chassis under a 6g acceleration load. The maximum stress is observed to be 5.19MPa, with the stress concentrating where the joints and mounting points would be. Medium level stresses also concentrate on the outer parts of the chassis. As all stresses are at 5.19MPa or below, which is less than the yield strength, it is evident that the chassis will withstand the launch load of 6g.

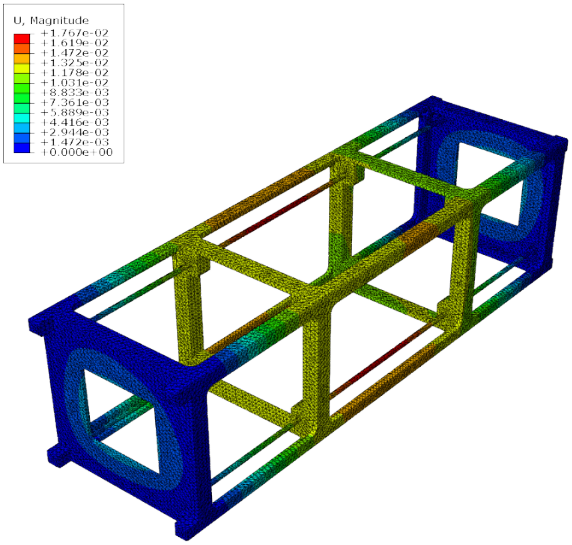

Figure 8.5: Deflection Distribution due to 6g Launch Load

As expected, the total displacement magnitude distribution depicted in Figure 8.5 shows that the middle of the chassis' rails experiences a maximum deflection at 0.0177mm, with the longer sections of the main body deflecting slightly less at 0.0162mm . The minimal deflection across the body suggests that the chassis is stiff enough to not drastically deform when experiencing the minimal launch load.

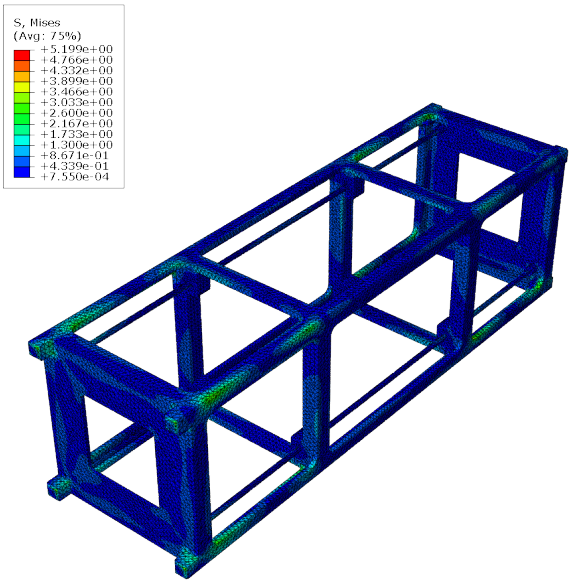

Figure 8.6: Von Mises Stress Distribution of 6g Launch Load

Maximum Launch Load

The overall Vonn Mises stress distribution profile almost mirrors that in Figure 8.7, but once compared to Figure 8.8, it is evident that the stress is more evenly distributed across the body due to load redistribution. The concentration points remain the same, but the deformation scale factor of 2578 shows that the chassis is experiencing tensive stresses further along the Z-axis, and compressive stresses closer to the origin.

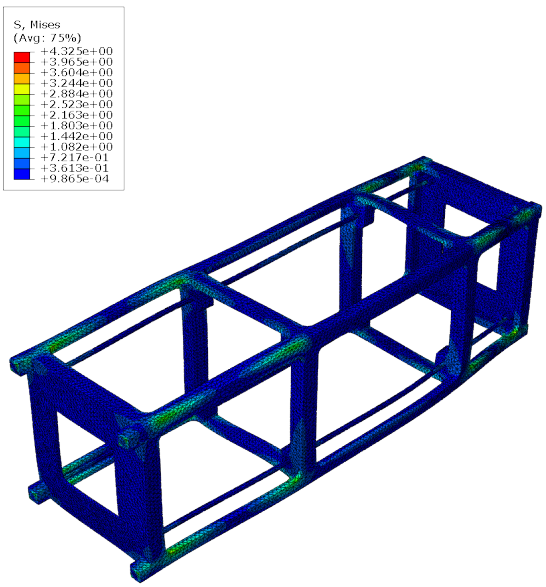

Figure 8.7: Von Mises Stress Distribution of 11g Launch Load

As a result of load redistribution, the maximum concentration of stress has been reduced to 4.32MPa, with the minimum stress increasing from the launch load of 6g. The maximum stress remains to be below the yield strength of Al-6082 and thus can withstand the assumed range of launch loads.

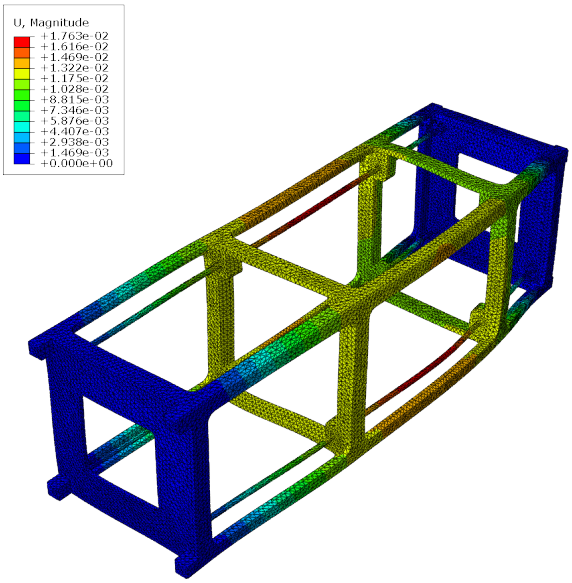

Figure 8.8: Deflection Distribution due to 11g Launch Load

The Figure above shows a similar displacement profile to that of the 6g launch load, which implies that the chassis is not overly susceptible to deflection upon increase of acceleration. The chassis experiences an insignificantly smaller maximum deflection of 0.0176mm. Overall, the simulations highlight key areas for weight reduction and show the chassis design and material choice are suitable for launch.

8.5.3 "Tuna Can" Volume

The "Tuna Can" volume of the chassis is a valid approximation recognised in CubeSat design can be calculated. It is found to be: $1.974E+06$ mm^3, this is equivalent to ≈2L. and represents the total "useful" volume of the chassis without any conflicts with parts of the chassis.

Figure 8.9: "Tuna Can" volume representation in WUSAT-4.

8.6 Final Chassis Design

8.6.1 3U Rail Element

Figure 8.10: 3U Member front view (left) and back view (right)

- Has countersunk holes for chassis assembly without intersecting with solar panels.
- Has threaded holes to ensure secure connections using Loctite.
- Anodized Al-6082, 120.579 grams x 2, engineering drawings in appendix.

8.6.2 1U Members

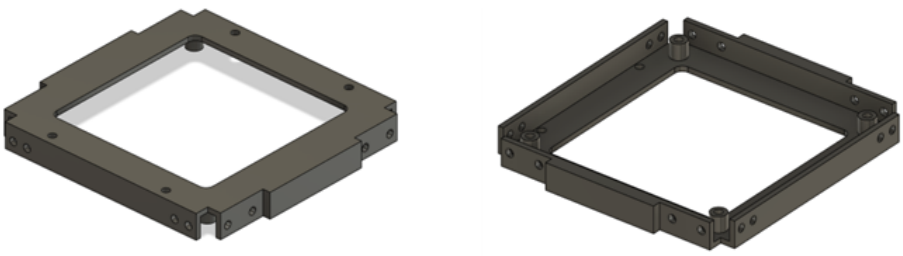

Figure 8.11: 1U Top Member top view (left) and bottom view (right)

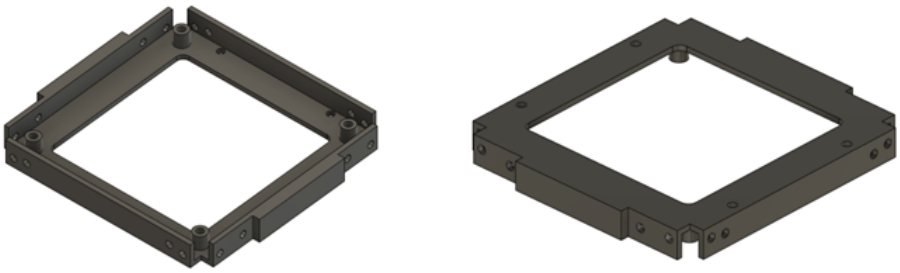

Figure 8.12: 1U Bottom Member top view (left) and bottom view (right)

- Includes mounting points for the solar panels, threaded rods, 3U members and antenna.
- Has threaded holes to ensure secure connections with M3 bolts using Loctite.
- Anodized Al-6082, 44.052 grams, engineering drawings in appendix.

8.6.3 Crossmembers

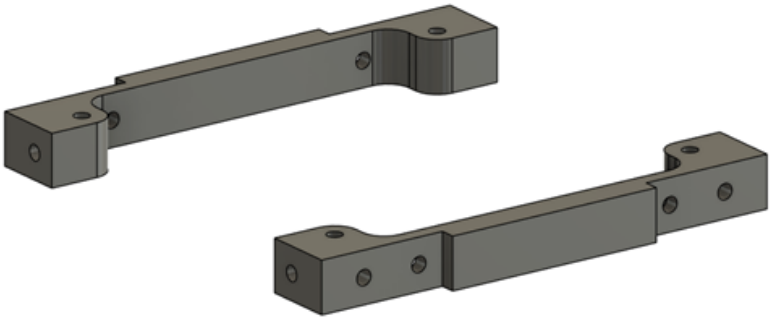

Figure 8.13: Chassis crossmembers

- Threaded holes for the solar panels, 3U and 1U members. Supports the threaded rods.
- Anodized Al-6082, 18.459 grams x 4, engineering drawings in appendix.

8.6.4 FDSPP Mounting Plates

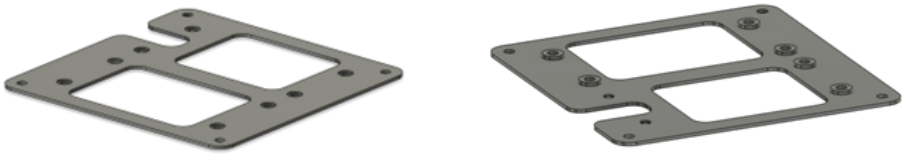

Figure 8.14: FDSPP Top Mounting plate top view (left) and bottom view (right).

- Used to mount onto the top of the FDSPP and the threaded rails.

- Countersunk holes for FDSPP bolts and spacing to ensure proper alignment with FDSPP geometry.
- Anodized Al-6082, 11.479 grams, engineering drawings in appendix.

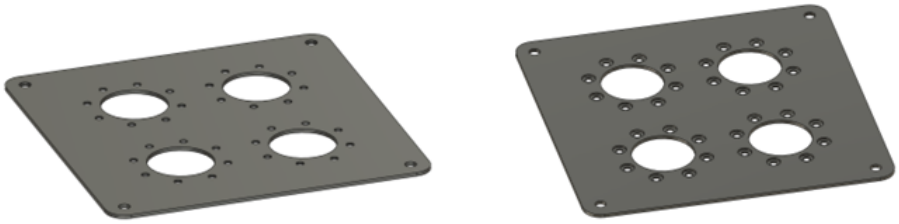

Figure 8.15: FDSPP Bottom Mounting plate top view (left) and bottom view (right).

- Used to mount onto the bottom of the FDSPP and the threaded rails.
- Countersunk holes for FDSPP bolts.
- Anodized Al-6082, 16.296 grams, engineering drawings in appendix.

8.6.5 Threaded Rod

Figure 8.16: M3 Threaded Rod up close side view

- Used to mount all other components and subsystems using nuts and spacers.
- Run the full length of the 3U CubeSat with a length of 324.5 mm.
- Anodized Al-6082, 4.775 grams x 4, engineering drawings in appendix.

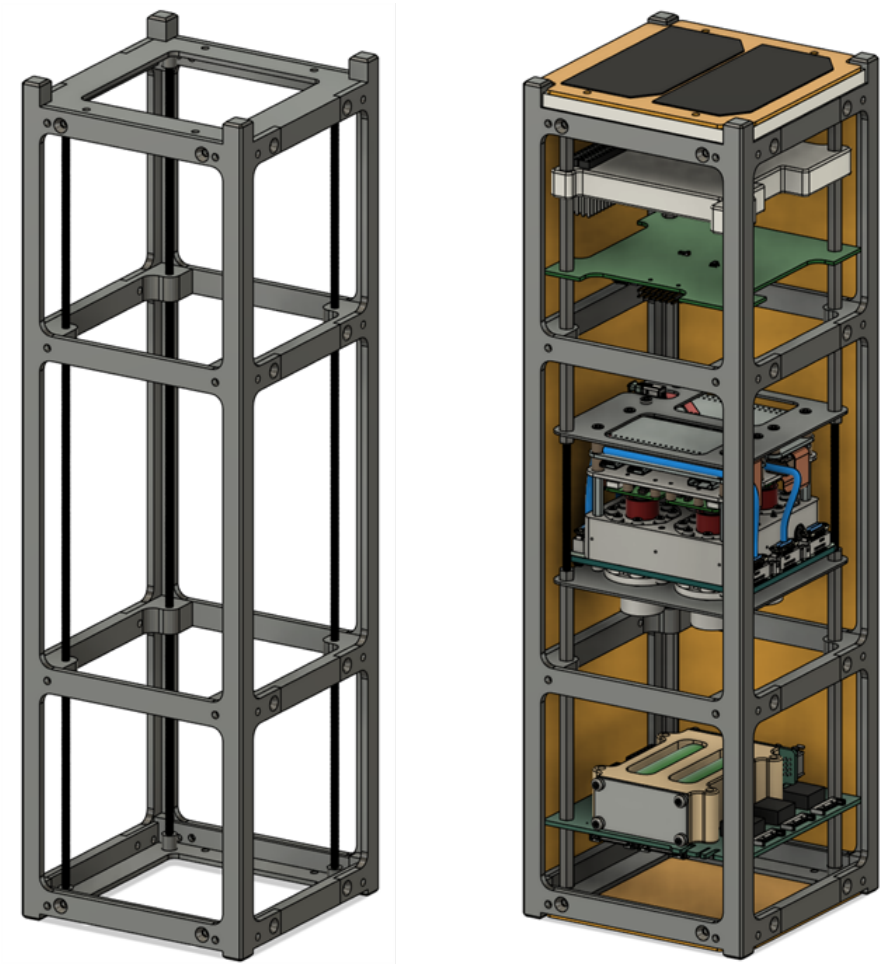

Figure 8.17: Final WUSAT-4 Chassis Design without (left) and with components (right).

Part No.	Component(s)	Material	Quantity	Mass (g)
1	3U Rail Element	Anodized Al-6082	2	120.579
2	1U Member	Anodized Al-6082	2	44.052
3	Crossmember	Anodized Al-6082	4	18.459
4	FDSPP Mount	Anodized Al-6082	1	27.775
5	M3 Threaded Rod	Anodized Al-6082	4	4.775
			Total Mass (g):	449.973

Table 8.1: Summary of all chassis components.

8.7 Prototyping

- Prototyping Stage 1: Cross-members and rails should be 3D printed, to examine the shape and size, at a much lower cost than manufacturing each part from metals. Mainly used to validate the design prior to any machining. Also in this stage, a detailed examination of component interaction should be completed, to understand how each component should assemble and integrate into the design.

- Prototyping Stage 2: A full prototype of the frame should be machined from a non-metallic material such as wood (not plastic). Like Phase 1, a non-metallic material would be cheaper meaning less risk with any prototyping complications. This stage would serve as a proof of concept for the frame, ensuring that each component can be successfully CNC machined, and the satellite can be readily assembled.
- Prototyping Stage 3: This final stage is the full qualification model, having the full configuration of the satellite, with components machined and finished from the material intended to be used in the final design. Assuming no unforeseen complications, this model is to be used for physical testing.

8.7.1 Prototype Component Mounting

All components are to be mounted on the M3 threaded rods in the WUSAT-4 prototype chassis structure spaced evenly in a 75mm square. This can be adjusted by ±2mm if necessary.

The components and mounting plates have a constrained maximum outer size from to the chassis in the form of a 94mm square as seen in the figure on the right. The components will be mounted on the threaded rod and then supported with nuts and other threaded supports. These dimensions will need to be changed in the final qualification model to accommodate for the various dimensions of standard off the shelf-parts such as the transceiver as seen in the appendix. However, this is not possible until all NDA's have been signed to obtain the relevant CAD files for all off the shelf parts.

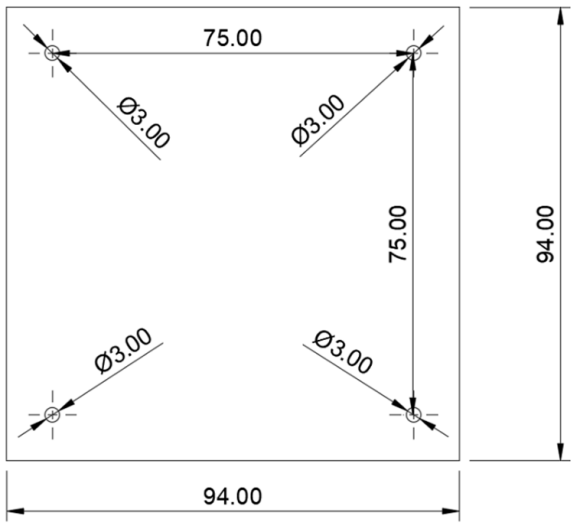

Figure 8.18: Drawing of component mounting points and outer boundary.

8.7.2 Stage 1 Prototype

The CAD model for the Stage 1 Prototype was made specifically for 3D printing. Due to the constraints in printing resolution and not being able to thread PLA, not all dimensions are representative of the final chassis and components. With the potential for 72 x M3 fasters, less than half are used, as only 2 solar panels are used. In this way, the prototype gives a clear view of the internal details and connections as well as the counter-sunk holes necessary for the assembly.

The Stage 1 Prototype was 3D printed on a Bambu Lab A1 Mini using PLA with 14 plates required to complete the print as shown in the figure below, taking 16 hours 45 minutes and using 339.73 grams of PLA using a 0.4 mm nozzle. The four 324.5mm M3 Aluminium threaded rods were manufactured in the engineering workshop.

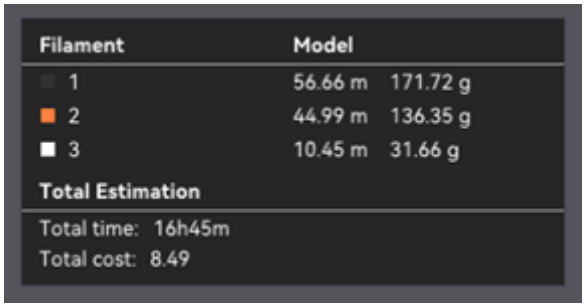

Figure 8.19: Total filament, cost and time estimation for 3D Print

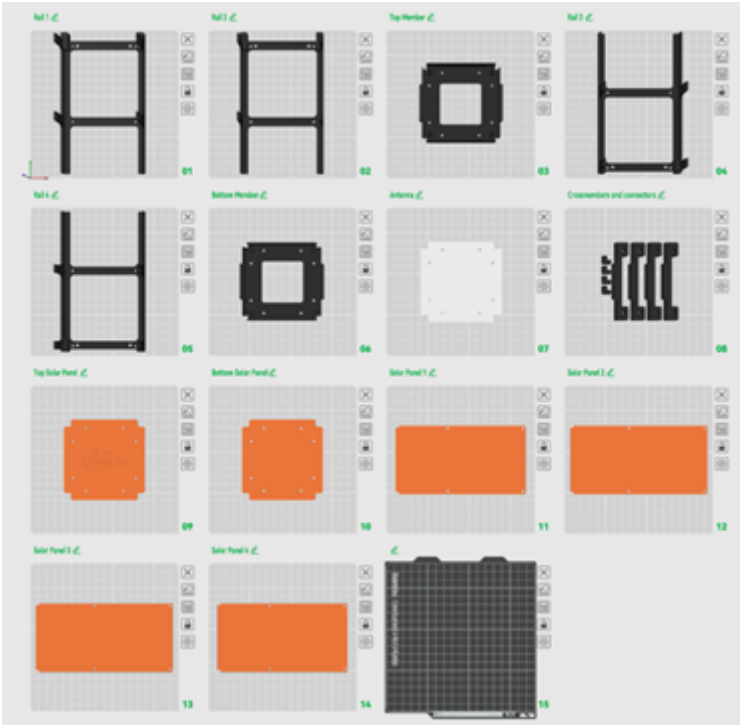

Figure 8.20: All plates required for Stage 1 Prototype

Figure 8.21: Final CAD (left) and render (right) of Stage 1 Prototype

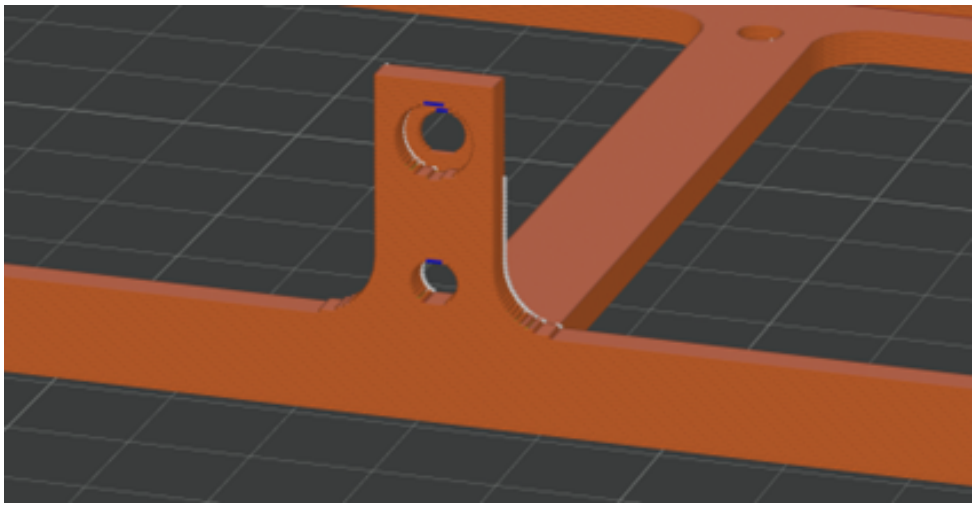

Figure 8.22: Close-up view of 3U Rail slice

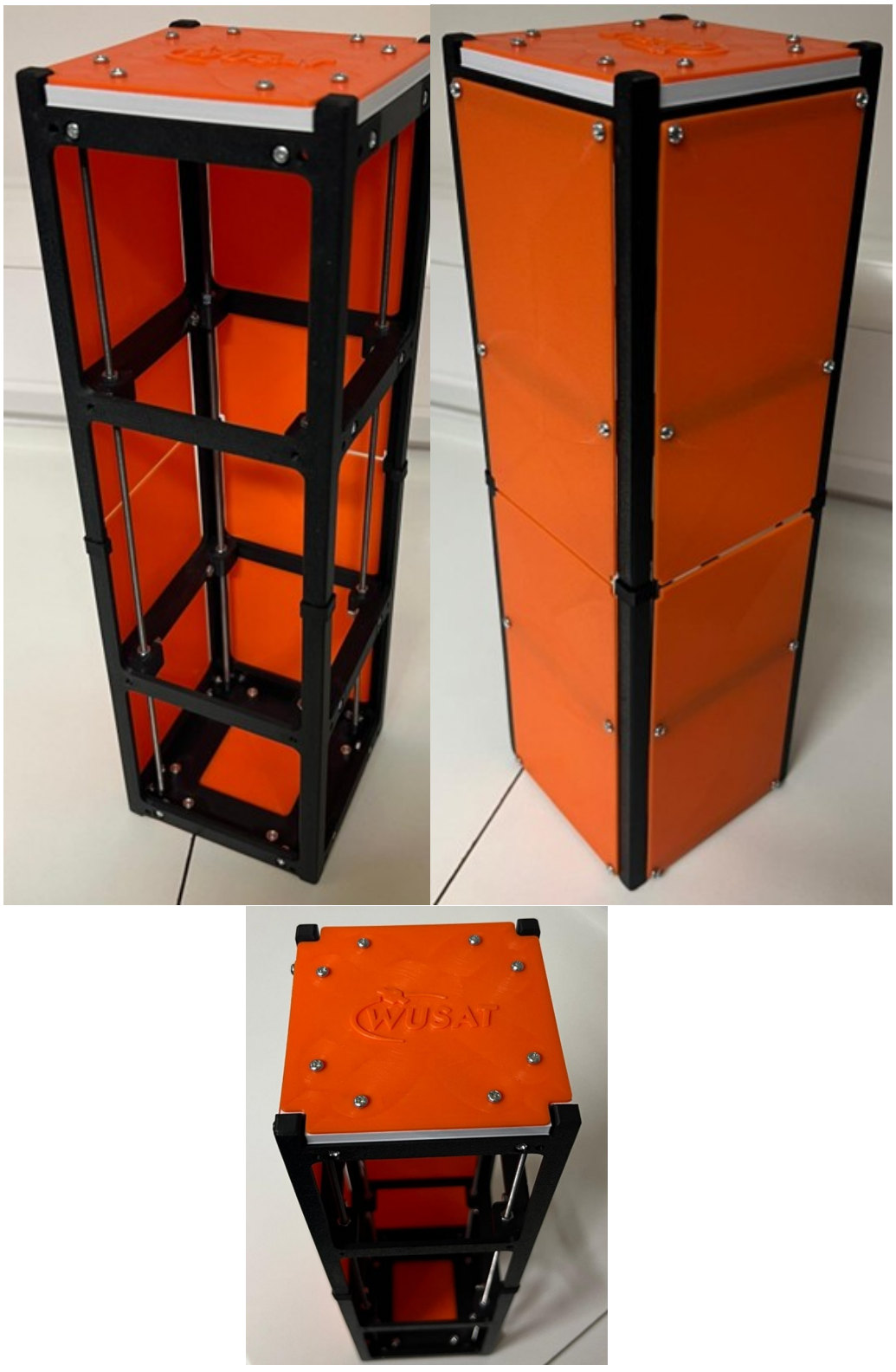

Figure 8.23: Pictures of completed Stage 1 Prototype Chassis

8.7.3 Physical Testing

FYS specification tests as per requirement **W4-STR-50** listed below:

- Natural Frequency Tests: The first natural frequency of the CubeSat should be determined through test and should be no less than 115 Hz. This can also be done analytically, but the natural frequency should be no less than 130 Hz.
- Quasi-Static Loads: Tests should show that the CubeSat shall withstand a launch quasi- static acceleration of 10 g in any direction.
- Random Vibrations: Vibration testing should be performed on the CubeSat, with results aligning in accordance with table supplied in the FYS specification.
- Shock Loads: The satellite should be compatible with the shock level supplied in the FYS specification.
- Sine Vibration Testing: This testing is entirely dependent on the launch vehicle, which is currently not selected. But it would be an important test to prepare to use when the launch vehicle is selected.

8.8 Open Points

- Iterate chassis design and finalisation of dimensions
  - FDSPP Mounting plate thickness and connections
  - Threaded rod spacing
  - 1U Member solar panel and antenna connections
  - Fasteners material selection
  - Centre of mass calibration
- Investigate weight reduction methods using ABAQUS and other simulations
  - FDSPP Mounting plates
  - Crossmembers
- Stage 2 Prototype
  - Finalise CAD Files and all connections for QM
  - Discuss with workshop technicians and produce CNC Files for manufacturing
  - Final production and assembly ready for physical testing
- Stage 2 Prototype Physical Testing
  - Carry out all FYS specification tests in Secion 8.7.3

9 Mechanisms

9.1 Requirements

W4-MECH-10 The antenna shall operate in the UHF frequency range of 430-438 MHz

W4-MECH-11 The antenna shall achieve circular polarization for signal transmission and reception

W4-MECH-12 The antenna shall interface with the satellite's onboard computer (OBC) via I2C protocol for deployment control

W4-MECH-13 The antenna shall integrate with a 1U CubeSat structure using standard mounting points

W4-MECH-14 The antenna mass shall not exceed 100 grams

W4-MECH-15 The antenna shall remain stowed within a volume of $10 \times 10 \times 1\text{cm}^3$ when non-deployed

W4-MECH-16 The antenna shall operate in a temperature range of -20°C to + 50°C

W4-MECH-17 The antenna shall withstand launch vibration frequencies

W4-MECH-18 The deployment mechanism shall include triple redundancy with at least two burn-wire systems

Considerations have been made to change the proposed antenna from the ISIS-Space 1U Antenna System to the 1U EnduroSat UHF Antenna III. Adhering to CubeSat integration standards, it is to be mounted on the Z-side of the CubeSat.

The Antenna III is designed to be configurable with solar panels of the same form factor, making it configurable with the DHV-Technology solar panel on the Z-face of WUSAT-4, which can be mounted on the top-plate.

The antenna's rods are stowed along the CubeSat body and is designed to align with standard mounting points, which ensures compatibility with common satellite structures. The rods are deployed using a triple redundant burn wire mechanism with verification feedback via I2C to confirm deployment status.

9.2 Analysis

- **W4-MECH-10&11**: The standard frequency range for a CubeSat mission is between 430Hz and 438Hz, which propagates through the atmosphere well. This range is also within the amateur radio band, which can be readily used for educational or hobbyist projects. Circular polarisation ensures that the signal transmission and reception is optimal regardless of orientation changes whilst in orbit.

- **W4-MECH-12&18**: For precise commands to the triple redundancy deployment mechanism, as well as precise telemetry feedback, I2C will be the main mode of communication to communicate with the on-board computer. The deployments mechanism should utilise at least two burn-wire systems and a fail-safe to mitigate the potential of deployment failure.
- **W4-MECH-13**: The antenna must fit within a 1U panel on the Z-face of the CubeSat using standard mounting points so that it is configurable with a solar panel to be mounted on the top plate. However, this may not be entirely necessary as deployable solar panels may be used instead.
- **W4-MECH-14&15**: The non-deployed form factor should minimise interference with the CubeSat's volume and shape during before and during launch. The maximum mass of 100g is relatively light to mitigate shifting the satellite's centre of mass and making it top-heavy.
- **W4-MECH-16&17**: The antenna must withstand the launch environment, namely forces such as vibrations and shocks. Which necessitates the use of damping systems and robust mounting to the main body. The antenna should also operate between -20°C and +50°C, so it should be made of materials with low thermal expansion coefficients.

9.3 Design

9.3.1 Progression from 2023-24 Group

Initially, the antenna for the CubeSat was to be the ISIS-Space 1U Antenna System, however it appeared to not have met their desires and promptly changed the antenna choice to the EnduroSat Antenna III. While their written work mentions that they made considerations, it appears that these considerations are not available to properly understand this change, however their decision will be adhered to for now.

9.3.2 EnduroSat Antenna III

Overview

The antenna is designed to cover the amateur satellite band, 435-438MHz, in the UHF band. The Antenna III has a circular polarisation and uses triple redundant burn wire mechanism with triple feedback for the deployment of the rods. The antenna is to be controlled and monitored via I2C interface. Additionally, the antenna is compatible with 1U solar panels for mounting.

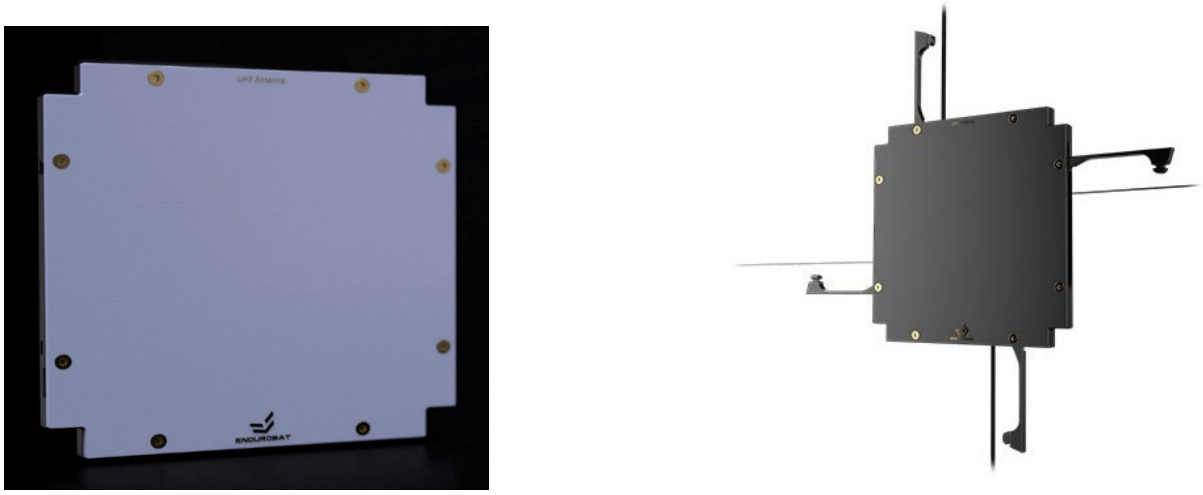

(a) EnduroSat Antenna III **(b)** EnduroSat Antenna III (Deployed)

Figure 9.1: CubeSat Antenna

Specifications Specifications taken from the Endurosat Antenna III Datasheet [18]:

- UHF band for amateur satellite communications 435 – 438MHz
- Circular Polarisation
- Max RF output power: 3.5W
- Supply voltage: 5V
- Current consumption: 250mA @ 5V
- Idle current consumption: 1mA @ 5V
- Gain >0dBi
- Mass: 85g
- Width: 98mm
- Length: 98mm
- Height: 12.25mm
- Operating temperature: -40°C to 125°C

Given these specifications, the Antenna III satisfies all of the requirements and is deemed suitable for integration into the design of the CubeSat.

The antenna attains a circular polarisation by having each rod be fed with a 90 degrees phase shift. The rods themselves are folded into the body and are held in place with the use of doors. These doors are held shut by a wire, which are cut by the burning resistors.

Each rod can be deployed by two independent resistors for redundancy. There is an additional level of redundancy provided by the ability to directly control the activation of the burning resistor chains. To prevent unwanted deployment, there is a test mode jumper for I2C verification.

Testing
Testing the antenna involves testing the deployment functionality, RF performance, an mechanical durability.

- Functional Deployment Test: The burn-wire mechanism is activated under controlled conditions to confirm full deployment in a typical scenario.
- Redundancy and Fail-Safe Testing: The backup burn-wire system is triggered to validate secondary deployment.
- Polarization Verification: Cross-checked using a reference antenna to confirm circular polarization.
- Vibration and Shock Testing: Simulates launch conditions using vibration tables and shock tests
- Thermal Vacuum Testing: Conducted in a thermal vacuum chamber to verify function in extreme temperatures (-20°C to +50°C) under near-space pressures.

9.3.3 Failure Mode and Effects Analysis (FMEA)

Failure Mode	Potential Cause	Effect on System	Detection Method	S	O	D	RPN	Mitigation Strategy
Antenna Deployment Failure	Release mechanism jammed, insufficient preload on burn wire	Loss of communication, mission failure	Deployment telemetry, signal strength monitoring	9	3	5	135	Use redundant channels for deployment. Perform thermal and vibration tests. Ensure low voltage drop by minimizing cable length.

Burn Wire Failure	Improper current delivery, wire fatigue	Deployment failure, no signal transmission	Voltage and current monitoring	8	4	6	192	Electrical verification, redundant burn wire, pre-flight resistance checks. Use feedback from deployment mechanism for monitoring and control.
Antenna Structural Failure	Launch vibrations, mechanical fatigue	Antenna deforms, signal degradation	Visual inspection, structural FEA	7	3	4	84	Vibration testing, material quality control, and ensure proper storage and handling as per the datasheet.
Connector Failure	Loose connection, cold welding in space	Intermittent or no signal transmission	Signal strength analysis, pre-flight connection tests	8	3	5	120	Secure connections with redundancy, vibration testing, ensure antenna is stored in a dust free environment.
RF Signal Loss	Faulty soldering, PCB degradation	Weak or no signal	Signal integrity tests, spectrum analysis	7	2	6	84	Quality control during manufacturing, redundant PCB pathways
Power Circuit Failure	Short circuit, overcurrent damage	No power to antenna, failure to transmit	Power system telemetry, current monitoring	9	2	5	90	Overcurrent protection, redundancy in power lines

Thermal Expansion Issues	Extreme temperature cycles in orbit	Deployment failure or antenna deformation	Thermal modelling, post-deployment analysis	6	3	4	72	Manufactured using materials with low CTE (Shape Memory Alloy rods, FR-4 for PCB), thermal cycling tests.
Contamination of Contact Points	Particles from spacecraft, oxidation	Poor electrical connectivity, signal degradation	Signal noise analysis, pre-flight inspections	7	2	5	70	Cleanroom assembly, protective coatings, redundant paths
Interference from Other Systems (EMI)	EMI from onboard electronics	Reduced signal strength, data loss	RF testing, EMI analysis	6	3	5	90	Shielding, grounding techniques, RF isolation testing

10 Thermal

10.1 Introduction

While in orbit, the CubeSat is subject to various internal and external thermal loads that result in large temperature fluctuations. A successful thermal design utilizes active or passive thermal control measures to ensure internal components are maintained at their respective operational and non-operational temperature limits. To analyse the thermal performance of a satellite, preliminary steady state and transient state calculations were done, followed by more comprehensive thermal environment simulations using ESATAN-TMS. The simulations were used to examine various thermal control techniques and minimise temperature fluctuation within the satellite.

10.2 Background and Methodology

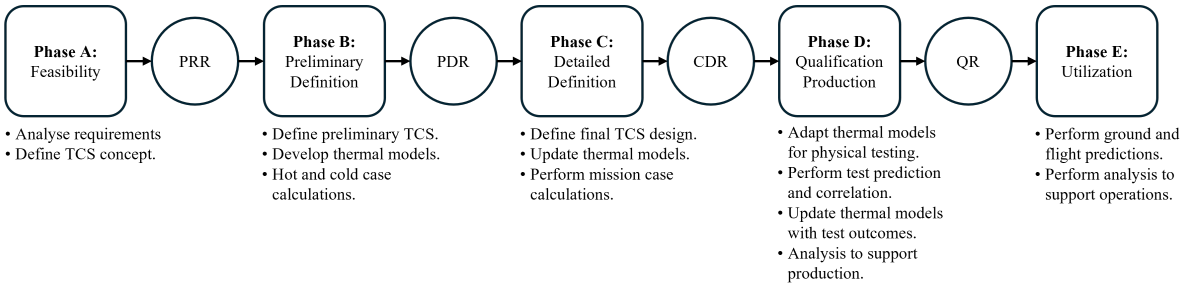

Figure 10.1: Thermal phase development

Thermal models are used during all phases of space system development, ranging from conceptual design to in-flight predictions [19]. The use of computational analysis can verify thermal requirements and minimise the need for physical tests that are expensive and time consuming. As mentioned in Figure 10.1, the first model used in thermal analysis is the thermal mathematical model. This model is primarily constructed based on heat loads and material properties.

10.2.1 Thermal Mathematical Model

The internal temperatures of a CubeSat are impacted by several heat loads described in Table 10.1.

Preliminary hand calculations are commonly used to verify simulation results. It involves modelling the satellite as a single node and averaging thermo-physical and thermo-optical properties of the satellite materials, hence calculating low-fidelity initial estimations. The steady-state thermal balance equation calculated the sum of all heat loads acting on the satellite at varying points in orbit. The steady-state equation is as follows [22],

	Heat Transfer	Internal/ External	Brief Description
Solar Flux	Radiative	External	Radiative heat resulting from exposure to solar rays. Large distance from Sun allows for the assumption of parallel solar rays. Can vary based on time of year, orbital parameters, satellite attitude and absorptivity of surface facing the Sun.[20]
Albedo	Radiative	External	Radiative heat resulting from solar energy reflecting off the Earth. Can vary based on solar flux, orbital parameters, satellite attitude and absorptivity of surface facing Earth.[20]
Planet IR	Radiative	External	Radiative heat resulting from solar energy being absorbed by Earth and re-emitted as long-wave IR. Can vary based on time of year, orbital parameters, cloud cover and emissivity of surface facing Earth.[21]
Internal Power Dissipation	Conductive	Internal	Heat generated from power dissipation by internal components necessary for satellite functions. Can vary based on satellite operational mode, material conductivity and contact area between components.[21]

Table 10.1: Internal and external heat loads.

$$\dot{q}_{in} = \sum_{i=1}^{L} \dot{q}_{solar,i} + \sum_{j=1}^{M} \dot{q}_{albedo,j} + \sum_{k=1}^{N} \dot{q}_{IR,k} \tag{10.1}$$

where,

- $\dot{q}_{in}$ refers to the sum of external heat loads acting on satellite.
- $\dot{q}_{solar,i}$ refers to solar energy absorbed by surface i.
- $\dot{q}_{albedo,j}$ refers to albedo absorbed by surface j.
- $\dot{q}_{IR,k}$ refers to Earth IR absorbed by surface k.
- L, M and K refer to the number of surfaces absorbing solar energy, albedo and IR respectively.

The transient thermal balance equation uses the heat flux acting on the satellite and calculates node temperature based on overall mass and specific heat capacity. The transient state equation a given node is as follows [22],

$$\dot{q}_{out} + \dot{q}_{stored} = \dot{q}_{internal} + \dot{q}_{in} \tag{10.2}$$

where,

$$\dot{q}_{stored} = \left(\rho c_p \frac{\delta T}{\delta t} \right) \Delta V \tag{10.3}$$

- $\dot{q}_{out}$ refers to heat rejected by satellite.

- $\dot{q}_{stored}$ refers to heat stored by the satellite.
- $\dot{q}_{internal}$ refers to heat generated by internal components.
- ρ refers to averaged node material density.
- c_p refers to the specific heat of the satellite.
- T refers to the node temperature in Kelvin.
- V refers to the overall volume of the satellite.

10.2.2 Computational Model

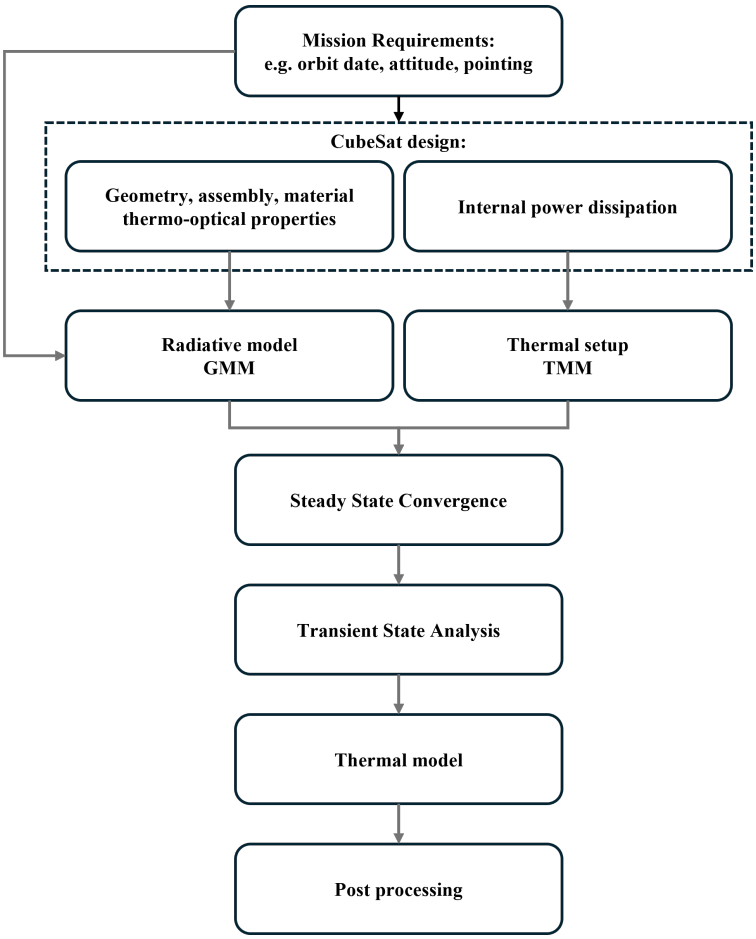

Figure 10.2: Simulation workflow

Preliminary thermal hand calculation is followed by higher fidelity modelling, done using thermal environment simulation software. The thermal simulations enable the modelling of individual component geometry, material properties and position within the satellite, hence modelling conductive and radiative heat transfer more accurately. Specifying satellite attitude ensures higher accuracy calculations of the heat loads defined in Table 10.1 [23]. The simulation is used to evaluate component temperature fluctuation in orbit. This is used to test thermal design against thermal requirements and evaluate thermal control

systems. In CubeSats, the chassis is the component with the highest geometric complexity. The chassis is the primary means for heat conduction [24]. Ensuring the chassis mesh resolution accurately captures contact area and heat transfer between components is crucial to producing accurate results. For 3U CubeSats, a node count between 200 and 600 is recommended [22]. Modelling the EPS unit plays a major role in evaluating the thermal performance of a satellite due to heat generated by batteries when charging and discharging. Most CubeSats use Lithium-ion batteries due to their lower weight and high energy storage capacity. As a result of its complex thermal behaviour, the EPS unit is often modelled using spatially averaged material properties [24].

10.2.3 Thermal Control Design

Due to the limited power budget on CubeSats, a passive control system is often preferred. Passive thermal controls can be categorised as follows,

- **Surface Coatings and Tapes**: Surface control methods are used to optimise the external heat flux absorbed and internal heat dissipated. Coatings like white paint can be effective in minimising incident heating, however, they can darken and degrade due to atomic bombardment in Low Earth Orbits. The change in thermo-optical properties are dependant on the mission duration. Adhesive tapes are cost effective and can be modified later in the assembly process [25].

- **Insulation**: MLI is commonly used in space missions to minimise heat transfer between internal and external components. It consists of multiple layers of low-emissivity material and a reflective outer layer. However, the limited space in CubeSats can result in the MLI being laterally compressed, reducing its effectiveness [21][26]. As a result, it is a less preferable thermal control feature in CubeSat missions.

- **Thermal Straps**: Thermal straps are used to form conductive links between components within a satellite. They can effectively conduct heat from internal components to radiators [21].

- **Radiators**: Deployable radiators are implemented in missions where the CubeSat has a high power density, resulting in large amounts of heat being generated by internal components. They consist of materials with low absorptivity and high emissivity, optimally dissipating heat [27].

- **Thermal Switches**: Thermal switches are used to control a conductive link passively. It consists of a normally open connection that closes when a connected component heats beyond a given threshold [28]. This is useful in optimally dissipating heat to radiators. However, they are spatially inefficient for most CubeSat applications.

10.3 Requirements

W4-THER-10 CubeSats shall withstand, as a minimum, a non-operational temperature range of -35°C to +80°C.

W4-THER-20 The thermal control provisions shall be able to maintain all units and parts within their non-operational and operational temperature ranges, as applicable.

W4-THER-30 Thermal vacuum bake-out shall be performed on the satellite to ensure outgassing of components prior to launch.

To meet requirements **W4-THER-10** and **W4-THER-20**, the operational and non-operational temperature ranges for internal components were determined based on manufacturer data sheets.

Component	Non-Operational (°C)		Operational (°C)	
	Min	Max	Min	Max
Antenna	-35	80	-35	80
EPS	-40	85	-40	70
OBDH	-40	125	-40	125
FDSPP	-40	85	-40	85
XCAM	-40	85	-30	65

Table 10.2: Component thermal requirements

10.4 Overview of 2023-24 Progress

The 2023-24 team completed phase B objectives and began defining the thermal model for phase C. In phase B, they established a single-node mathematical model for the satellite and developed it to determine hot and cold case temperatures. Passive thermal control options were explored and preliminary thermal simulations were developed.

10.4.1 Preliminary Calculations

The following steady state equation was used to create a single node heat transfer model,

$$\dot{q}_{stored} = \dot{q}_{IR} A_{IR} + (1 + a)\dot{q}_{solar} A_{solar} \hat{s}\alpha + \dot{q}_{internal} - A_{out}\sigma\varepsilon T^4 \tag{10.4}$$

where,

- $\dot{q}_{stored}$ refers to heat stored in the satellite.
- $\dot{q}_{IR}$ and $\dot{q}_{solar}$ refers to the heat energy absorbed by the satellite as a result of IR and solar radiation respectively.

- A_{IR} and A_{solar} refers to the surface area absorbing heat as a result of IR and solar radiation respectively.
- a refers to the albedo fraction of solar energy reflected back to the satellite.
- $\hat{s}$ refers to a 1/0 step multiplier based on whether the satellite is in eclipse or not.
- α refers to the absorptivity of satellite surface.
- ε refers to the emissivity of the satellite surface.
- σ refers to the Stefan-Boltzmann constant.
- T refers to the satellite temperature.

The following transient temperature equation was used to estimate hot and cold case temperatures,

$$T_{i+1} = T_i + \dot{q}_{stored,i}\frac{\Delta t}{c_p m} \tag{10.5}$$

where,

1. T_i refers to satellite temperature at time, i.
2. $\dot{q}_{stored,i}$ refers to energy stored in the satellite at time, i.
3. Δt refers to the time step.
4. c_p refers to the spatially averaged specific heat capacity of the satellite.

The above equations were modelled in MATLAB to measure satellite temperature for both the hot and cold cases.

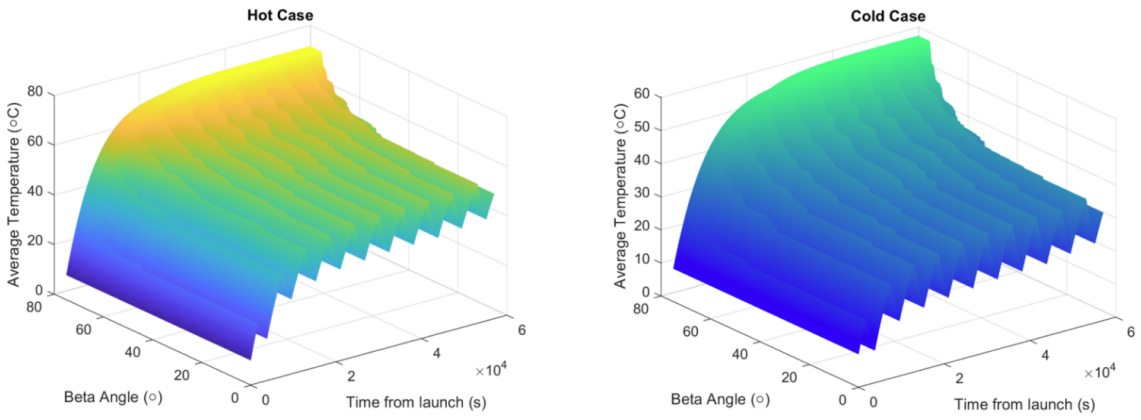

Figure 10.3: Average temperatures across 10 orbits.

The hot case estimates satellite temperature in the worst-case scenario during the year with the highest solar irradiance. The cold case estimates satellite temperature in the worst-case scenario where the satellite faces minimal sunlight. Figure 10.3 indicates that

the satellite may not meet the operational and non-operational temperature range requirement. While minimum temperatures in the cold case meet the temperature requirements for all components, a maximum temperature of $70°C$ in the hot case would exceed the operational temperature range of XCAM. This indicates a need for thermal control to dissipate heat.

10.4.2 Preliminary Thermal Control

The team explored various surface coating options. It was determined that using clear or black anodised aluminium for the chassis would minimise temperature fluctuation within the satellite. The team considered the use of copper foil tape for insulation and thermal straps to reduce temperature fluctuation.

10.5 Thermal Simulation Set Up

To assess the satellite's thermal performance against the stated requirements, the satellite mission was modelled using ESATAN-TMS. This section discusses the CubeSat assembly model, material selection, radiative case and thermal boundary conditions.

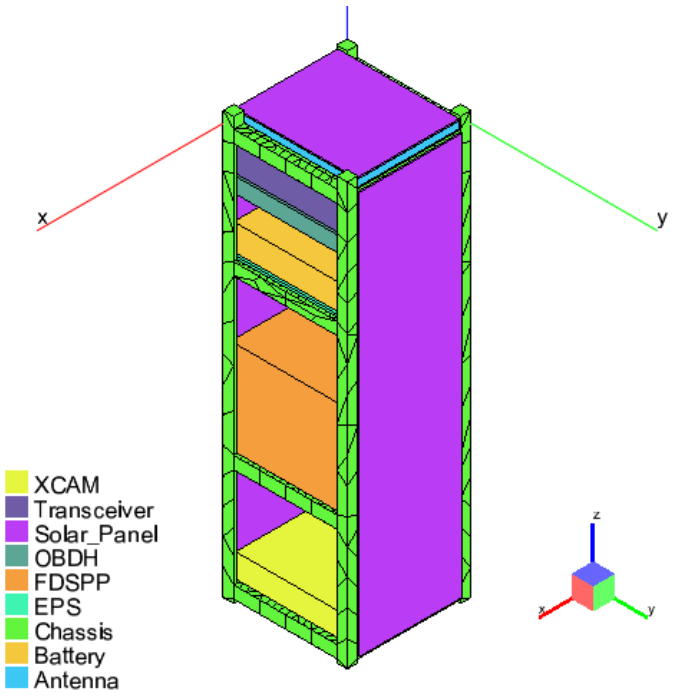

Figure 10.4: Model Geometry

10.5.1 Geometry and Materials Definition

To ensure efficient computation, the satellite structure was simplified. This involved only including geometry that impacts conductance while retaining key thermal characteristics [22]. The assembly model is shown in Figure 10.4. Materials used to model internal components is shown in Table 10.3.

Component	Bulk Material	Density ($kg\,m^{-3}$)	Specific Heat ($J\,kg^{-1}K^{-1}$)	Conductivity ($W\,m^{-1}K^{-1}$)	Surface	Emissivity	Absorptivity
Chassis	Al 6082	2700	900	200	Al 6082	0.21	0.18
Solar Panels	FR4[29]	1900	1100	0.4	Solar Photovoltaic	0.92	0.91
Antenna	Al 6082	2700	900	200	Al 6082	0.21	0.18
Transceiver	Al 6082	2700	900	200	Al 6082	0.21	0.18
OBDH Board	FR4[29]	1900	1100	0.4	Green Coat	0.89	0.65
EPS Board	FR4[29]	1900	1100	0.4	Green Coat[29]	0.89	0.65
Battery	Li-ion[24]	2448.5	454.89	200	Al 6082	0.21	0.18
FDSPP	FR4[29]	1900	1100	0.4	Al 6082	0.21	0.18
XCAM	FR4[29]	1900	1100	0.4	Al 6082	0.21	0.18

Table 10.3: Material bulk definition and thermo-optical properties.

The chassis geometry includes the external rails and cross-members without fixtures and small internal joints. The internal components were modelled based on the respective external dimensions to model cross-component conductance. The payloads, battery and antenna were modelled to be within an aluminium casing to simulate the impact of passive thermal control features like coatings and paints. The PCBs were modelled to be made of the standard FR4 substrate and a green coating, as per manufacturer description.

Component positions were estimated to distribute mass such that the centre of mass is positioned near the geometric centre of the satellite. Lumped parameterisation was used to model the satellite due to the minimal geometric detail. As the team progresses with subsystem designs, more detail can be incorporated into the simulation model, and FEM techniques could be used to produce fine mesh, high accuracy results.

10.5.2 Radiative Case Set Up

To determine external heat loads acting on the satellite in orbit, a radiative case must be defined in ESATAN-TMS. In our mission, the external heat loads result from solar radiation, albedo and earth infrared radiation. The planetary parameters are documented in table 10.4.

Planet	Earth	Sun
Radius (km)	6371	6.958×10^5
Gravitational Acceleration ($(\mathrm{m\,s^{-2}}$)	9.798	N/A
Albedo	0.306	N/A
Temperature (K)	254.3	5778
Infrared Emissivity	1	N/A
Solar Constant Override ($\mathrm{W\,m^{-2}}$)	N/A	0

Table 10.4: Radiative case planet definition

The orbital parameters are in table 10.5[30];

Parameter	Value
Eccentricity	0.00021
Semi-Major Axis (m)	6829450
Altitude at Apogee (m)	408000
Inclination (°)	51.64
Right Ascension (°)	336.826
Argument of Periapsis	2.4591
Zenith Pointing	+X axis (refer Figure 10.4)
Normal To Orbit Pointing	+Y axis (refer Figure 10.4)

Table 10.5: Orbital parameters

Due to minimal attitude control, the satellite was assumed to be oriented such that the positive X-axis solar panels are always facing perpendicularly away from Earth. This was determined to be a safe estimate for initial simulations; however, simulating varying satellite orientations would ensure the internal component temperatures meet requirements in all scenarios.

The radiative case in Figure 10.5 illustrates external heat load in the form of heat flux ($\mathrm{W\,m^{-2}}$). The yellow arrow indicates the position of the sun. A total of 15 orbital positions were calculated to determine radiative heat flux.

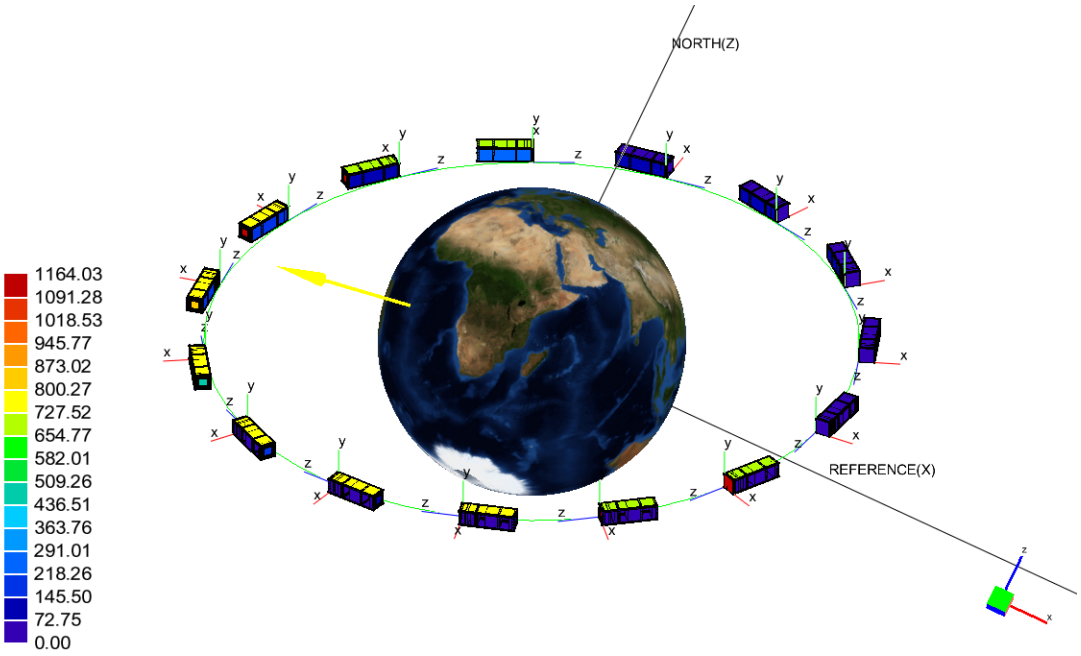

Figure 10.5: Heat flux due to external heat load.

10.5.3 Boundary Conditions and Internal Heat Loads

Calculating internal and external heat loads determines the boundary conditions required to simulate thermal performance. The external heat loads were measured by the radiative case in section 10.5.2. The internal heat load is a result of heat dissipated by subsystem components. A majority of heat produced by internal components is a result of ohmic power dissipation. This was estimated by the following equation,

$$P_{heat} = I^2 R_{effective} \tag{10.6}$$

where I is current draw and $R_{effective}$ is effective resistance. For components where effective resistance could not be determined, an approximate 15% power dissipation was assumed. This value shall be revised as component designs are iterated. Table 10.6 displays component operational heat loads.

Component	Total Volume Heat Load (W)
Antenna	0.5
Transceiver	0.4
EPS	0.036
Battery	3.2
FDSPP	1.624
OBDH	0.16
XCAM	1

Table 10.6: Internal heat load

The solution setup combines steady-state and transient-state solutions. 100 iterations of steady-state analyses are run till convergence is observed. This is followed by transient analysis at varying orbit positions.

10.6 Thermal Simulation Results

For each analysis case, two simulations were run. The first simulation is run with no internal heat loads; hence, non-operational temperatures are evaluated. The second simulation includes heat loads among other boundary conditions to assess operational temperatures. On completion of the thermal analysis case, component data was extracted in csv format and plotted in MATLAB.

10.6.1 Base Analysis

The base simulation was used to evaluate thermal performance in the absence of thermal control systems. The resultant transient temperatures are plotted in Figures 10.6 and 10.7. The antenna and XCAM board were positioned furthest away from the satellite centre of mass and had the largest contact area with external components like the solar panels and chassis. As a result, they had the highest temperature peaks and fluctuation, as shown in table 10.7. On the other hand, the payload was positioned furthest away from the Z-axis solar panels, and as a result, had the lowest temperature peak and was the least reactive to changes in external temperatures. Additionally, unlike components nearer to COM that observe a dip in temperature around the eclipse (t$\sim$3000), components located at the Z-axis extremities (antenna, XCAM) observe a shift in temperature dip due to facing normally away from the sun at different points of the orbit.
The EPS board displayed a significant increase in transient temperature when operational due to its conductive link to the battery. Despite this, all internal components meet operational and non-operational thermal requirements by being well within the survival ranges.

Component	Non-Operational (°C)		Operational (°C)	
	Min	Max	Min	Max
Antenna	28.3	25.1	71.0	74.3
EPS	9.6	13.8	61.8	66.0
OBDH	12.2	13.8	55.9	57.6
FDSPP	12.1	12.6	54.4	54.9
XCAM	15.9	17.2	65.2	66.6

Table 10.7: Base Simulation Results

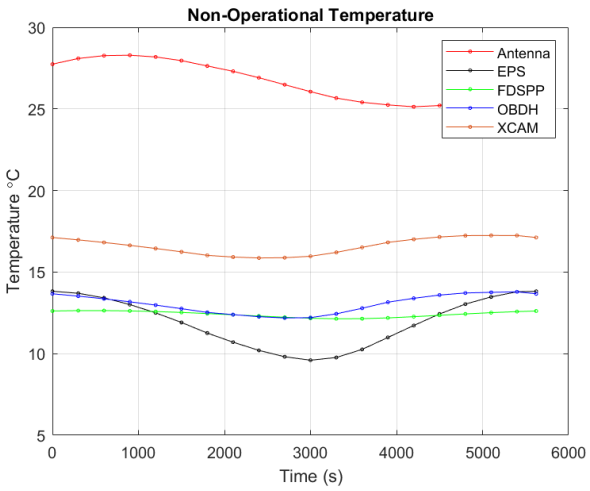

Figure 10.6: Component non-operational temperatures.

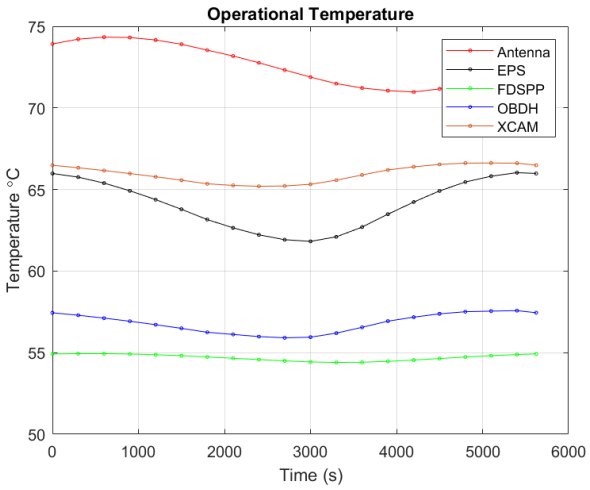

Figure 10.7: Component operational temperatures

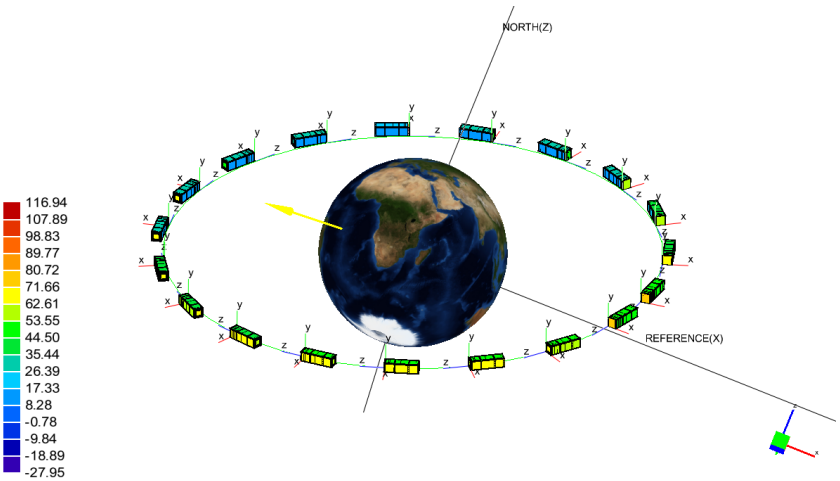

Figure 10.8: Thermal analysis temperature range

10.6.2 Simulation Validation

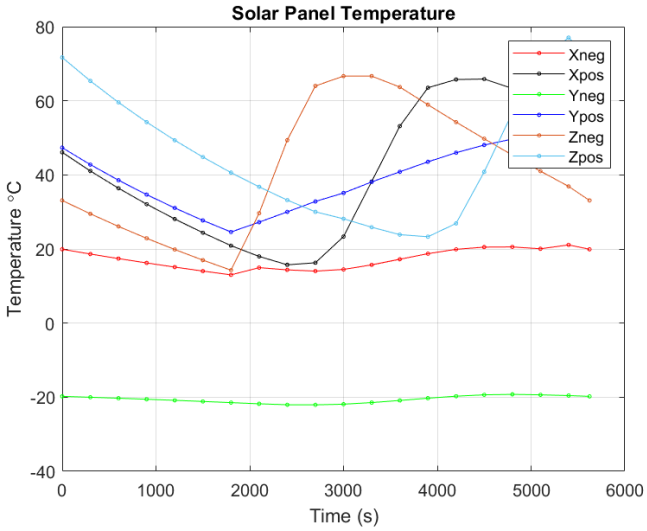

Figure 10.9: Solar panel transient temperatures

Simulation validation is crucial to ensuring the thermal model is an accurate representation of the satellite. The computational thermal model must be validated against the results derived from the mathematical model described in sections 10.2.1 and 10.4.1. Since the mathematical models assumed a single-node satellite, the external components could be used to achieve the closest correlation between models. Hence, to validate the computational model, the solar panel temperatures were compared. The mathematical model estimated the satellite to have a hot case maximum temperature of about 70°C and a cold case minimum temperature of about 10°C. As shown in Figure 10.9, the solar panels have a max temperature of 77°C, which is closely validated by the mathematical model. On the other hand, the solar panel in the negative Y direction appears to reach a much lower minimum temperature of -22°C. This, however, is expected, as the simulated surface is faced away from the solar vector at all points of the orbit. The minimum temperature among the other solar panels is 13°C, which is closely validated by the cold case calculations.

10.6.3 Passive Control – Black Surface Coating

Component	Non-Operational (°C)		Operational (°C)	
	Min	Max	Min	Max
Antenna	7.32	8.77	79.6	81.0
EPS	8.58	13.2	65.8	70.6
OBDH	10.6	12.3	58.4	60.1
FDSPP	11.6	12.1	54.1	54.7
XCAM	15.0	16.5	63.6	65.2

Table 10.8: Black Coating Simulation Results

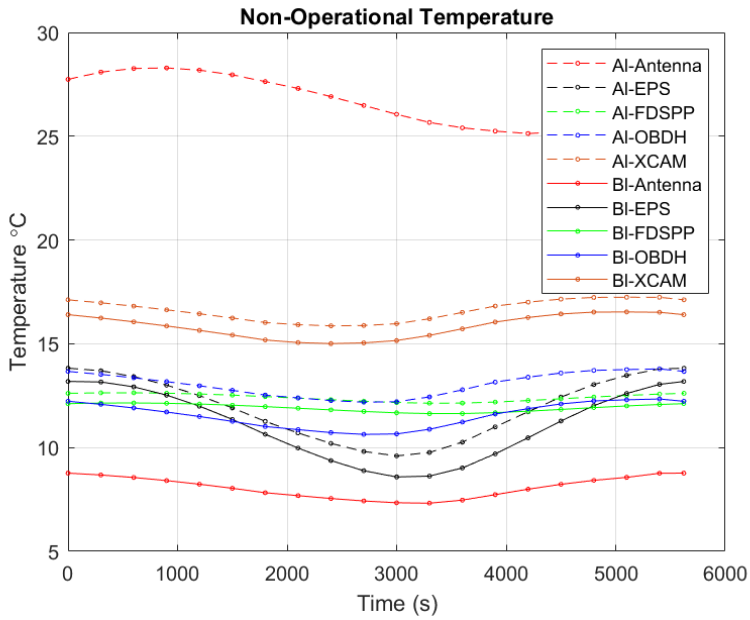

Figure 10.10: Component non-operational temperatures with black coating

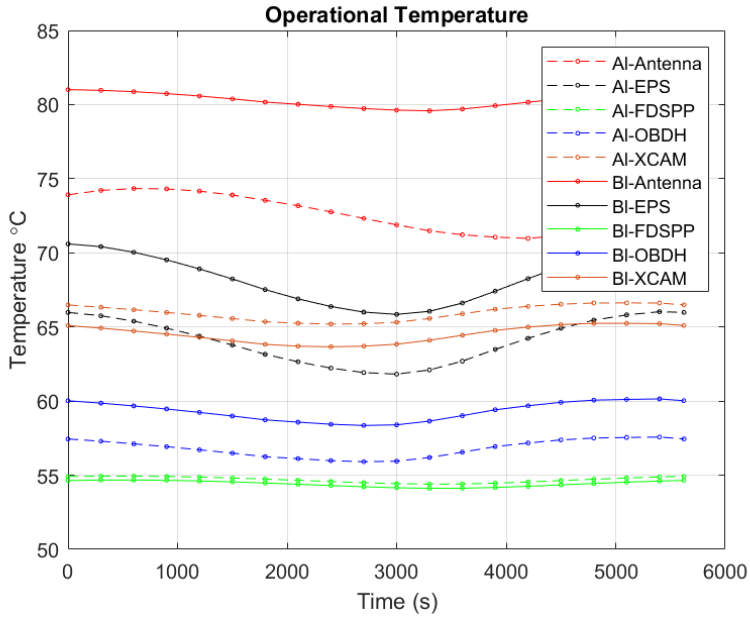

Figure 10.11: Component operational temperatures with black coating

As concluded from the simulation results presented in section 10.6.1, the internal component temperatures are maintained within the range defined in section 10.3. However, the antenna and XCAM transient temperatures are closer to the upper end of the operational limit, therefore establishing the need for thermal control. As mentioned in section 10.2.3, CubeSats are limited in their power budget due to the limited surface area for solar panels. To minimise power consumed by the thermal control system, the team aims to use passive control measures to reduce peak temperatures.

A thermal analysis case was run to evaluate the thermal performance of the satellite with the chassis coated in black paint. Black paint was defined to have an emissivity of 0.86 and an absorptivity of 0.8 [22]. With a high emissivity value, the coating was hypothesised to increase heat dissipated through radiative transfer, reducing antenna and XCAM temperatures, as observed from the non-operational temperatures plotted in Figure 10.10. However, the coating had high absorptivity, resulting in increased heat absorbed by surfaces facing the sun. This is reflected in the operational results documented in Table 10.8 and 10.11. The antenna peak temperature significantly increased, while XCAM saw a slight decrease in peak temperature. This discrepancy is caused by satellite attitude while in orbit, indicating that attitude control would play a crucial role in minimising the peak temperature of the satellite.

10.6.4 Passive Control – White Surface Coating

Component	Non-Operational (°C)		Operational (°C)	
	Min	Max	Min	Max
Antenna	-4.92	-3.17	73.0	74.5
EPS	4.50	8.25	63.6	67.5
OBDH	5.92	7.49	55.3	57.0
FDSPP	8.43	8.90	52.0	52.5
XCAM	10.5	11.8	60.8	62.2

Table 10.9: White Coating Simulation Results

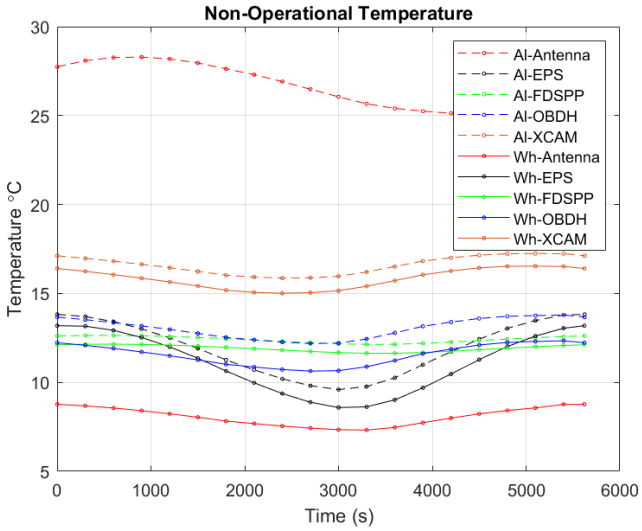

Figure 10.12: Component non-operational temperatures with white coating

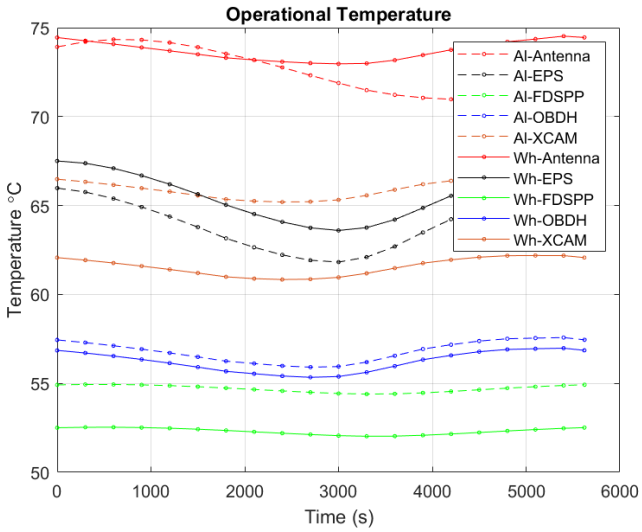

Figure 10.13: Component operational temperatures with white coating

A thermal analysis case was run to evaluate the thermal performance of the satellite with the chassis coated in white paint. White paint was defined to have an emissivity of 0.89 and absorptivity of 0.26[22]. The white paint has emissivity similar to the black paint, resulting in similar non-operational temperatures, as can be observed in Figure 10.12. This coat has an absorptivity significantly lower than the black coat. This reduces heat absorbed by surfaces facing the sun, in turn greatly reducing operational temperatures, as observed in Figure 10.13. However, unlike black coatings, white coatings degrade due to atomic oxygen bombardment.

10.6.5 Passive Control - Silver FEP Tape

Silver FEP tapes are commonly used as second surface mirrors in CubeSats minimise absorption of external heat load [23]. Silver FEP tapes have low absorptance between 0.06 and 0.09, minimising solar flux absorbed into the chassis. A tape of 1 mm thickness exhibits an emissivity of 0.52, lower than black coatings [31]. Therefore, to optimise the external thermal radiative properties of the chassis, the silver tape was placed on the outer chassis surface, and the inner surfaces were coated black. As shown in Figure 10.14, this increases the internal heat absorbed and radiated outward.

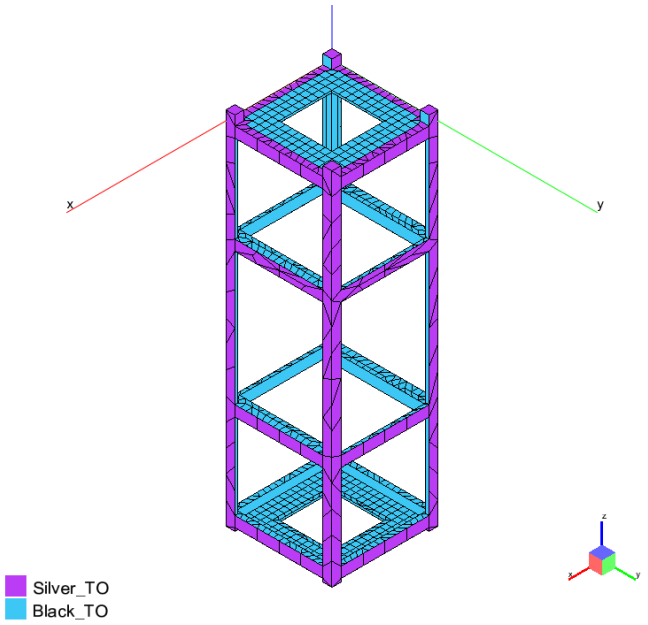

Figure 10.14: Chassis surface thermal control

Component	Non-Operational (°C)		Operational (°C)	
	Min	Max	Min	Max
Antenna	-3.25	-1.54	75.9	77.4
EPS	4.63	8.21	64.3	68.0
OBDH	6.17	7.71	56.3	57.9
FDSPP	8.47	8.92	52.3	52.8
XCAM	10.9	12.2	61.5	62.8

Table 10.10: Silver FEP Tape and Black Coating Simulation Results

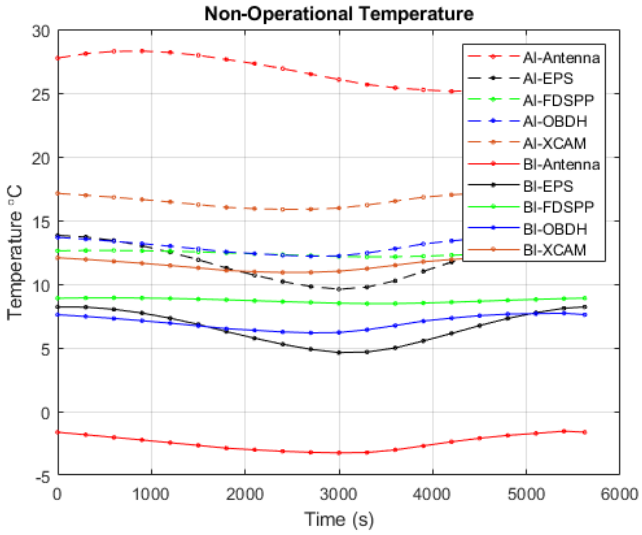

Figure 10.15: Component non-operational temperatures with FEP tape and black coating

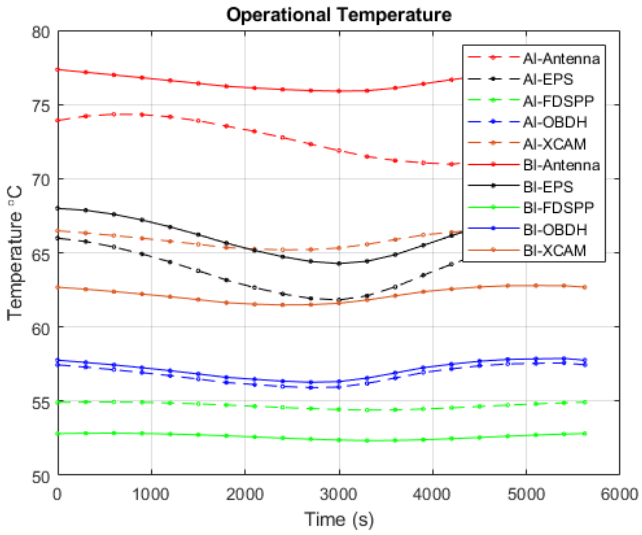

Figure 10.16: Component operational temperatures with FEP tape and black coating

Figure 10.15 indicates that using silver FEP tape significantly reduced the external radiative flux absorbed in the satellite. Additionally, internal temperatures are more stable throughout the orbit as the difference between maximum and minimum EPS temperature peak is reduced. Figure 10.16 indicates that the use of silver tape saw a reduction in operational temperature peak as compared to black coating, due to its reduced solar absorptivity. However, this reduction was relatively small as the FEP tape has an emissivity higher than the black and white coatings.

10.7 Conclusion

Following the computational thermal analyses, it is determined that the subsystem components are maintained at their operational and non-operational temperature requirements. It was observed that antenna and XCAM temperatures peaked at high temperatures nearing the operational limits. Thermal surface coatings were analysed and compared to minimise temperature peaks for components at the Z-axis extremities. Black, white and silver coatings observed a reduction in non-operational temperatures, with the silver FEP tape resulting in the lowest temperature peaks. The use of white coating resulted in the lowest operational temperature peaks due to its low absorptivity and high emissivity. However, white coatings tend to degrade due to atomic oxygen bombardment and can be costly to make stable [21]. Alternatively, the combined use of silver tape and black coating was feasible to manufacture and resulted in internal temperatures well within operational limits.

10.7.1 Phase C Progression

Phase C of thermal analysis and control involves developing the thermal model and defining a final thermal control system design. This involves developing higher fidelity simulations that capture the complete internal configuration of the satellite and more accurately

calculate contact surfaces between internal components. This may include modelling screw fixtures, adhesives and detailed payload geometry. The thermal model can then be used to design and evaluate thermal control systems and determine the final thermal design. Phase D would begin with defining the thermal balance test to verify the thermal design against requirements.

10.7.2 Open Points

As the team develops the subsystem designs, more detail can be incorporated in the simulations to achieve better accuracy. There are several ways to build upon the current thermal model, as follows,

- The current simulation tests two modes, operational and non-operational. The boundary conditions could be adjusted to test thermal performance at each mission mode to ensure internal temperatures are maintained within the thermal requirement limits.
- The screws and fixtures used to assemble the satellite could be modelled to improve the accuracy of measured conductive heat transfer between components.
- The above simulations test for the effectiveness of surface coatings on the satellite chassis. Other methods of passive control to reduce antenna and XCAM temperatures could be examined through thermal modelling. These include thermal straps, insulation, and thermal tapes.
- The simulations measure one form of satellite attitude control, with the X-negative face oriented towards earth at all times. A small angular rotation speed could be implemented to simulate the satellite without attitude control.
- The payload could be modelled with greater geometric detail to achieve accuracy in transient temperature readings.
- Power dissipation was calculated for most components within the satellite. However, a 15% power dissipation was estimated for a few of the components due to changes in design. As each subsystem approaches final designs, establishing a power dissipation budget would be beneficial to document and assess the internal heat load at each power mode.

11 Electronic Power System

11.1 Introduction

The electronic power system (EPS) is a core subsystem that will underpin the functioning of all other subsystems. For the entire operating lifetime of WUSAT-4, a consistent power supply is required for all modes of operation. The CubeSat's design topology includes neither ADCS nor deployable solar panels. Such restrictions require that all faces of the satellite be covered with solar panels to maximize power generation. However, some additional considerations have been identified that may prevent the Z panel from being mounted. The aim is, after accounting for all constraints, the CubeSat battery level on board maintains a net positive charge trajectory over time, ensuring that it does not fall below the defined critical threshold under nominal operating conditions.

11.2 Requirements

W4-EPS-10 The electronic power system unit shall be able to continuously power all on-board systems via the power from the solar panel array and the battery.

W4-EPS-20 Solar power generation must be optimized by installing a Maximum Power Point Tracking Unit (MPPT).

W4-EPS-30 The output from the solar panels shall be conditioned, regulated, and stepped down to meet the power specifications of all components and subsystems.

- **W4-EPS-31** Output power from the PV array shall be stepped down to ensure the voltage operates within the functional input range of the MPPT.

W4-EPS-40 The battery's state of charge, output voltage and current, and its temperature must be monitored and accessible to the on-board data handling system.

W4-EPS-50 Comprehensive simulation and test results shall be conducted before component procurement.

- **W4-EPS-51** PV array output power shall be simulated for varying load cases.
- **W4-EPS-52** The State-of-Charge (SoC) of the onboard battery must be evaluated under all operational modes and sunlight conditions to verify its ability to sustain mission requirements.

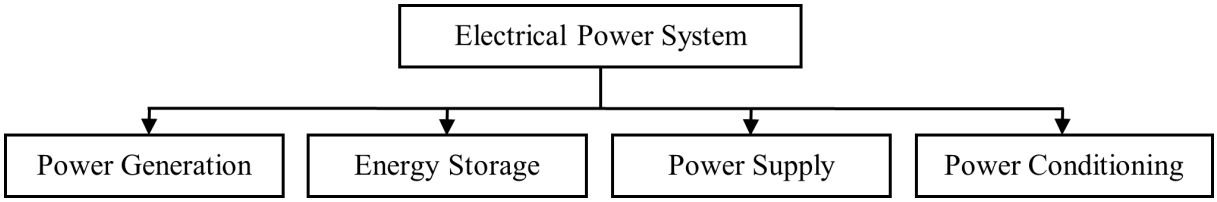

Figure 11.1: EPS Requirements Summary

W4-EPS-60 Power delivery must be dynamically managed based on the operational needs of each mission phase, meeting the idle, nominal and peak loads.

W4-EPS-70 The system should include control capabilities for EPS performance and health, i.e., via ground station or on-board control.

W4-EPS-80 The circuitry should be designed to include sufficient redundancies to mitigate the risk of single-point failures in the power system.

11.3 Review of 2023-24 EPS Progress

The 2023/24 team made significant strides in the solar panel configuration, outlined the subsystem and operational-phase power budgets, and identified potential integration issues of the EPS with other subsystems. After finalizing the CubeSat structure as 3U, the team also decided to implement two parallel branch structure to wire the solar arrays. The chosen configuration maximizes power output while still offering redundancy advantages. Further power analysis studies and simulations can now be conducted on the panels to determine the power capacity over varying operating conditions and on-board requirements.

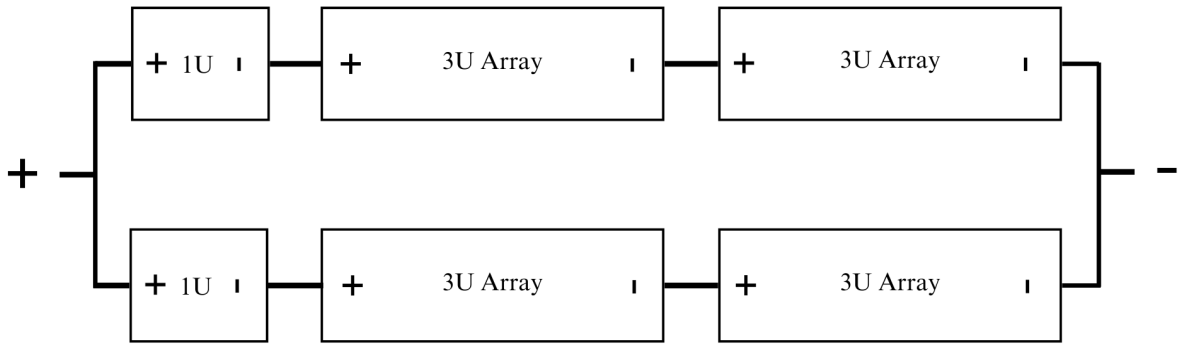

Figure 11.2: Solar Panel Configuration for WUSAT-4

The subsystem-wise power budget provided fundamental insights, comprising of average and maximum power requirements. These can now be translated into idle, nominal, and peak operational modes that would represent a more realistic implementation of individual subsystems. Furthermore, a cold and hot case analysis was conducted for power consumption, this needs to be extended to the entire temperature range of LEO, and similar tests need to be carried out for the LEO irradiance range as well. With these parameters, the on-board battery levels need to be modelled for the varying operational modes' power requirements.

The mounting challenges between the transceiver and solar panels were also identified. The proposed solutions will be evaluated in alignment with this year's new design developments. Additionally, the solar panel output voltage levels were found to exceed the functional range of the MPPT system. Thus, further work with voltage conditioning will

be required to address this issue and ensure compatibility.

The current team has also explored the integration of an onboard camera, which would impact certain previously conducted simulations. As a result, these tests and simulations will need to be reconducted if the camera is added as a payload. Cabling, routing and connector-type choices will also be impacted if such design changes are undertaken.

11.4 Analysis

The simplified CONOPS summary is presented in figure 5.1. This will serve as a reference for the requirements analysis.

11.4.1 W4-EPS-10: Continuous Power Supply

To ensure the CubeSat can supply power to all onboard systems, the solar panel subsystem must be capable of generating sufficient energy under nominal sunlight condition. Additionally, the total energy used during eclipse and transmission phases must be less than the power generated in sunlight modes like nominal and safe mode [32]. This will allow the CubeSat to maintain a net positive battery percentage for every orbit. For this, the power budgets for each operational phase will be comprehensively evaluated.

Additionally, passive de-tumbling of the CubeSat is a significant requirement to optimize the output power because the sunlight exposure would be very limited if the satellite has an uncontrolled orientation [33]. Magnetorquers facilitate passive de-tumbling for the CubeSat. They will require power during initial stages of operation to slow down the CubeSat (See section 7.2) [33].

The battery subsystem must provide sufficient capacity and discharge capability to meet peak power demands during eclipse phases or high-power operations, such as the downlink mode and payload data-collection during the nominal mode. Additionally, the robust power distribution system must ensure efficient and loss-minimised delivery of power to subsystems.

11.4.2 W4-EPS-20: Maximum Power Point Tracking

To optimise solar power generation, a Maximum Power Point Tracking (MPPT) unit will be incorporated. The choice of the Power Conditioning and Distribution Unit (PCDU) is the ISIS iEPS-A, which incorporates an on-board, hardware based MPPT [34]. This unit dynamically adjusts its input to operate the solar panels at their maximum power point across varying illumination conditions caused by orbital eclipses and CubeSat attitude changes [34].

It should be noted that the MPPT system must be compatible with the solar panel voltage and current ranges and should provide real-time telemetry data, such as voltage, current, and power, to aid in monitoring and optimization. The ISIS iEPS-A PCDU provides telemetry data, however, it has a limited functional input MPPT range (3.5V – 7V) [34]. This will need to be taken into account and corrected.

To prepare for a critical battery level, the EPS will integrate with the OBDH to prioritize core subsystems while shutting down or reducing power consumption of other systems. This is the survival shown in the CONOPS reference diagram.

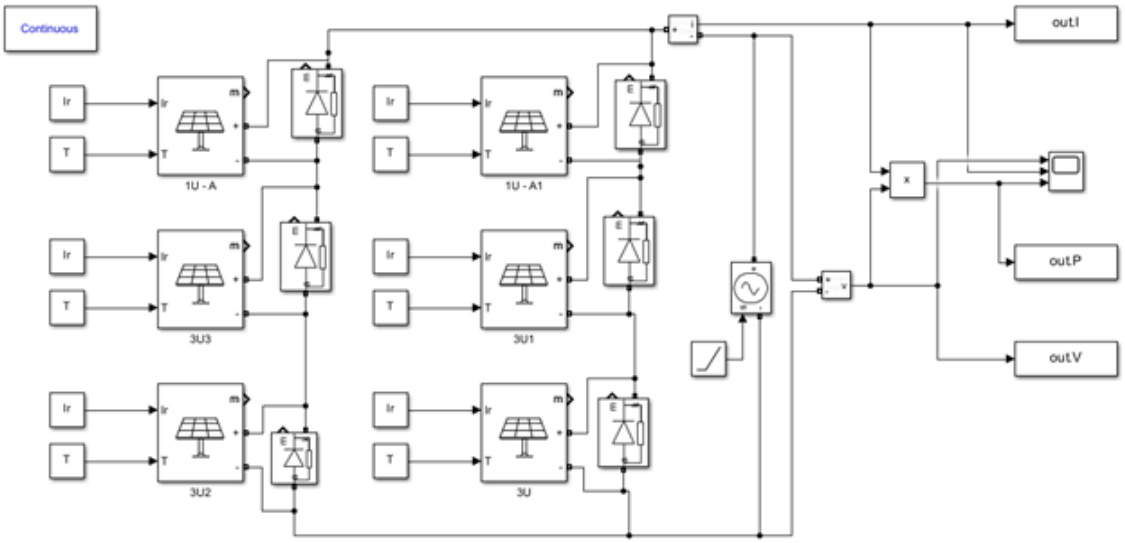

Figure 11.3: Simulink model of the PV array configuration

The Simulink model highlights the 6 PV array blocks used – one panel for each face of the CubeSat. These include two 1U and four 3U panels with a blocking diode in parallel to each panel. A ramped-input voltage source is used to simulate the varying load across panels. These are, however, idealistic conditions at a constant irradiance of 1000W/m^2 and a constant temperature 25℃. Moreover, ambient lighting is assumed, i.e., lighting from all sides, which is also impractical in LEO. These simulations only allow us the find the Maximum Power Point (MPP) for the chosen panel configuration.

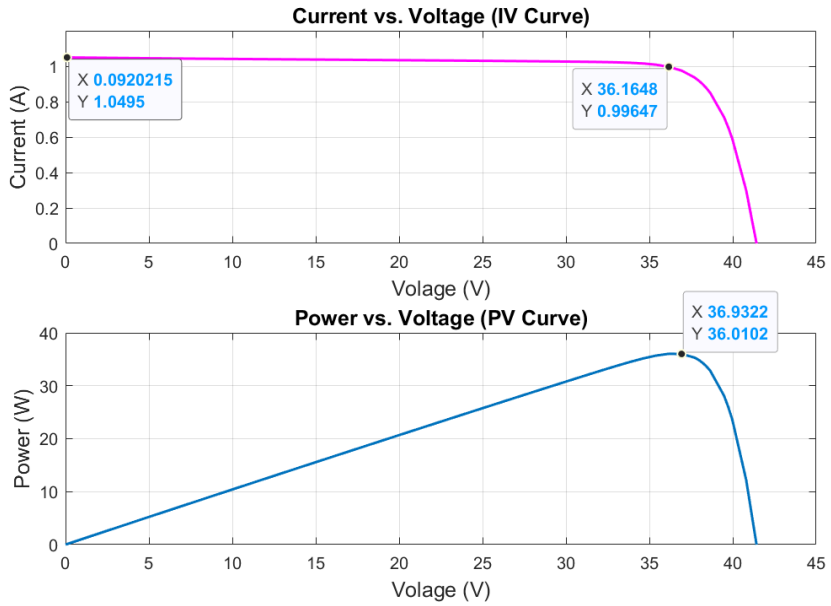

Figure 11.4: IV and PV Curves for Solar Panel Configuration

The short-circuit current is 1.04A, and the open-circuit current is near 41.5V. The MPP is found at 36.2V and 0.99A, 36W. These highlight the maximum achievable voltage, current, and power figures at BOL from the panel configuration. The purpose of this study was to determine the absolute extremes of the power figures that can be used as a point of reference while designing the EPS.

The foremost observation from this analysis is that the voltage exceeds the functional MPPT input range, therefore, requiring a DC-DC step-down. This will be further scrutinized in the Analysis section of EPS. Secondly, the power losses from the bypass and protection diodes, power conversions, conduction losses, and the overall system degradation (BOL to EOL) need to be accounted for in the power calculations.

11.4.3 W4-EPS-30: Power Conditioning and Regulation

The power output from the solar panels must be properly conditioned and regulated to match the operating requirements of the CubeSat's components and subsystems. This involves stepping down the solar panel output through voltage regulation units, i.e. a buck converter, to provide stable voltage levels for power buses (e.g., 3.3V, 5V). No subsystem requires more than a 5V input except for the thermal management unit of the FDSPP payload (See Appendix H). This requires a 12V and 27V input which will require a step-up (See Appendix H).

The system must also adhere to the specific tolerances required by the payload, OBDH, and communications systems.

11.4.4 W4-EPS-40: Battery and Solar Panel Monitoring

The PCDU includes monitoring capabilities to continuously monitor the state of charge (SoC) and temperature. These parameters would prevent overcharging, deep discharging, or overheating. Moreover, the DHV solar panels have a temperature sensor and a photodiode for irradiance measurement [35]. These sensors shall provide real-time measurements to OBDH system that will compare them to reference values to implement safety precautions for either subsystem if required. This can be seen in figure 11.5.

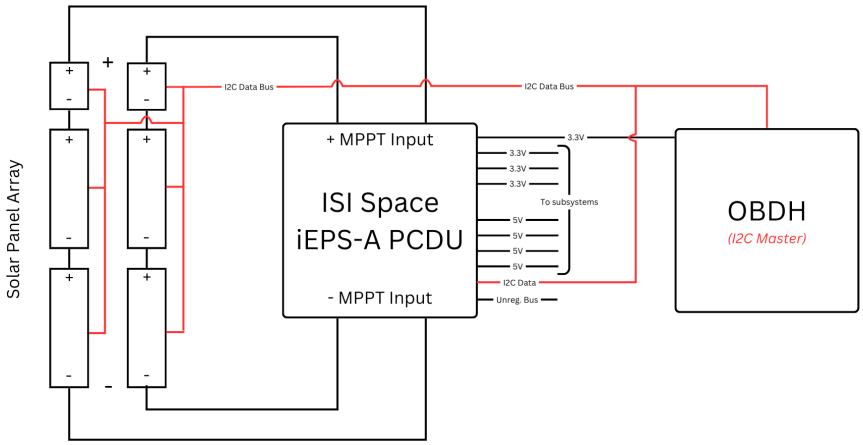

Figure 11.5: Interfacing of the solar panel array, the PCDU and the OBDH

The purpose of such integration is to extract relevant sensor data from the PCDU and solar panels that will guide the CubeSat's operational mode. For each mode, the OBDH system will alter the power consumed by individual components depending on the power requirements of the respective mode. This data will also be transmitted to the ground stations to serve as a guide for manual decision making.

11.4.5 W4-EPS-50: Simulations and Procurement

Before procuring components for the WUSAT project, comprehensive simulation and test results must be conducted to ensure system reliability and performance. Specifically, the power output of the PV array shall be simulated across varying temperature and irradiance conditions to assess its efficiency and stability (**W4-EPS-51**). The graphs below highlight the increase in current and power curves from the solar panels as the irradiance levels rise from 600 (Black) to 1000 (Blue) to 1400 (Red) W/m2. Assumptions for these plots include ambient lighting, and all sides of the CubeSat covered with panels.

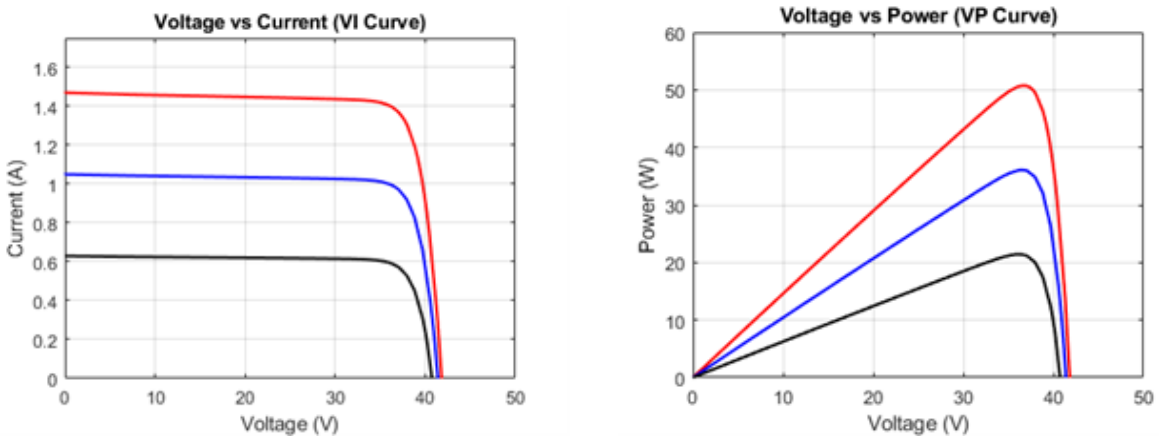

(a) IV Curve **(b)** PV Curve

Figure 11.6: PV & IV Curves variations for different irradiance levels

This relationship can be better visualized with a three-dimensional view of this relationship.

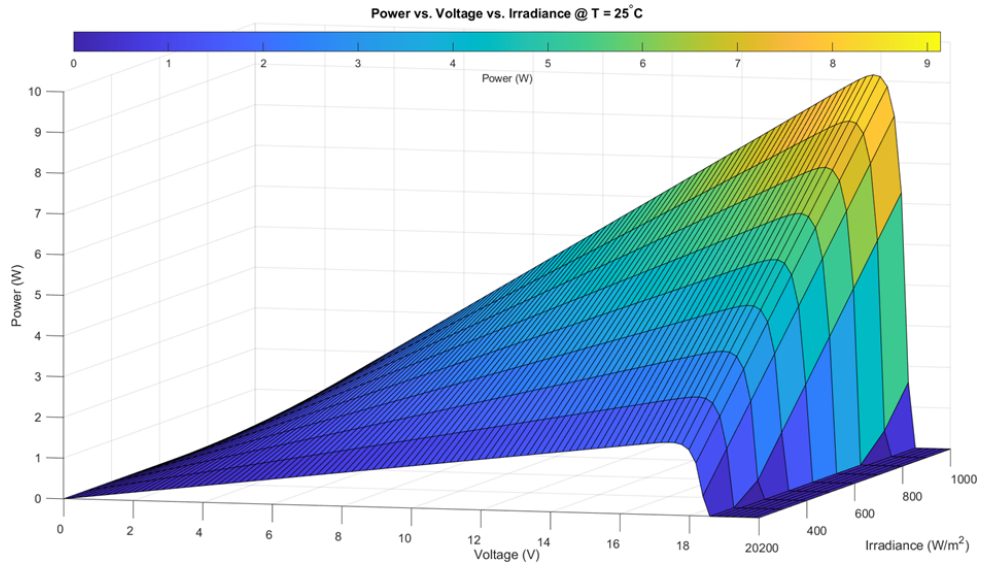

Figure 11.7: Surface plot of a 3U solar panel's output power across varying voltage and irradiance levels at 25°C

The surface plot visualizes the power output against voltage and irradiance at a constant 25°C for a single 3U panel with standard 3U DHV specifications. The impact of irradiance on power output is positively linear, directly impacting the MPP, and therefore, the power output. Considering an average of 1360 W/m^2 of irradiance at LEO, which is outside the range of the surface plot, would produce more than 9W at its MPP. It is also observed that the voltage level at the MPP remains relatively constant, while the power output increases with irradiance. This is ideal because the MPPT system, which employs the Perturb and Observe (P&O) algorithm, adjusts the applied load voltage to maximise extracted power. The P&O algorithm constantly changes the voltage and observes the corresponding power change to track the MPP [36]. The voltage level at which

MPP occurs remains largely unaffected by changes in irradiance; thus, the MPPT system does not experience significant power loss while recalibrating at different irradiance levels.

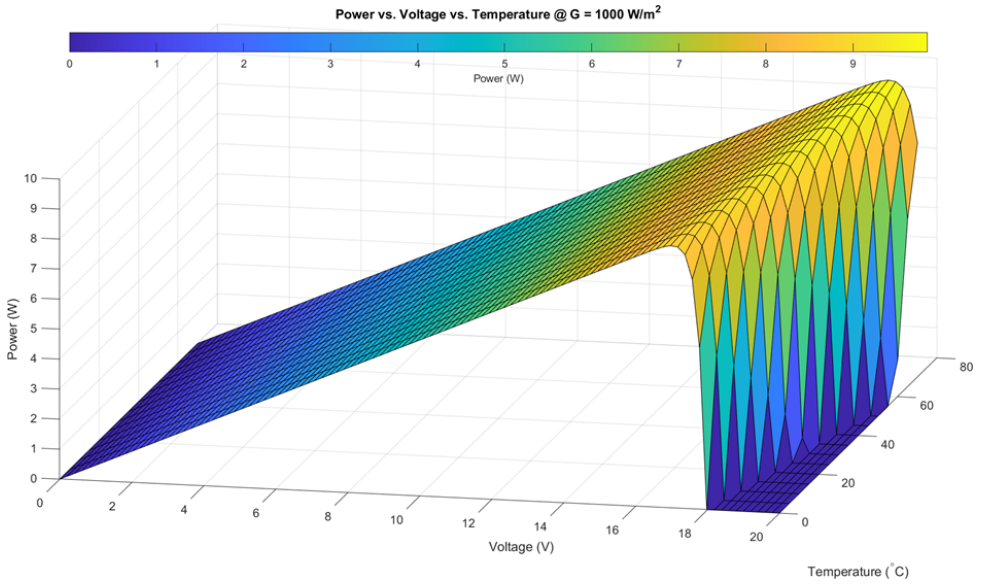

Figure 11.8: Surface plot of a 3U solar sanel's output power across varying voltage and temperature levels at 1000W/m^2

The impact of temperature on the MPP is relatively less than the irradiance, however it does affect the voltage point at the MPP. This translates to energy losses when the temperature changes as the MPPT system would readjust its operating point to the MPP. Additionally, the State-of-Charge (SoC) of the onboard battery must be evaluated under all operational modes and sunlight conditions to verify its ability to sustain mission requirements (**W4-EPS-52**). To do this, the power budgets must be studied.

Table 11.1 shows the duration ratios spent in each operational mode. These are assumptions for a typical orbit.

CONOPS	
Phase	**Ratio per orbit (Avg.)**
Nominal	0.611222222
Downlink	0.044444444
Eclipse	0.333333333
Safe	0.01
Survival	0.001
Total	1

Table 11.1: Operational Phases and Their Ratio per Orbit

To convert this into an operational-mode power budget, the power generated and consumed for each mode is needed. Table 11.2 highlights the required parameters for this.

Power Generation	
Parameter	**Value**
Avg. No. of Illuuminated Solar Cells	9
Incident power per solar cell (W)	3.429
Average solar cell efficiency	30%
Power Generation per Solar cell (W)	1.0287
Solar Incidence Time per Orbit (hrs)	1
Safety Margin	20%
Power Generation per Orbit	7.40664

Table 11.2: Power Generation Parameters

The parameter *'Avg. No. of Illuminated Solar Cells'* is a control parameter that can be varied to determine the power generated during different operational modes.

Orientation-Scenarios

The three possible CubeSat orientation scenarios, nadir-pointing, sun-pointing, and free orientation, are highlighted by the figures below. Nadir-pointing is an orientation scenario where the satellite is locked to allow the satellite to constantly view the Earth [37]. This requires precise orientation control, and since magnetorquers are passive de-tumbling devices, this scenario is highly unlikely. Sun-pointing produces the most power, however, this also requires active control measures to direct the satellite towards the sun, making this scenario also improbable [37]. Free orientation is the most probable with a passive detumbling system. Each of these scenarios can be used to estimate how many solar panels would be illuminated through an orbit [37]. It should be noted that the reflections from earth have been ignored for these power calculations.

Nadir-Pointing

For a Nadir-pointing scenario, the maximum number of solar cells being illuminated would be when the entire X+ face is illuminated, i.e., when $\theta = 0°$. This would be 6 solar cells. At an angle of 45°, this would mean that both the X+ panel and Z panel are illuminated at 45°. Translating to $8\cos(45°)$, i.e., 5.66 solar cells. Lastly, the number of illuminated solar cells would be 2 when $\theta = 90°$. Therefore, the average number of panels receiving sunlight would continuously move between these numbers.

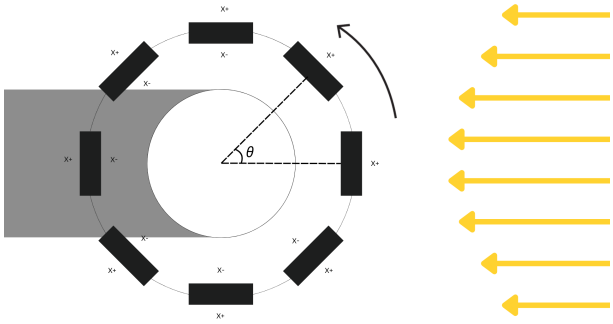

Figure 11.9: Nadir-pointing

Sun-pointing

For a sun-pointing scenario, only one side, i.e., 6 solar cells face the sun during orbit.

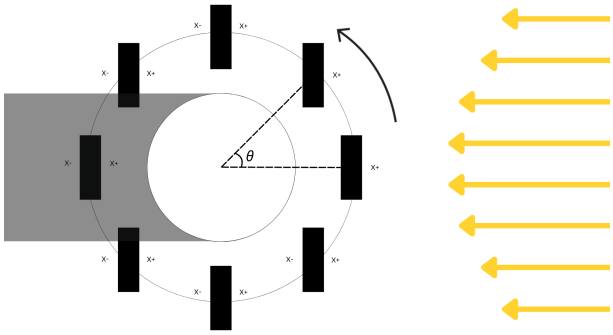

Figure 11.10: Sun-pointing

Free-orientation

For free orientation, at a given time, a maximum of three faces of the CubeSat can be illuminated from sunlight. This translates to 14 solar cells as the longer sides have six solar cells each and the Z-axis panels have two cells. Moreover, the light will incident on the panels at an angle, so the intensity will be reduced.

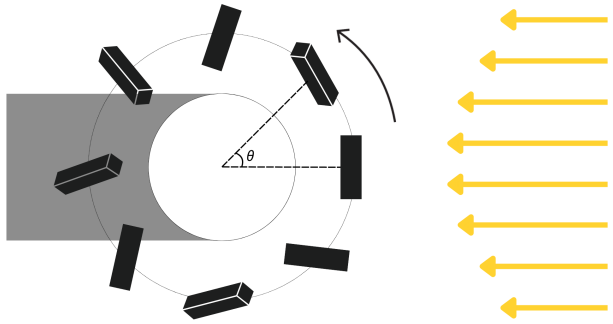

Figure 11.11: Free-orientation

To get a maximum figure, it can be assumed that all three faces are at an equal angle, i.e., 45°. This gives 14*cos(45), an average of 9.89 solar cells being illuminated. For the

minimum figure, this will be the case when the CubeSat is parallel (lengthwise) to the incident light, and only the Z-axis panel is illuminated. This translates to 2 cells.

Nadir and Sun-pointing orientations require active control [37]. WUSAT will not be equipped with such angular control systems, thus, the free-orientation case best represents its orbital orientation. Based on this, the power budget can be calculated.

Operational Mode Power Profiles			
Phase	**Power Consumption (W)**	**Power Generation (W)**	**Net Power (W)**
Nominal	5.47	7.41	1.93
Downlink	17.21	7.41	-9.80
Eclipse	1.43	0	-1.43
Safe	5.47	7.41	1.93
Survival	6.60	7.41	0.81

Table 11.3: Mode Power Profiles - FDSPP min

WUSAT Orbit Parameters	
Parameter	**Value**
Orbital Period (h)	1.5
Starting Battery Capacity (Wh)	26
Battery Decay per period	0.0005
Number of periods	30

Table 11.4: Graph Parameters

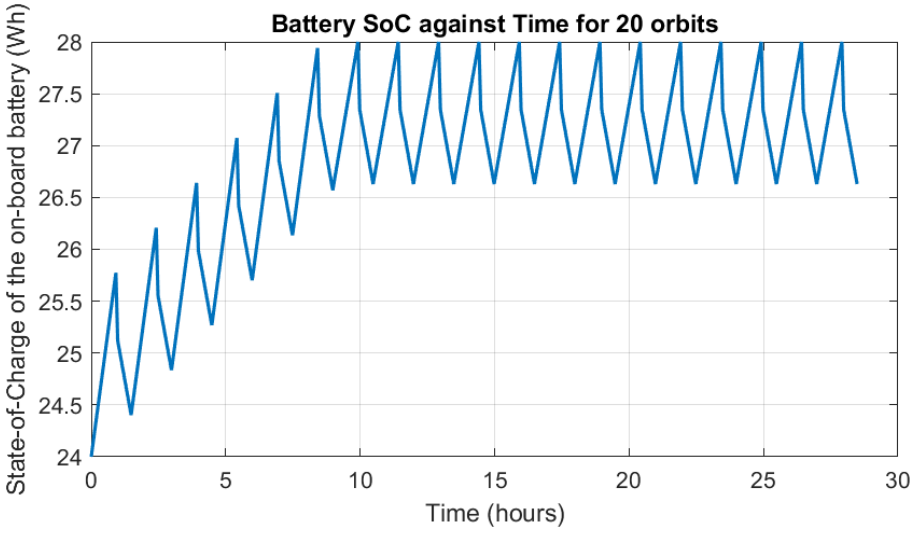

Figure 11.12: Battery State-of-Charge for 20 orbits with only FDSPP Payload

Sub-Systems Power Budget														
Subsystem	Component	Power Draw (W)			Nominal		Downlink		Eclipse		Safe		Survival	
		Idle	Nominal	Max	Duty Cycle	Power Draw (W)	Duty Cycle	Power Draw (W)	Duty Cycle	Power Draw (W)	Duty Cycle	Power Draw (W)	Duty Cycle	Power Draw (W)
RF Comms	Endurosat UHF Antenna	0.005	1.25	3.5	1	0.005	1	1.25	0.1	0.005	0.2	0.005	0.2	1.25
	Endurosat 1U Transceiver	0.005	1	1	1	0.005	1	1	1	0.005	1	0.005	1	1
Payload	FDSPP module	1.05	1.05	4.06	1	4.06	1	11	1	1.05	1	4.06	1	4.06
	Xcam	0.5	5	5	0.01	5	1	0.5	0	0.5	0	0.5	0	0.5
	Pi_1	1	1	1	1	1	1	1	1	1	1	1	1	1
	Pi_2	1	1	1	0	0	1	1	0	0	0	0	0	0
	Pi_3	1	1	1	0	0	1	1	0	0	0	0	0	0
OBDH	On board computer	0.1	0.4	1	1	0.4	1	1	1	0.1	1	0.4	1	0.1
EPS	ISI Space 1U Solar Panels	0	0	0	0	0	0	0	0	0	0	0	0	0
	ISI Space 3U Solar Panels	0	0	0	0	0	0	0	0	0	0	0	0	0
	ISIS iEPS A	0.09	0.09	0.09	1	0.09	1	0.09	1	0.09	1	0.09	1	0.09
Total		4.75	11.79	17.65		5.61		17.84		2.2455		5.556		6.5

Figure 11.13: Sub-Systems Power Budget for Different Operational Modes

Battery SoC with FDSPP and XCAM Payloads

A slower, positive SoC trend is obtained with XCAM on-board, see figure 11.14. However, this is only possible when only one Raspberry Pi is powered from the FDSPP payload (See Appendix H).

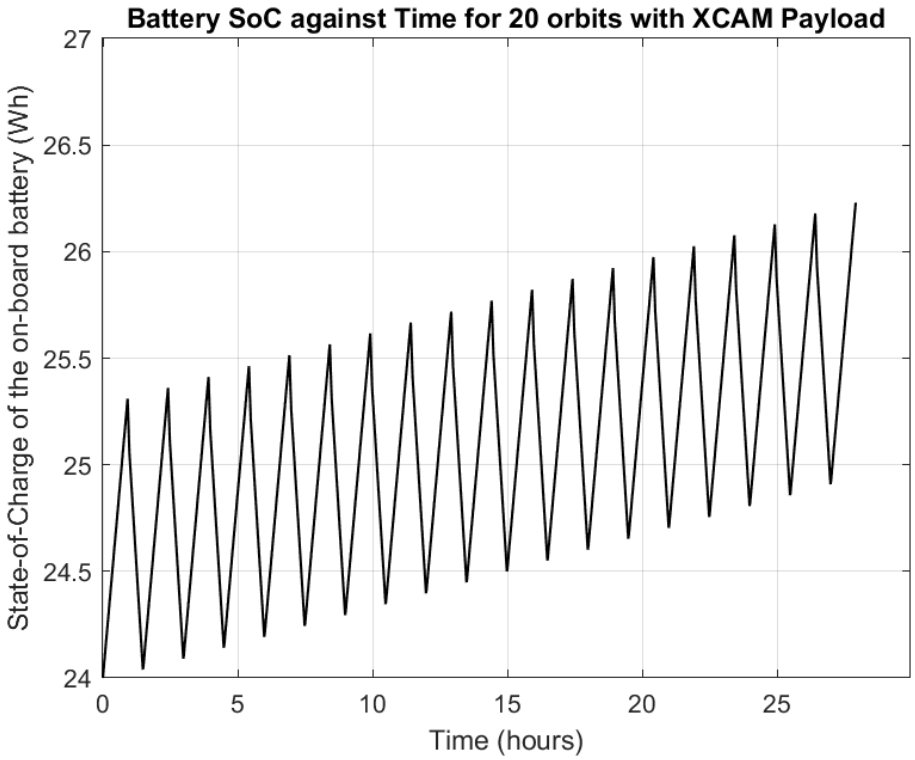

Figure 11.14: Battery State-of-Charge for 20 orbits with FDSPP and XCAM Payloads

11.4.6 W4-EPS-60: Dynamic Power Delivery

Power delivery must be dynamically managed according to the CubeSat's mission phase. For instance, during the launch phase, only housekeeping subsystems should be powered to preserve the battery charge, while during downlinking, the comms system must be prioritized. The CONOPS state-flow diagram (see Figure 5.1) provide an idea of how this will be carried out. Using the sensor data, such as the battery's SoC, incident irradiance, subsystem temperatures, and voltage readings, the OBDH can decide the CubeSat's operational mode.

11.4.7 W4-EPS-70: Protection Mechanisms

The EPS must incorporate over-voltage, under-voltage, and over-current protection mechanisms to safeguard components and subsystems. Over-voltage and under-voltage lock-outs will ensure the electronic components are safe from power fluctuations.

Current-limiting must also be included to prevent excessive current flow from damaging components. Additionally, fault isolation mechanisms, such as blocking diodes, should be

implemented to ensure faults in one part of the system do not spread to other systems.

11.4.8 W4-EPS-80: System Redundancy

To mitigate the risk of single-point failures, the EPS design must have redundancy for individual systems. The solar panel subsystem, for example, features a parallel diode configuration that ensures that a single component or solar cell failure does not result in total power loss. Additionally, the PCDU incorporates multiple MPPT inputs, which further enhances the redundancy available for the solar array. In essence, there should not be an independent point in the subsystems whose failure or malfunction may lead to the failure of the entire system.

11.5 Design

11.5.1 Solar Panels

Initially, work continued with the choice of the previous team of DHV solar panels, comprising 1U and 3U panels built with AzurSpace 3G30A solar cells [35]. These are triple junction GaAs solar cell assemblies offering 30% efficiency in LEO [35]. Apart from being flight-proven (TRL-9), these solar assemblies offer a bypass diode for each cell and two blocking diodes in parallel to the array [35]. This configuration provides partial-shading and fault tolerance, meaning that the cells receiving sunlight would continue power generation even when other the other series-connected cells are shaded or damaged. This is especially important because of the absence of an active ADCS system and provides redundancy advantages in the event of individual solar cell failure. However, when the DHV team was approached for a quote, it was learned that a single COTS 3U panel would cost between 15,000 and 20,000 euros (£12,400 - £16,500). This would be excessively overbudget and the cost per watt would be unjustifiable.

The ISI Space solar panels were considered as an alternative. This would offer direct compatibility with the ISI Space PCDU, and the price was around £12,000 for all four 3U panels. This information, however, was learned from a fellow CubeSat team that was encountered at the ESA Design Booster Week in Netherlands (See Section 3.1.2). Thus, the ISI Space pricing will require further confirmation. Nevertheless, it is clear from the specs of the panels that the supply voltage of the panels is also within range with the ISIS iEPS-A PCDU [38]. Therefore, the solar panel outputs could be connected directly with the MPPT inputs, eliminating the need for a buck converter between the panel outputs and the PCDU inputs. This not only increases efficiency by eliminating the buck converter's losses, but it would also reduces the number of possible single-point failures in the system. Furthermore, the previous team also identified ISIS panels as a solution to the mounting issues with the transceiver. But, the DHV panels offers 7 solar cells, thereby offering a maximum power output of 8.4W [35], while the ISI Space panels carry 6 cells offering a peak power of 6.9W [38]. Therefore, these figures need to be accommodated in

the power budget before the final decision.

	3U DHV Panel	**3U ISI Space Panel**
Cell Type	Triple-junction GaAs assembly	Triple-junction GaAs assembly
Efficiency	30%	30%
Max Power (BOL)	8.4W	6.9W
Mission History	Yes	Yes
3U Panel Price	£12400–16500	£3000 (approx.)
PCDU Compatibility	Low	High
Supply Voltage within MPPT range	No – buck conversion required before MPPT	Yes

Table 11.5: Comparison of 3U DHV and ISI Space Solar Panels

11.5.2 XCAM Payload

To accommodate the XCAM payload (a camera and an image processing module) the panel configuration of the 2023-24 team would have to be modified. It is intended to capture external images from the CubeSat. The main change is the elimination of the ±Z-axis 1U panels to ensure an unobstructed field of view for the onboard camera. Figure 11.15 highlights the new configuration.

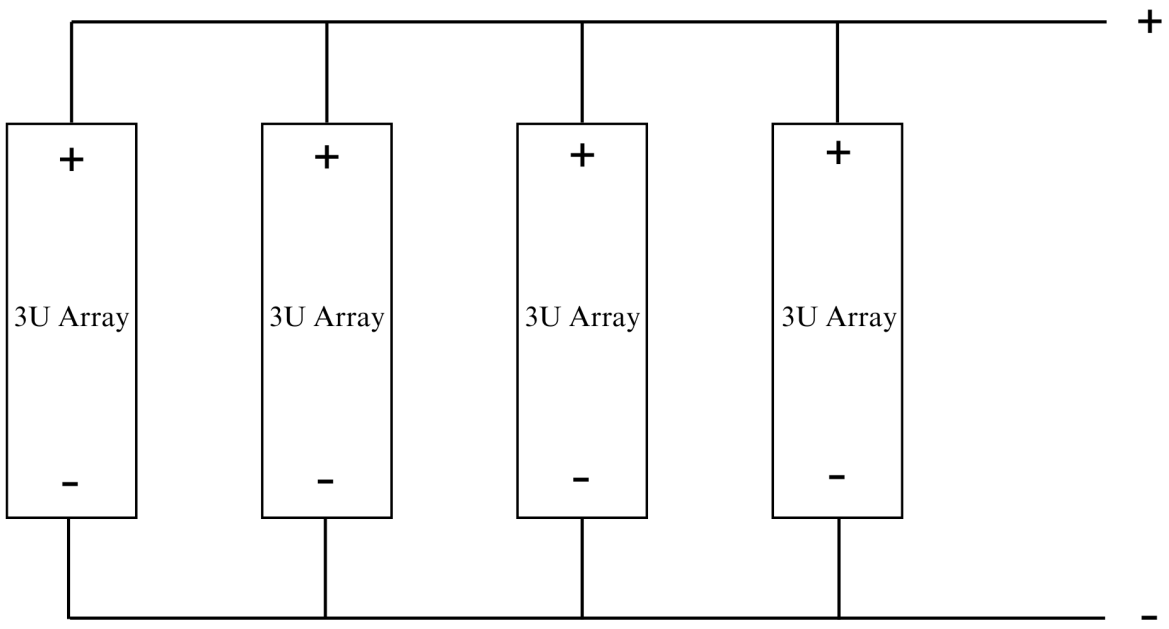

Figure 11.15: Solar panel configuration with XCAM Payload

Adopting this configuration would reduce power generation, therefore, the addition of XCAM will only be finalized after examining its impact on the subsystem budgets, especially power.

11.5.3 ISI Space iEPS-A PCDU

The chosen power conditioning and distribution unit has 3 in-built, independent MPPT units (**W4-EPS-20**), of which two will be utilized, allowing room for redundancies (**W4-EPS-80**). It provides telemetry data in I2C for the battery's temperature and SoC (**W4-EPS-40**). More importantly, it has output load switches that allow direct interfacing with the OBDH system to control each voltage rail independently (**W4-EPS-60**). In the case of a system update command from the ground station or a communications failure, it also has a stack reset watchdog (**W4-EPS-70**). This also carries undervoltage and overvoltage protections for the battery to prevent short-circuits and circuit lockouts. Lastly, the PCDU has step-down converters to provide stable voltages of 3.3V and 5V, with 4 rails for each voltage level (**W4-EPS-30**). [34]

As of the writing of this report, the non-disclosure agreements have been signed for the acquisition of a quote for this PCDU with ISI Space, and the initial meeting has been scheduled. Thus, a quote and some rudimentary data about the panels and the PCDU can soon be accessed.

11.5.4 DC-DC conversion

Since DHV solar panels are no longer being used, the need for a buck converter that was identified by the previous team is no longer relevant. This is because the supply voltage of the ISIS solar panels is within the MPPT input range (**W4-EPS-31**). More information on this will be available after the initial meeting with ISIS. However, since the PCDU only has 3.3V, 5V, and an unregulated voltage rail, the need for a step-up converter is noted. This is because the power budget provided by SPL (Appendix H) noted 12V for the laser driver and 27V for the heater.

These requirements, however, can perhaps be circumvented as the 27V heater uses four 3 kΩ resistors in parallel to heat the pod. This translates to a 0.24W power output, which can alternatively be achieved with a 102 Ω resistor with a 5V input. In theory, this produces the same power output, which could be used as a heater. This will, of course, need to be confirmed with SPL.

Moreover, for the 12V requirement, it is recommended to use a radiation-hardened boost converter. This could also be circumvented as SPL would be developing a bespoke payload for WUSAT; therefore, the 12V lasers could be replaced with 3.3V/5V lasers with a similar output light intensity. This would require a feasibility analysis and a confirmation with SPL.

11.6 Open Points

To finish Phase-C, the following is required:

- For estimating the power consumption of components, certain assumptions were made in the power budget. This includes the duty ratios for subsystems under different operational modes. The charge rates and the duration of each phase was also assumed. For instance, it is assumed that downlinking would require four minutes, this may change as the CONOPs become more clearly defined. These assumptions need to be replaced with empirical data.
- Contact SPL to check if the 12V and 27V requirements can be substituted with a 5V input instead. If not, then a boost-converter integration is required.
- Like the DHV simulations, the ISIS solar panels are required to be tested via simulations. The DHV simulation files will be uploaded on Microsoft Teams that can be accessed by future WUSAT teams. By changing basic parameters such as the open-circuit current and short-circuit voltage, the MPP can be determined for the ISIS panels.

Additional open points:

- The power consumption of the de-tumbling method needs to be analysed. If magnetorquers are integrated into the design, they will require power. Their integration

with OBDH, i.e., identifying the operational modes for which the magnetorquers will be powered, would also have to be studied.

- If XCAM is on-board WUSAT-4 as a payload, its power consumption analysis would need to be conducted. This is imperative as carrying the XCAM payload would also mean removing the ±Z panels.

11.7 Next Steps

- Setup an initial meeting with ISI Space and acquire the data sheets, user manuals, and the quotes for the PCDU and solar panels. Ask about possible 12V/27V voltage outputs from the PCDU.
- Look at boost converter implementations that are radiation hardened and integrate into the OBDH for the 12V and 27V outputs required for the FDSPP payload.
- Get storage access for a clean room that meets ISO standards for storing the PCDU, Solar Panels are the routing cables. Ideally, all testing, including the flat-sat test, should be conducted in a clean room.

12 OBDH Software

12.1 Introduction

This section gives an overview on the progress of the on-board data handling (OBDH) software development. This software is responsible for interfacing with and controlling the other on-board subsystems, as well as ensuring communication with the ground station.

12.2 Requirements

The requirements were built upon from last year, expanding them to include reliability measures. They have also been reworded to conform to ESA standards — where "must" and "shall" denote mandatory requirements, and "should" indicates a lower priority.

W4-OBDH-SW-10 The OBDH shall packetize the data before transmission.

- **W4-OBDH-SW-11** The OBDH should store all data to be transmitted in contiguous memory to ease packetization.
- **W4-OBDH-SW-12** The data buffer should be able to hold the maximum amount of payload data that could be added.

W4-OBDH-SW-20 The OBDH shall transmit one image per six orbital periods.

W4-OBDH-SW-30 The OBDH should include reliability measures to facilitate consistent data transmission.

- **W4-OBDH-SW-31** The OBDH should store previously transmitted packets to facilitate retransmission in case of packet loss.
- **W4-OBDH-SW-32** The packet buffer should be able to store n packets, where n is the number of packets that can be sent without acknowledgement.
- **W4-OBDH-SW-33** n should be sufficiently high to not cause excessive retransmission and jeopardize **W4-OBDH-SW-20**.
- **W4-OBDH-SW-34** n should not be so high that retransmission affects transmission of the next image.

W4-OBDH-SW-40 The OBDH shall control power to the subsystems.

W4-OBDH-SW-50 The OBDH shall systematically turn power off to components in the event of survival mode.

W4-OBDH-SW-60 The OBDH shall update its software upon completely receiving a latest version from the ground station.

- **W4-OBDH-SW-61** The OBDH should verify that the packets were not corrupted during transmission.
- **W4-OBDH-SW-62** The OBDH should keep a copy of the software in an external memory to mitigate the severity of software corruption.

12.3 Summary of 2022-24 Progress

Software progress so far has been minimal.

The beginning of packetization was explored, with the suggestion of adding some bits to the beginning of each transmission to determine what data was being sent. This has been built into the application layer protocol, described in Section 12.5.1. Further, only housekeeping data was considered in this identification scheme.

A state diagram was given, which describes how the operating state of the CubeSat changes with respect to the current conditions, e.g., battery level. This has been absorbed into the software design this year – see Section 12.4.

Finally, JPEG was briefly considered in the case of no compression from the FDSPP. This is still considered to be the case this year, as the camera chosen by the FDSPP manufacturers – the ZeroCam – does not indicate it performs any image compression.

12.4 Analysis

This section discusses open points carried forward from last year.

12.4.1 Compression

The required data rate to transmit only the 5MP image, without any packet headers, can be calculated as:

$$\text{Image size (bits)} = 1944 \times 2592 \times 24 = 120932352$$
$$\text{Data rate (kbps)} = 120932352/(6 \times 6 \times 60 \times 1024) = 54.7 \text{ (3 s.f.)}$$

Where:

- 1944×2592 is the image resolution [39]
- 6 minutes is the average contact time per orbit
- There are 6 orbits to transmit the image (**W4-OBDH-SW-20**)
- 1kb = 1024 bits

The resulting data rate is almost 6 times the legal limit for data rates in the amateur radio band. This, coupled with the fact that headers will be needed to fulfil **W4-OBDH-SW-30**, and this calculation did not include any other payload data, means that some form of image compression will be required.

There are a few options for image compression, the most notable being Joint Photographic Experts Group (JPEG). In an average case, JPEG compression results in a 10x reduction

in file size, meaning our 14MB image will be reduced to approximately 1.4MB [40]. The caveat of this method is that there is a reduction in image quality, as information is lost during the compression. However, any lossless compression techniques, such as Portable Network Graphics (PNG), will not be suitable for this application, as they are incapable of the required levels of compression. Thus, a compromise needs to be reached between WUSAT and the University of Exeter researchers as to how much image quality can be degraded whilst still being useful for their experiments, such that we can still ensure the images are transmitted within the time limit.

12.4.2 Programming Language

The integrated development environment (IDE) for the microcontroller supports both C and C++ [41]. C++ is often considered to be far more memory safe, bug-free, and performant than C. It also allows programmers to make use of a larger variety of data types, such as vectors, as well as allowing classes to be defined. As a result of these, development in C++ is regarded as easier and faster [42].

C is often used in embedded development due to its far smaller memory footprint. C is known for being a "close-to-the-metal" programming language, allowing for direct hardware control with little overhead. Given the microcontroller has a limited memory, C appears to be the better choice for this application. The downside of choosing C is the developer cannot rely on many common data structures, or must implement them themselves, which may inadvertently introduce bugs [42].

In theory, both languages could be used in tandem with each other, as C code is compatible with the C++ compiler. This is not advised though, as it is extremely likely to cause bugs where the interface between functions and data within C++ and C are not explicitly defined, as is the case with much of the C language. Using the two languages together, especially in such a small-scale project, is more likely to double development time rather than reduce it.

12.4.3 Protocols and Reliable Data Transmission

The OSI model is a tried-and-tested model for protocol stacks, used as the structure of any Internet communications since its inception in the 1970s [43]. Adaptations will be necessary, as many of the features of the TCP/IP suite ensure the correct routing of packets among a large network, but here, communications will only ever be sent between the ground station and satellite. Lightweight protocols will be especially important, as we need to reduce the amount of extra data added to each of the packets, to ensure we are well within margins for transmitting the image within 6 orbital periods. To meet **W4-OBDH-SW-20**, reliability measures will need to be implemented to ensure that the image is transmitted correctly, especially considering the enhanced challenges of transmitting into

space. Common reliability measures include checksums, acknowledgements, and sequence numbers, though the measures used will depend on the selected protocols.

12.5 Design

This year focussed on finalising the design of the software. Unit tests were also developed to aid the developer next year. Code files are hosted on a GitHub repository, found here [44].

12.5.1 Packet Structure

Following guidelines from CCSDS, the maximum packet size will be 65536 bytes [45], which includes both the packet header and the payload data. The packet header has been divided into three layers of services: application, transport, and data-link, which correspond to the OSI model. The network layer has been omitted as it is primarily concerned with routing packets across different networks. Since WUSAT communications are point-to-point, routing information is not needed so can be removed. The physical layer is discussed in Chapter 9. The remainder of this section introduces the protocol stack chose for WUSAT communications between the CubeSat and ground station.

Telemetry (TM) Space Data Link Protocol was selected for the data link layer. To reduce header size, the synchronisation and channel coding sublayer has not been implemented as it was deemed that its functions overlapped with those provided by higher-level protocols [6]. Further, the secondary header will not be included in the transfer frame. The structure of a TM transfer frame primary header is given below:

Bit Position	Data
0-11	Master Channel ID
12-14	Virtual Channel ID
14-15	Operational Control Field (OCF) Flag
16-23	Master Channel Frame Count
24-31	Virtual Channel Frame Count
32-47	Transfer Frame Data Field Status

Table 12.1: Structure of the TM header without trailer. Total header size is 6 bytes. [6]

TM also provides the option to include a trailer, consisting of an operational control field and frame error control field. The purpose of the OCF is to report real-time functions; whilst the frame error control field provides the capability to detect errors introduced in the transfer frame. If these fields are used, the packet structure is:

Bit Position	Data
0-11	Master Channel ID
12-14	Virtual Channel ID
14-15	Operational Control Field (OCF) Flag
16-23	Master Channel Frame Count
24-31	Virtual Channel Frame Count
32-47	Transfer Frame Data Field Status
48-524223	Payload Data
524224-524271	Operational Control Field
524272-524297	Frame Error Control Field

Table 12.2: Structure of the TM header with trailer. Total size is 12 bytes. [6]

The selected transport layer protocol is Reliable User Datagram Protocol (RUDP). This was chosen over UDP as UDP does not contain any reliability measures, such as ordering and retransmission of lost packets. This is not suitable for this communication as incorrect, unordered, and potentially malformed data can mean that the recovered image could become corrupted and unusable. TCP also is not suitable due to the overhead imposed by its handshake – this would require at least three round-trip time (RTT) to establish a connection which heavily cuts into the data transmission time, especially if this were repeated at the start of each contact period [46].

RUDP was selected as a compromise between UDP and TCP – this implementation contains acknowledgement and retransmission, without the unnecessary overhead required by TCP [7]. The RUDP packet header is shown below.

Bit Position	Data
0-7	Control Flags
8-15	Header Length
16-23	Sequence Number
24-31	Ack Number
32-47	Checksum

Table 12.3: Structure of the RUDP header. Total header size is 6 bytes. [7]

Finally, a customised application layer protocol has been defined. The purpose of this layer is to provide identification of the data contained within the packet. It has been named Warwick University Satellite Application Protocol (WUSAPP). The WUSAPP packet header structure is shown below.

Bit Position	Data
0-7	Data ID Flags
8-15	Header Length
16-31	Checksum

Table 12.4: Structure of the WUSAPP header. Total header size is 4 bytes.

The structure of the entire packet can be summarised as follows:

Bit Position	Data
0-31	WUSAPP Header
32-79	RUDP Header
80-127	TM Header
128-524287	Payload Data

Table 12.5: Packet Structure (No TM trailer). Total packet overhead is 16 bytes.

If the TM Transfer Frame trailer is used:

Bit Position	Data
0-31	WUSAPP Header
32-79	RUDP Header
80-127	TM Header
128-524223	Payload Data
524224-524271	OCF
524272-524287	Frame Error Control Field

Table 12.6: Packet Structure with TM trailer. Total packet overhead is 22 bytes.

12.5.2 Software Functionality

The software has six main functions it needs to perform over the mission lifetime:

- Retrieving housekeeping and payload data
- Recalculating the operating mode, based on current environmental conditions
- Alter power consumption of onboard components
- Transmitting received data to the ground station
- Receiving data from the ground station
- Update itself when software patches are transmitted and verified

Retrieving housekeeping and payload data will require interfacing between the MCU and other onboard components. In accordance with **W4-OBDH-SW-11**, all collated data will be stored in a data buffer. Payload data will add complexity as the ZeroCam communicates via CSI, which is not supported by the MCU. Hence, OBDH hardware will require a transceiver to be placed between the payload and MCU.

The operating mode can be thought of as a finite state machine (FSM), where state changes are triggered by external conditions meeting certain thresholds. These changes are summarised in the Figure 5.1.

In the event of the OBDH moving into critical mode, it should selectively power down components so that power consumption is reduced. This should be reversed when the OBDH exits critical mode. Implementation of this function has not been explored as it would require MCU- and component-specific protocols to send the power down and power on messages.

Transmitting the collected data to the ground station requires packetization as discussed in 12.5.1. For **W4-OBDH-SW-31** to be fulfilled, each of the formed packets should be stored in a packet buffer, which is kept distinct from the data buffer. Packets should only be discarded from the buffer when they have been acknowledged by the ground station. For the software's purpose, a packet is considered transmitted when the packet has been passed to the physical layer. The flowchart for this process is given below.

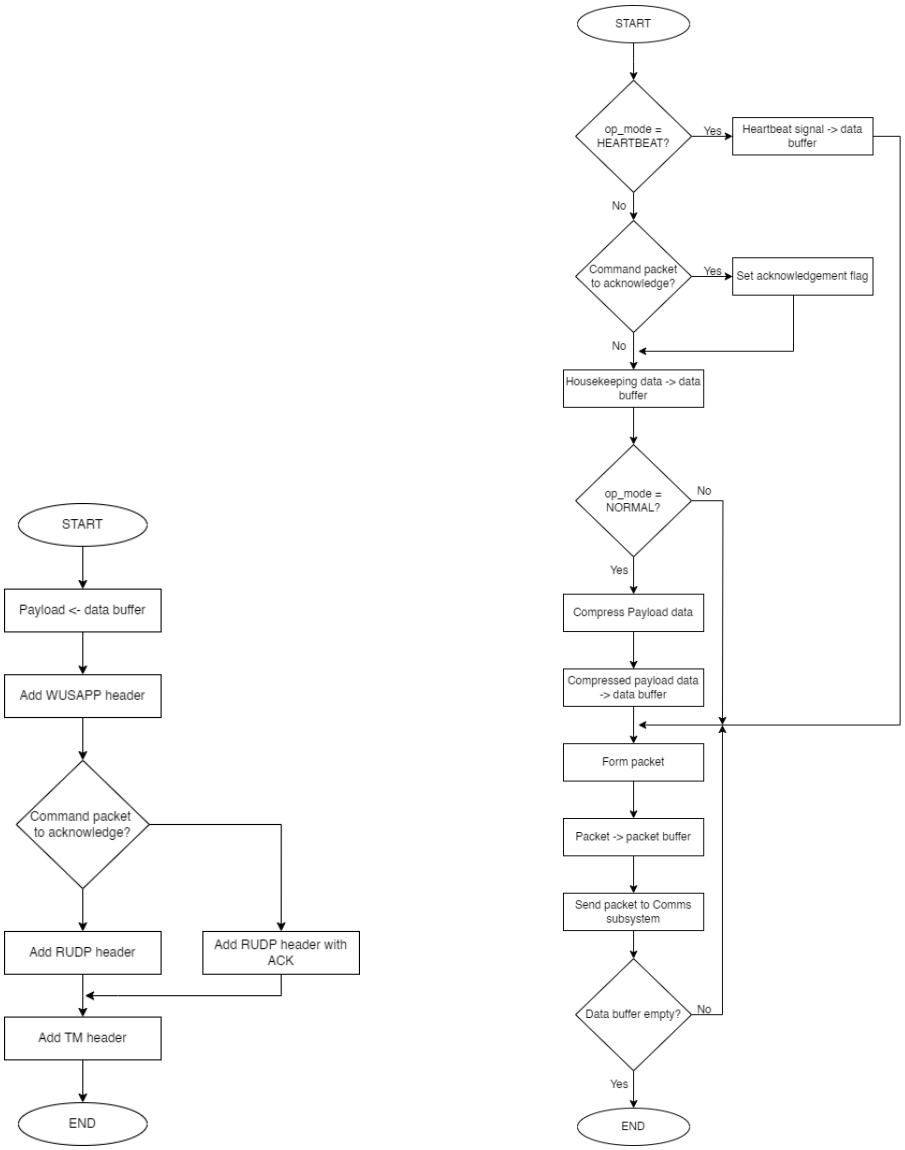

Figure 12.1: Process for data transmission. Form packet flowchart expands the "form packet" step in the right flowchart

Upon receiving data, its checksum should be verified. The packet is only acknowledged if the checksums are equal. Data from received from the ground station is expected to be one of three options: a heartbeat reply, acknowledgments for previously transmitted packets, or a software update (discussed in the next paragraph). Importantly, receiving data need not disrupt transmission from the satellite to the ground station, as any necessary acknowledgments can be added as part of the packet header.

Allowing for remote software updates requires the software to be separated into two separate entities: a bootloader, and the program. When a software upgrade is sent (without error) to the CubeSat, it should be written into a region of memory not used by the OBDH software. Once the entire update is read into memory, a reboot needs to be triggered. This will be controlled by a watchdog timer (see Section 13.4.3). Once rebooted, the bootloader can detect the update in memory and pull it into RAM to begin execution.

The initial CONOP for any software update should be HEARTBEAT, where transmission of the heartbeat signal indicates successful update of the software.

This functionality can be summarised in the flowchart below:

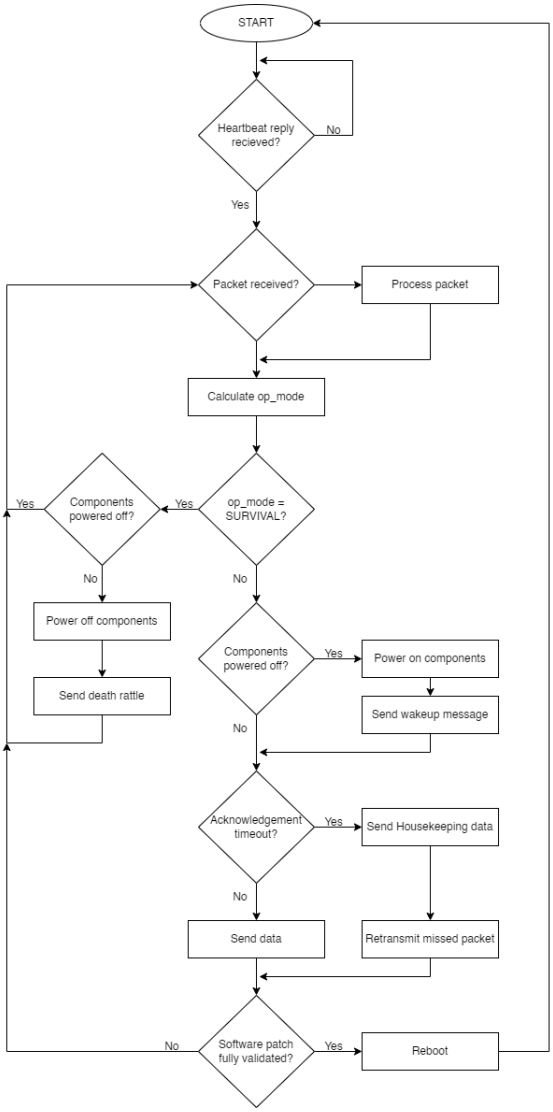

Figure 12.2: Software overview. "Death rattle" means the satellite's last words, such as [1].

Larger versions of the flowcharts presented in this section are available in Appendices E, F, and G, respectively.

12.5.3 JPEG Compression

As mentioned in 12.4.1, compression will be required to meet **W4-OBDH-SW-20**. JPEG compression has been selected as the most viable compression technique for this case, as it has a strong compression rate.

JPEG compression is based on the Discrete Cosine Transform (DCT). This represents the image as a sum of sinusoids with different amplitudes and frequencies. Image compres-

sion via DCT works by discarding sinusoids whose amplitudes are close to zero, as these have little effect on the quality of the reconstructed image. Once discarded, the inverse two-dimensional DCT of each block in the image is calculated and combined to form the compressed image [47].

A MATLAB implementation of JPEG compression is shown below:

```
T = dctmtx(8); % dctmtx returns the N-by-N DCT transform matrix

% compute the DCT of the image
dct = @(block_struct) T * block_struct.data * T';
B = blockproc(I,[8 8],dct); % I is the image

% discard all but 10 of the coefficients
mask = [1   1   1   1   0   0   0   0
        1   1   1   0   0   0   0   0
        1   1   0   0   0   0   0   0
        1   0   0   0   0   0   0   0
        0   0   0   0   0   0   0   0
        0   0   0   0   0   0   0   0
        0   0   0   0   0   0   0   0
        0   0   0   0   0   0   0   0];
disc = @(block_struct) mask .* block_struct.data;
B2 = blockproc(B,[8 8],disc);

% Compute the inverse DCT to recover the image
invdct = @(block_struct) T' * block_struct.data * T;
I2 = blockproc(B2,[8 8],invdct);
```

Listing 1: DCT compression of an image in MATLAB, reproduced from [47]

Since this code example is MATLAB, a C implementation will have to be explored for use within the WUSAT MCU software.

12.5.4 File Structure

The following is a brief overview of the sub-folders and files found in the repository.

Makefile

This file is responsible for compiling the source code files and the unit tests. There are four compilation options:

- `make all` — this makes an executable binary, `obdh-controller`, located in the build/ directory. This is the final product which should be run on the microcontroller.

- `make build` — this compiles all src/ files, except the `main.c` file. It is a necessary step before running the test suite.
- `make check` — this compiles and runs the tests stored in the test/ directory. `make check` cannot be ran if make all has been run, unless preceded by make clean. Otherwise, the run will fail as there is more than one `main()` function.
- `make clean` -– this recursively removes the files in build/, and the directory itself

.github/
This folder contains all the `.yaml` files used to run automated checks in the GitHub repository. There are two files: `build.yaml` checks that the binary can be built (but does not guarantee correctness). `test.yaml` compiles all but `main.c` and runs the test suite.

build/
This folder contains the compiled object files for the software. If `make all` has been run, it will also contain the `obdh-controller` executable. If `make check` has been run, a test/ subdirectory will be created containing all compiled and run tests.

src/
This folder contains all source code written by the programmer. Currently, it contains template files to demonstrate intended layout and verify that the .github/ files behave as expected.

src/osdlp/
This folder contains code taken from the Libre Space Foundation's open-source implementation of the TM protocol, found here [48].

test/
This folder contains the unit tests written this year. Each test verifies that one of the requirements are met. To aid traceability, the header of each test file explains what the test checks, and which requirement this pertains to.

This directory structure is visualised below:

```
obdh-sw/
├── .github/
├── build/
│   ├── osdlp/
│   └── test/
├── Makefile
├── src/
│   └── osdlp/
└── test/
```

12.6 XCAM

Whilst a final decision has not been made regarding whether we will take XCAM onboard, its impact on the software and data transmission has been considered.

Since they would be joining onto the mission as secondary clients, they would be given lower priority compared to transmission of the FDSPP packets. It is proposed that XCAM packets "steal" any packets left over after the transmission of the FDSPP image and data. The maximum number of packets that XCAM will be able to use, per six orbits, can be calculated as follows:

$$\text{Number of packets required to transmit FDSPP data} = 33$$
$$\text{Bits per packet} = 65536 \times 8 = 524288$$
$$\text{Data rate (kbps)} = 9.6$$
$$\text{Average contact time per 6 orbits (minutes)} = 6 \times 6 = 36$$
$$\text{Bits wasted} = (36 \times 60 \times 9.6) \times 1024 - (524288 \times 33) = 3932160$$
$$\text{Spare packets (per six orbits)} = \lfloor 3932160/524288 \rfloor = 7$$

Of course, this assumes that no packets for the FDSPP need to be retransmitted. XCAM has also stated they do not provide optics, so no assumptions can be made about file size and thus the number of packets needed to transmit an image. In conclusion, we can make no guarantees about the number of orbits it may take for XCAM to get a complete image.

12.7 Proposed Next Steps

The selected MCU is the Texas Instruments F2800132RGZR, which has its own IDE provided by Texas Instruments [41]. The MCU also has a development board which is used for interfacing between it and a laptop.

It is recommended that functionality is developed using the mock subsystems provided in `dummy_subsystems.c`, so that the unit tests can verify correctness. Once all unit tests pass, the developer can begin replacing mock functions with microcontroller-specific ones, and testing on the microcontroller and its development board.

Finally, the developer should be aware of NASA Power of 10 Coding, which is NASA's 10 rules for developing safety-critical code [49]. While not strictly required, following the guidance of industry experts can only benefit WUSAT's mission.

13 OBDH Hardware

The On-Board Data Handling (OBDH) is the brains of the computer with aims to pull data from other subsystems, process the data into spendable packages and parsing this data to the communications system for downlink.

13.1 Requirements

To align with the specificity and terminology standards of the ESA, the requirements were adapted to be more specific, with mandatory requirements with the words "shall" and "must" and optional features highlighted by the word "should".

W4-OBDH-HW-10 The OBDH Microcontroller shall have the processing power to process an image of up to 15MB in size.

W4-OBDH-HW-11 The OBDH Microcontroller should have a secondary microprocessor in the event of an emergency.

W4-OBDH-HW-20 The OBDH storage component shall store data for each housekeeping data item.

W4-OBDH-HW-21 The OBDH storage component should have a secondary external memory to store data in the event of software corruption.

W4-OBDH-HW-30 The OBDH storage component shall section data for each housekeeping data item.

W4-OBDH-HW-40 The OBDH MCU shall have a watchdog timer to easily reboot the OBDH when in orbit.

W4-OBDH-HW-50 The OBDH shall interface with the FDSPP subsystem.

W4-OBDH-HW-51 The OBDH should interface with XCAM payload.

W4-OBDH-HW-60 The OBDH shall interface with the EPS subsystem.

W4-OBDH-HW-70 The OBDH shall interface with the Communications subsystem.

W4-OBDH-HW-71 The OBDH shall be able to deploy the antenna once in orbit

W4-OBDH-HW-72 The OBDH must be able to interface with the RF transceiver with a setting of 9.6kbps

W4-OBDH-HW-80 The OBDH shall have an accurate time reference capability based on its altitude.

W4-OBDH-HW-81 The OBDH shall be able to synchronise all subsystems.

W4-OBDH-HW-90 The design should include sufficient redundancy to mitigate the risk of single-point failures in the OBDH subsystem.

13.1.1 OBDH Objectives Relative to CONOPS

CONOPS Phase	OBDH Operation	Physical Requirement
Launch	Power off	Use of a "Remove Before Flight" or "Apply Before Flight" pin
Initial Connection	Send Heartbeat signal to ground station	N/A
Early Operations	Sending Housekeeping data	OBDH must be able to collect, store & process housekeeping data before sending to the Communications subsystem
Commissioning	Request Payload data	Needs a large enough storage to store payload and housekeeping data simultaneously
Processing	Process and package data	OBDH requires good enough processing power to handle the image and housekeeping data
Transmit	Send the processed data to the communications subsystem	May require source encoding capabilities
Survival	Rebooting OBDH	OBDH Microcontroller Unit (MCU) must contain a watchdog timer

Table 13.1: CONOPS taken from [2]

13.2 Review of Past Progress (2022-24)

The previous years of WUSAT have developed OBDH to phase B (a preliminary definition) with substantial research into how requirements link to the CONOPS phases and further analysis defining the hardware interfaces and types of data that will be processed.

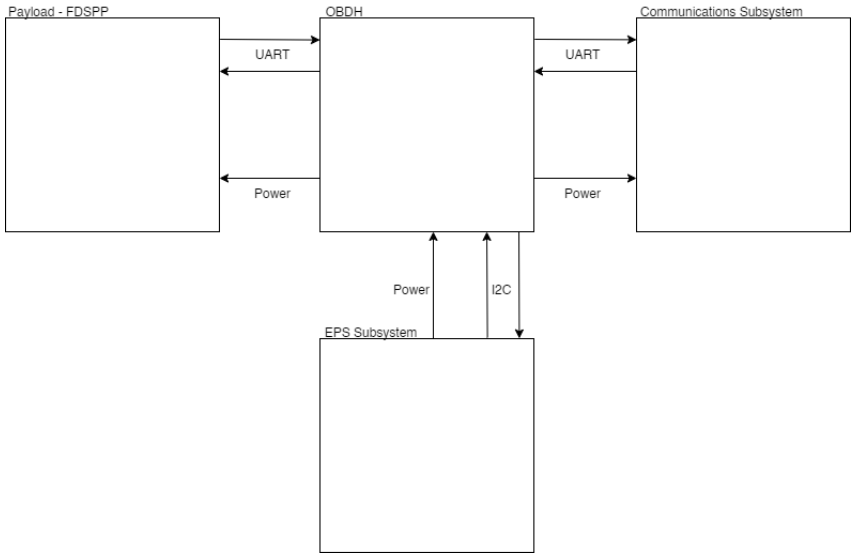

Figure 13.1: Interconnections between OBDH and other subsystems [2]

A functional architecture was created to give a high-level view of how the subsystems would be connected i.e. power flow and communication interfaces, for which the further requirements were created.

The important components chosen were: MCU, Memory, passive components (for noise prevention, JTAG circuitry and connectors. A general hardware design was attempted by connecting these components in Altium with an organised library and exploration of protection methods (EMI and EMC).

This year, the system requirements were further refined to align with ESA standards, and research into active redundancy schemes was initiated. The objective is to advance the On-Board Data Handling (OBDH) system from Phase B to Phase C, wherein the design process will involve circuit development using Altium, followed by fabrication and testing against the Engineering/Qualification model. To achieve this transition, a comprehensive analysis must be conducted to evaluate the design's **functionality** and **complexity**; as well as **reliability** *(the probability of performing the required function under specified conditions over a given time interval)* and **availability** *(the resilience of a system against single-event upsets).*

13.3 Payload

13.3.1 FDSPP

The original design for the FDSPP is a self-sufficient 3U spacecraft [50]. This will be adapted such that only the 1U FDSPP (see Chapter 2) will be housed in the WUSAT-4 spacecraft. The interface to the FDSPP is a 15-way D-SUB connector that is connected to various pins i.e. NREP signals from the original platform of Space Park Leicester device [50]:

P1	NREP Signal	P2	Wire	FDSPP Signal	Note
15	Power +	1	20awg FEP	Power +28Vdc	FDSPP Main power
8	Power +	7	20awg FEP	Power +28Vdc	FDSPP main power
13	Power Return	2	20awg FEP	Power 0V RTN	FDSPP common 0V
6	Power Return	8	20awg FEP	Power 0V RTN	FDSPP common 0V
5	Power Shield	9	20awg FEP	CHASSIS	Connected to FDSPP baseplate (CHASSIS) via PSU
12	Ground	3	20awg FEP	CHASSIS	Connected to FDSPP baseplate (CHASSIS) via PSU
10	USB DATA+	5	26awg FEP STP	USB DATA+	TE 0026A0024-9X cable
9	USB DATA-	6	26awg FEP STP	USB DATA-	TE 0026A0024-9X cable
2	Power Shield	12	26awg FEP STP	CHASSIS	Connected to FDSPP baseplate (CHASSIS) via PSU
-	USB PWR+	-	-	-	Unused
11	USB PWR-	9	20awg FEP	USB PWR-	Connected to FDSPP common 0V
4	USB PWR SHLD	10	20awg FEP	CHASSIS	Connected to FDSPP baseplate (CHASSIS) via PSU
-	SPARE	-	-	-	Unused
-	SPARE	-	-	-	Unused

Table 13.2: NREP signals from the original platform of Space Park Leicester device

Payload and housekeeping data is transferred from the payload via USB, hence the OBDH must account for this with a bridge chip connecting to the UART port of the MCU. To align with the power budget provided by the EPS, the functionality of the original FDSPP

module will be reduced ideally to only one Pi Zero and one Pod hence OBDH must regulate a 5V power rail and USB for data transfer.

13.3.2 XCAM

XCAM offers a board that can be used in conjunction with an off-the-shelf camera, with functionality for I2C and SPI [51]. This will be connected via SPI to ensure high integrity of the signal. Further investigation needs to be conducted to whether XCAM will be implemented as a secondary payload based on mass, power and data budgets.

13.4 Hardware Development

WUSAT-4 emphasises the use of COTS components due to their widespread adoption in successful CubeSat projects and their ability to significantly reduce development time and costs compared to using solely radiation hardened components [52]. Utilising COTS components ensures target launch window of 2026/27 can be met while adhering to the project's educational goal to maintain accessibility and hands-on learning for university students. Furthermore, their widespread availability and established supply chains reduce procurement risks, ensuring the project remains on schedule and within budget.

Permanent failures and transient errors can be protected against using shielding, error correcting codes and latch up current breakers [53]. Radiation hardened components are able to withstand against radiation of 100 krads, whereas typical CMOS components can survive nearly 5 krads before physical damage [54], further demonstrating the importance of reducing exposure to radiation as much as possible.

A library of radiation tested of COTS components has been created by the ESA [55]; choosing components from this repository will reduce the time in the testing phase (after Phase C in the Space Systems Engineering methodology).

Furthermore, all components should be surface mounted devices for space saving and high density mounting such that weight and dimensions can be reduced [56]. The objective is to transition from a configuration model to an engineering model, with an emphasis on optimizing functionality, rather than solely prioritizing the use of high-reliability components and the full implementation of redundancy. Even without a full design a lot can be learned from initial tests [57].

13.4.1 MCU

To meet **W4-OBDH-HW-10** and **W4-OBDH-HW-40**, the microcontroller chosen was the F2800132RGZR (part of the C2000 family) due to its flexibility, availability and ample supporting documentation. Points of interest being a large programmable memory

of 256kB, 120MHz clock, JTAG pins for programming and debugging, multiplexing of pins to increase level of functionality [2].
The trade-off which choosing such a component over a radiation hardened component is that the MCU will have to undergo rigorous testing in design stages beyond Phase C.

13.4.2 Memory

Mass memory is a non-volatile memory used to store housekeeping and payload data during periods of no contact with ground stations [58]. This will be used to meet **W4-OBDH-HW-20** and communication should be fast and have a low latency (the delay between when a read/write action is requested and when it is performed). Previous year [2] chose W25N02KVZEIR, a NAND flash memory due to these properties:

- 2G-bit memory (high memory capacity)
- Serial Peripheral Interface (SPI) interface
- 3.3V power supply
- 50MB/s sequential data transfer
- Lower susceptibility to vibrational issues

To meet **W4-OBDH-HW-21**, the secondary memory would have a higher latency since it is lower priority than the main memory and if there are size constraints, there is possibility that it can be housed on a different board. Devices will need to manage load wearing (equally distributing access to memory across the entire device) to improve memory durability but this will require a software driver [59].

13.4.3 Watchdogs

Watchdogs provide fault detection and recovery of flight computer transient failures. The watchdog monitors a heartbeat signal from the computer and reboots it if a failure is detected. It can also be commanded from the ground through the UHF radio to force power resets of the flight computer. They need to implemented at various levels:

- Subsystem, i.e., in microcontroller
- System level, i.e., at the power subsystem monitoring bus communication (**W4-OBDH-HW-40**)
- Ground-based watchdog, i.e., when no comms for 24 hours, reset or system in SAFE MODE

13.4.4 Time Reference

To meet **W4-OBDH-HW-80** a GPS will be used. GPS receivers provide a clock signal and time stamp referenced to the GPS satellite network. This was chosen over simple clocks (such as crystal oscillators or 555 timers) to mitigate the problems from drift. Accurate time reference is important as we need to be able to synchronise the downlink, but will also be used to synchronise all the subsystems [59]. An accurate time reference will be especially critical if a secondary processor is to be used [60].

13.4.5 Remote Terminal Unit

W4-OBDH-HW-20 and **W4-OBDH-HW-30** implies the need for sensors that monitor the health of the system - which can be categorised as the Remote Terminal Unit. This is used for interfacing sensors, actuators and discrete signals. Temperature, voltage, current sensors will be distributed across the different subsystems to serve diagnostic data that will be assessed by the OBC, stored and transmitted back to ground station. Digital sensors are preferable to analog sensors since they are more robust to radiation.

13.4.6 Antenna deployment system

In order to meet **W4-OBDH-HW-71**, Endurosat UHF Antenna III was chosen to deploy once the CubeSat is in orbit. It operates by burning resistors to cut a wire that releases the antenna rods with a typical current consumption of 500mA at 5V with an I2C redundancy signal [18], hence the Power bus must interface with the resistors that are triggered once in orbit and the MCU must interface with the I2C redundancy signal to ensure that deployment has occurred.

13.4.7 Connections

The general philosophy is to use COTS connectors which will allow for more seamless Assembly, Integration and Verification in the later design phases. In the Space industry, communication protocols tend to be reserved for certain functions which has informed the connection type between certain interfaces [57]:

- I2C – bus known from commercial applications, used on CubeSats for platform and payload applications. Better used within a single board, i.e., interfacing temperature sensors, mainly used for the RTU.
- SPI – known from commercial applications, used on CubeSats, i.e., for memories, ADCs, etc.
- RS-232/422/485 serial interfaces – interface between sub-systems/payloads.
- Wireless network technologies – slowly entering industry, i.e., for remote sensor acquisition.

MCU functionality can be extended (if needed) through the use of multiplexers in order to achieve all of these connections:

Connector and Routing Summary				
Requirement	From	To	Connection	Purpose
W4-OBDH-HW-60	EPS (Power rails)	OBDH	Samtec SSM-106-L-DV	Provide OBDH access to all power rails needed to power the other subsystems.
W4-OBDH-HW-60	EPS (Interface)	OBDH	Samtec SSM-106-L-DV	Obtain housekeeping data
W4-OBDH-HW-50	OBDH (FDSPP Connector)	FDSPP	15-way male D_SUB connector (A28100-015), and female to female wiring; UART to USB	Supply power to FDSPP module and obtain payload and housekeeping data.
W4-OBDH-HW-51	OBDH (XCAM Connector)	XCAM module	SPI data interface	For transferring payload and housekeeping data
W4-OBDH-HW-71	OBDH (5V Rail)	Antenna	Six pin Molex Pico-Lock™ 504050-0691	Deploy the antenna once in orbit
W4-OBDH-HW-71	OBDH (Interface)	Antenna	I2C; Six pin Molex Pico-LockTM 504050-0691	Redundancy for deployment
W4-OBDH-HW-72	Transceiver	Antenna	MCX connector (from Endurosat UHF Antenna III)	Data transmission and reception
W4-OBDH-HW-80	OBDH	GPS (OBDH)	Undefined	Accurate time keeping

W4-OBDH-HW-20	OBDH	Mass memory (OBDH)	SPI	Storage of data
W4-OBDH-HW-30	OBDH	RTU (dispersed)	I2C within board and CAN	Housekeeping data to monitor the health of the satellite

13.5 Redundancy

Redundancy is the ability of the system to have back up plans in the event of error. Such errors that a design must account for are [53]:

- Single event upsets: temporary effects due to ionising radiation such as noise in data, random switching events, changes in memory location and changes in the data itself. Error correction codes can be used to minimise this effect, as known as memory scrubbing
- Total dose: damage due to accumulative effects of ionising radiation over time, leading to device failure. Shielding devices can be used to minimise dose effects via housing, specific device packaging, or spot shielding.
- Latch up: device failure caused by one energetic ion causing runaway current flow. This can be prevented through shielding, as well as current sensing and current limiting to block the runaway affects. The device can return to operating normally afterwards.

These can be mitigated or managed through the use of redundancy schemes, which can be passive (e.g. capacitors to be used as noise filters) or active schemes (e.g. function in the MCU).
The functions of the OBDH can be visualised through a diagram adapted from SAVIOR [61].

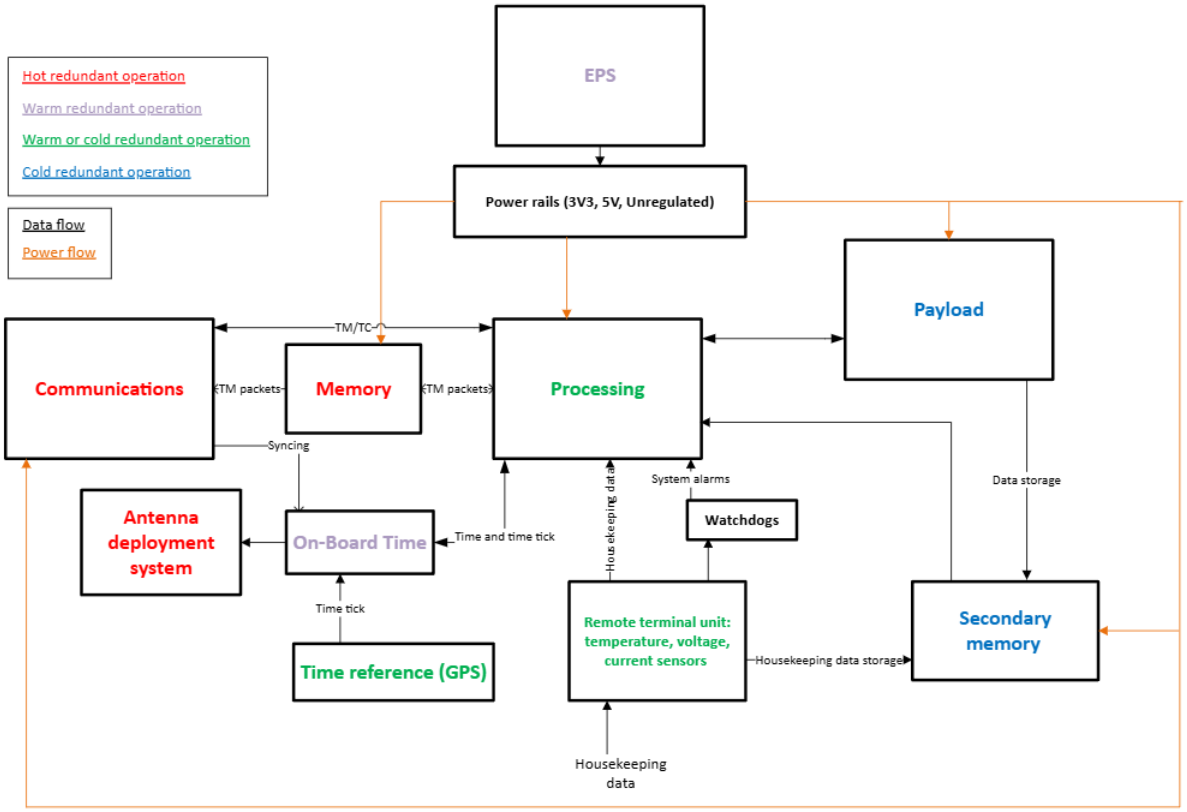

Figure 13.2: Data flows between subsystems, colours represent their redundancy levels

- **Hot redundancies** are for processes where outage can occur and requires instant process correction when failure is detected. The most critical functions are regarding Communications (tele-commanding, telemetry), memory and the antenna deployment system.
- **Warm redundancies** are for functions where a momentary outage is acceptable, and it usually operates in shadow mode. Time reference depends on connection to GPS, hence temporary disconnection to this means that the OBDH system can rely on the internal clock of the processor until power is restored.
- **Cold redundancies** are non-critical processes where human intervention (from ground station) is possible. Secondary memory is to be accessed in the case of an emergency, where OBDH-SW system will be able to retrieve relevant housekeeping and payload data to diagnose the problem.

Defining functions as such allows for a hierarchy which can be used to determine where critical and/ or active redundancy schemes [60] need to be implemented to manage the impact of single point failures (**W4-OBDH-HW-90**). Hence the lower the priority of the redundancy scheme needed, the less likely it will be implemented into the hardware design to save mass and reduce complexity.

13.5.1 CAN Protocol

There are a high number of mission failures reported due to I2C in CubeSat missions [3], where CAN provides a more robust and reliable alternative for communication. CAN is a communication protocol that operates at 1Mbps, with a realistic data rate of 100-200 kbps. The CAN communication protocol that operates with differential signalling, making it more robust to noise compared to single-ended signalling methods such as I2C. CAN also has greater protection for EMC issues, hardware-based error detection and tolerance to failures that avoids global bus hanging (persistent error conditions) [62].

CAN is advantageous because even though the effective data throughput is around 20% lower than for I2C, in absolute terms the data throughput is still higher by a factor of 1.7, when considering the default baud rate of 1 Mbps for CAN bus and the 400 kHz clock frequency for I2C [3].

However, CAN has added software/hardware complexity and higher power consumption. As can be seen in the graph below, the power consumption increases with the number of nodes, especially with a lower power consumption when I2C is in idle mode. This must be accounted for in the power budgets. Despite the higher power consumption, there are methods to reduce this through introducing the transceiver into a sleep mode (which reduces the power consumption by a factor of 10) while frames are being received on the bus [3].

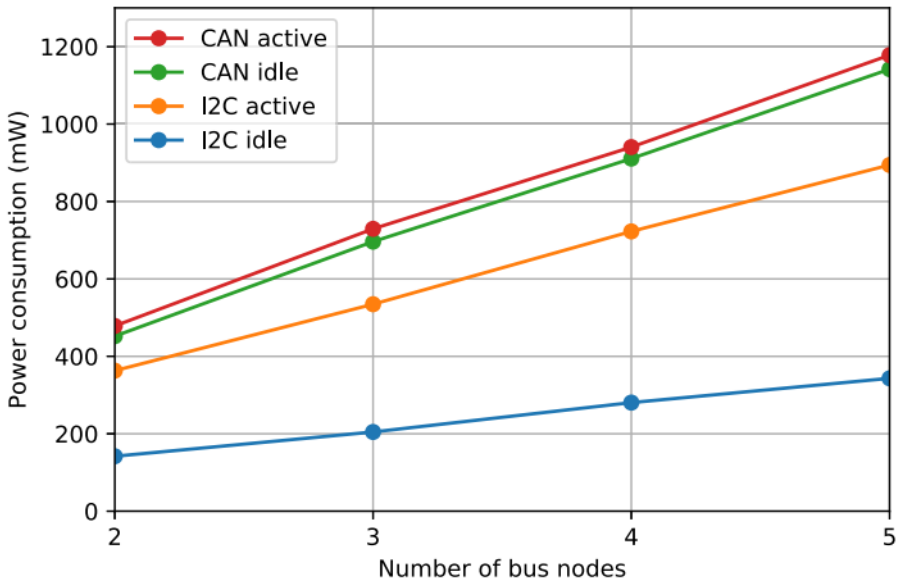

Figure 13.3: CAN vs I2C power consumption [3]

CAN should be implemented as a ring architecture (see figure below) and with 120Ω termination to reduce reflections [63].

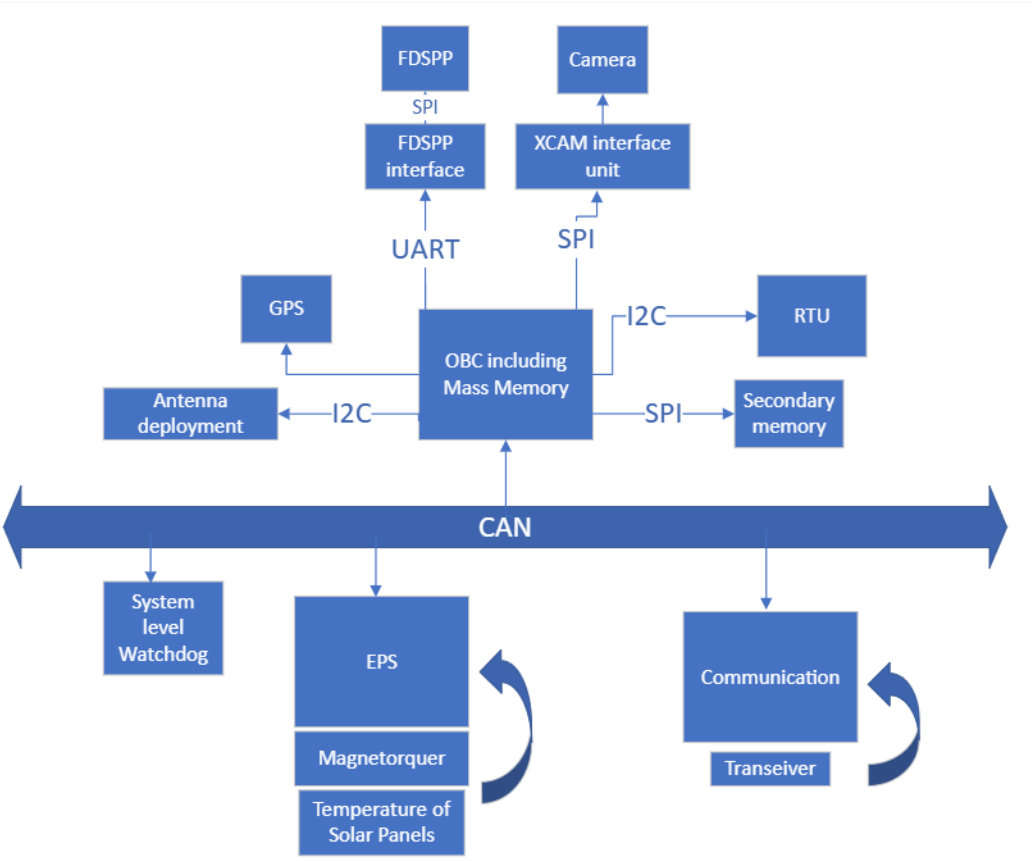

Figure 13.4: Data flows between OBDH functions

13.5.2 Latch up protection

Latch up protection should be implemented for individual components with their known consumption. It is difficult to implement at a subsystem level because the more components you have the harder it is to detect the current increasing on the power line [64].

13.6 Wiring

WireViz is a Python (3.7 or above) based programme used to organise the wiring between circuit components. This can be used when designing the final circuit board on Altium and will help in the ideation of implementing redundancy methods in conjunction with figure 13.2.

The repository is saved on the WUSAT-4 GitHub [65].

13.7 BOM

A rough BOM was generated in order to get a current inventory of components and cost. Indeed this is not final as there are other components to be chosen and considered (such as resistors).

Component	Price (GBP)	Quantity	Total	SUBSYSTEM
F2800132RGZR Microcontroller	1.5	1	1.5	
USB bridge chip	2	1	2	PAYLOAD
W25N02KVZEIR	3	1	3	OBDH Memory
Space-grade PCB	200	1	200	OBDH
Samtec SSM-106-L-DV	1	1	1	EPS connector
Voltage and current sensor: INA219	1.5	25	37.5	RTU
GPS: STMicroelectronics Teseo-LIV3F	14	12	168	OBDH
DS18B20 temperature sensor (for payload)	1	10	10	PAYLOAD
LM75 temperature sensor (for OBDH, Comms, EPS)	2.5	20	50	RTU
Total			473	GDP

Figure 13.5: Rough OBDH budget

13.8 Comparison with successful solutions

The current solution of the WUSAT-4 OBDH solution has been compared against other solution to serve as a benchmark for solutions with flight heritage; one designed by a university team of similar caliber and the other from leading aerospace manufacturer, Endurosat [66]. The purpose of this analysis is to ballpark a price range for the cost of WUSAT-4 OBDH design.

EQUISat (Brown University) is a 1U CubeSat that aims to shine various LEDs such that the satellite it visible from earth. It was chosen for its very low production cost of ∼5000 USD, where only the PCB production was outsourced [67].

Feature	WUSAT proposed solution	EQUiSat[68]	Endurosat	Analysis
Processor	F2800132RGZR	Atmel SAMD21J18A microcontroller (32-bit ARM Cortex-M0+, 48 MHz)	ARM Cortex M7	ARM Cortex is radiation hardened whereas WUSAT MCU is not.
Memories	Internal MCU 258KB Flash, 36KB RAM External W25N02KVZEIR NAND flash 2GB.	minimum 256KB Flash, 32KB RAM	2 MB program storage, 1MB internal SRAM, 8Mb external MRAM; 2MB NAND Flash for data storage; 1 SD card slot	

Compatibility	Standard connectors to interface EPS, Comms, Payloads and RTU	Custom-built to interface radio, flash panel (payload, sensors and antenna deployment), Voltage regulator board, and battery	Full set of drivers for EnduroSat modules	
Redundancy	CAN bus	N/A	3-axis Magnetometer	
Clock Type	GPS to synchronise system clocks	Internal oscillator	RTC	
Power Saving	N/A	Software-selectable sleep modes (idle and standby)	Flexible frequency (dynamically adjust frequency to optimise power consumption)	
Power consumption	Unknown	Not mentioned	1.5W peak	
Mass	Unknown	100-150g (estimated from total 1kg 1U cubesat)	130g	
Interfaces	x2 I2C, x1 CAN, x1 SPI, x3 UART	I2C, SPI, UART/USART, USB	4x RS-485, 2x RS-422, 3x UART, 2x I2C, SPI, USB, CAN	Fewer interfaces need for WUSAT-4
JTAG/ debugging	Yes	Supports JTAG and SWD (Serial Wire Debug)	Yes	
Fully radiation tested	No	Not mentioned	Yes (at 40krad TID)	Radiation testing will increase development time
Flight heritage	No	Yes, launched 2018 and re-entry in 2020	Yes	

Cost	£473 * 1.5 ≈ £710 (with 50% overhead costs)	∼$450 (£360) from total cost mission of $5000 (£4000) Estimate from OBC components: consists of processor(∼$5), memory(∼$35), demuxes and subsystem interfaces (∼$30), sensors (∼$30) and PCB (∼$200) Sum = $300 With 50% overhead margin (to account for testing and unforeseen/unspecified costs) estimate OBDH cost to be $450	£3,900	Reduced functionality of the WUSAT solution means that the costs can be brought down compared to Endurosat. Endurosat also have the advantage of buying components in bulk which will further reduce the costs, but these will be made up for in labour costs. But more functionality than EQUISat hence cost is projected to be more.

Table 13.4: Cost analysis and comparison[8][9]

13.9 Open Points

For future development, it is feasible to consider parallel processing [59], where functions of the MCU can be distributed to various processors, in order to reduce the load on an individual main microprocessor. It is an emerging trend in CubeSat design and there are various demos which demonstrate its success [58].

Further ideation to how the CubeSat can be disassembled [64], which depends upon reliable connections between each of the subsystems.

13.9.1 Further suggestions for future activities:

- FMEA documentation
- FDIR for failure senarios
- Create circuit board on Altium and conduct functional testing; tasks include implementing testing points adjacent to the JTAG connector and PSPICE simulations.
- EMC and Grounding methods based on what is required by components
- Obtain further information for XCAM payload and analyse whether payload is feasbile to include in the mission

- Research how power buses are to be implemented and regulation techniques for 3.3V, 5V and unregulated power rails
- Consideration of the interfacing with passive AOCS – additional sensors will need to be integrated as part of the RTU
- Implementation of stubs (required for preventing signal reflections and ensure signal integrity)

13.9.2 Failure Modes Analysis

The purpose of this analysis is to determine the failure modes more precisely such that points of failure can be reduced and protected against with compensating provisions. Examples of such situations are low battery, high temperature, rebooting of OBDH and software problems.

Another important example is in regards to PCB solder. The design must account for vacuum effects that cause the solder to 'grow' dendrites [4]. This can be mitigated by outsourcing the design to a manufacturer that specialises in space-qualified PCBs.

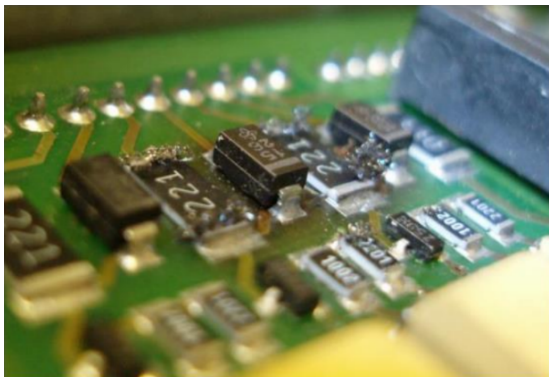

(a)

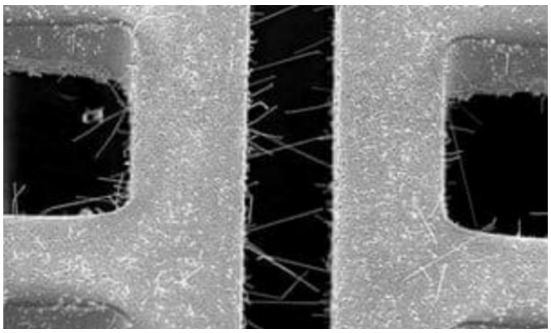

(b)

Figure 13.6: PBC dendrite growth [4]

13.9.3 Testing Suggestions

Test	Equipment	Purpose
Power Measurements	Multimeter, Oscilloscope	Verify voltage levels, current draw, ripple noise
CAN Bus Testing	Oscilloscope, CAN Analyser	Signal integrity, error frames, bit timing.
JTAG Debugging	JTAG Debugger	Verify programming capability
Sensor Testing	Magnetometer, Gyroscope, GPS Receiver, Voltage, Current and Temperature sensors	Verify sensor readings vs. expected values
Grounding & EMC	Oscilloscope (Differential Mode), Near-field Probe	Identify grounding issues, EMI sources
Watchdog & Fault Testing	MCU Debugger, Software Fault Injection	Test watchdog reset time, fault recovery
Breadboarding	Multimeter, Oscilloscope	Verify connector types between subsystems for configuration model
FlatSat testing (Phase C)	Example test (see Figure 13.7) Tests should be automated with simple python scripts	Validate software, memories, interfaces within OBDH and between the other subsystems i.e 1 on 1 testing between two subsystems, before assembling entire CubeSat.

Table 13.5: FlatSat Testing Suggestions[10]

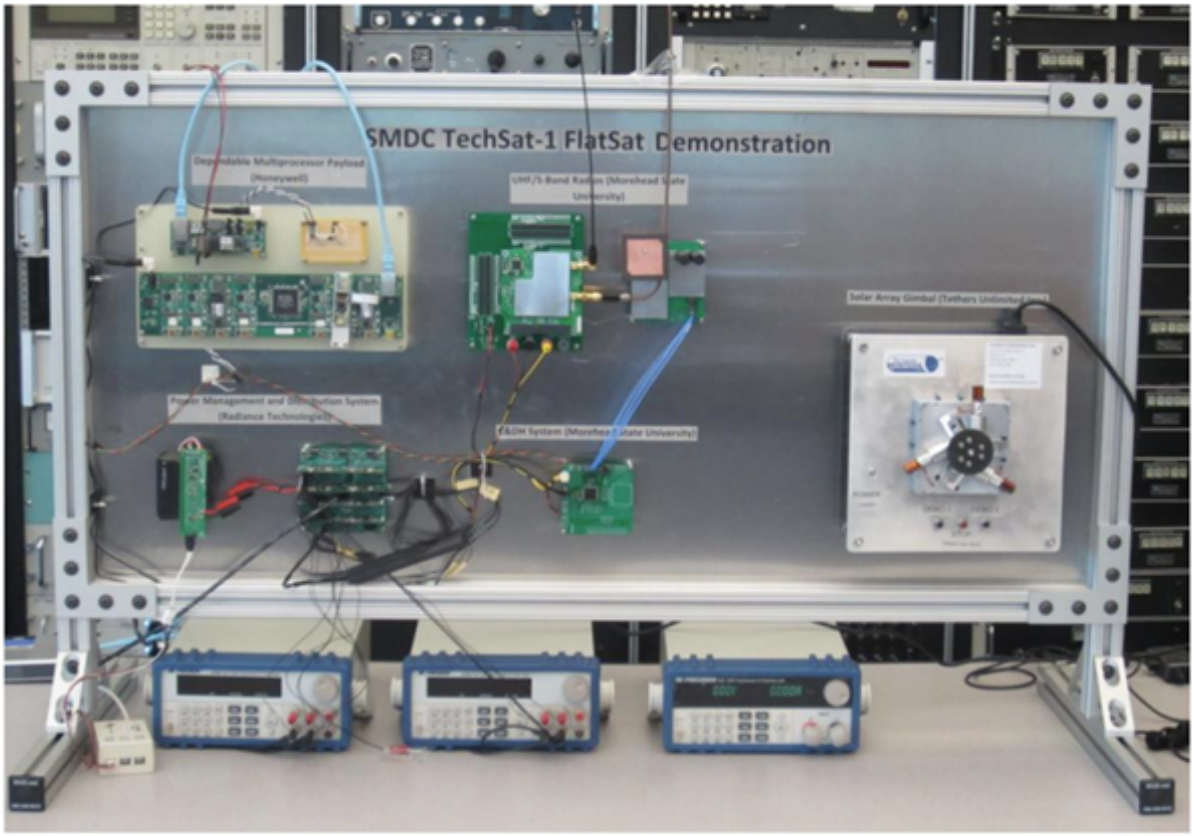

Figure 13.7: Morehead State University Flatsat Test Demonstration [5]

13.10 Conclusion

In conclusion this iteration of WUSAT-4 defined a more comprehensive list of requirements, which were met with additional hardware that includes active redundancy schemes and other desirable but non-mandatory requirements such as a secondary MCU. Initial wiring and BOM were initiated, with direct comparison to successful OBDH designs in order to determine a range in which the final cost is expected to be. Test suggestions were also given with emphasis on consideration of the assembly and integration of the different subsystems.

14 RF Communications

14.1 Requirements

W4-TTC-10 The CubeSat shall have the data rate to transmit a full image within six orbital periods to the ground station with 20% margin

W4-TTC-11 The CubeSat shall have the data rate to transmit all housekeeping data gathered each orbit alongside the payload image data

W4-TTC-20 The Link shall be closed with 3dB margin without a directional antenna on the space segment, due to no AOCS.

W4-TTC-30 The selected CubeSat antenna should fit within the defined allowable space, either deploying after launch or being of a form factor small enough initially (patch)

W4-TTC-40 The Uplink and Downlink shall use readily available amateur frequency bands, to ensure no legal limitations on communications.

14.2 Analysis

14.2.1 Previous Work

Last year's work withing this sub-system focused heavily on link budget analysis and accurate representation of this. However, this resulted in underdevelopment in certain areas of the communications system, such as modulation techniques, access time analysis, and legal considerations. Due to the knowledge gained on the ESA FYSDB course mention in section 3, it was decided that a system redefinition was required to ensure the work completed covered all of the required information.

A significant reconsideration was also the component selection for this sub-system – the Endurosat Antenna and Transceivers are exceptional parts, but may be over engineered for the mission, resulting in unnecessary expenditure when cheaper options are sufficient.

14.2.2 Subsystem Definition

The RF Communications sub-system investigates and defines the connection between the satellite and the ground station, in the space industry this is referred to as the 'Link'. The parts of the sub-system can then be defined as the space segment (satellite), the gap between the segments (link), and ground segment (ground station). When the satellite sends data to the ground station it is referred to as 'downlinking', and when the ground station sends data to the satellite it is 'uplinking'. The following diagrams represent the sub-system with these abstractions:

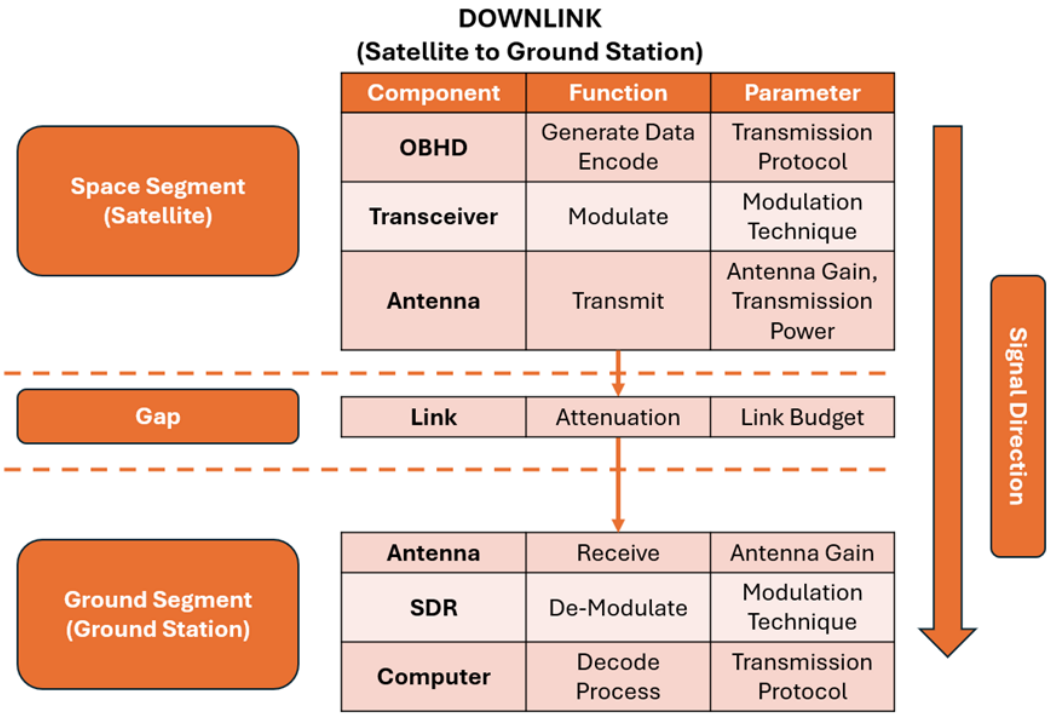

Figure 14.1: Downlink System Abstraction

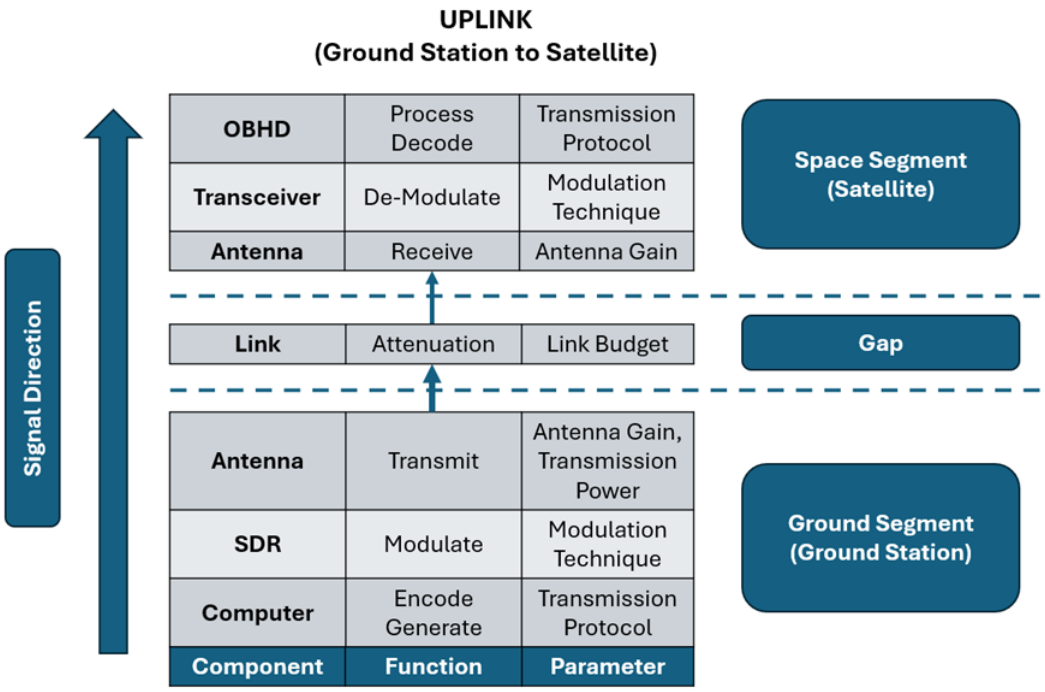

Figure 14.2: Uplink System Abstraction

These diagrams lay out the main components, functions, and parameters of the system, for both uplink and downlink. It should be noted that most of the parameters will stay the same between both links, except for the transmission power – the ground station is limited only by legal factors [69], but the satellite transmission power will be limited by the available power in the budget.

The components and parameters to select can be summarised as follows, with the following format:

Segment	Component	Parameters
Space	Antenna	Gain
		Downlink Power Consumption
	Transceiver	Modulation Technique
	OBDH	Encoding Protocol
Link	N/A	Path Attenuation
		Losses (de-pointing etc.)
Ground	Antenna	Antenna Gain
		FOV
		Tracking Precision
	SDR	Modulation Capabiliites
		Encoding/Decoding Capabilities

Table 14.1: RF sub-system analysis

With this definition, each segment can now be analysed for constraints and optimisations.

14.2.3 Space Segment

Architecture Selection

With the system defined, the architecture and complexity need to be selected, which will drive component selection. These will be selected to optimise the sub-system within the constraints of the mission.

Complexity

In a communications system, the complexity must be defined. This can be simplex (one-way communication), half-duplex (two-way communication, but not simultaneously) or duplex (two-way communication simultaneously).

Simplex communication would remove the ability to acknowledge the satellite or report errors or verify connection. As it will not be suitable to fulfil the requirements, this is ruled out. The mission requires the satellite to transmit science data to the ground station, but the only uplink data is the 'handshake' to verify that the satellite is within range at the start of communication. Both half- and full-duplex can accommodate this, but full-duplex requires an extra antenna on the satellite and increases cost. As such, half-duplex is selected for the system.

Frequency Band
The frequency band used by the system will determine multiple factors – maximum data rate, transmission power required, directionality, and antenna size. It should be noted that a driving factor of the frequency selection will be legal and mechanical constraints. Legally, the UK Office of Communications (OfCom) designates certain frequency bands for amateur communication [69]. The ones typically used for amateur satellite communication are VHF, UHF, S and X band, in increasing frequency and decreasing wavelength. Higher frequencies provide faster transmission, but have decreasing field-of-view (need to be pointed at the target) [70]. A significant consideration when selecting the frequency band was the lack of active AOCS on the satellite, meaning that it would not be able to point at the ground station. As such, an omni-directional antenna is required. This rules out the S- and X-bands. Of the remaining bands, both are omni-directional but UHF offers higher possible data rates. Since the payload data generation was unknown at this stage, the decision to maximise data rate was taken, resulting in the selection of the UHF band for transmission. In this range, the 432MHz band was selected.

It should be noted that another requirement for OfCom is that, to occupy space on an amateur band, one of two requirements must be met;

- All data downlinked must be decodable by a COTS amateur decoder
- OR an amateur transceiver must be on board the satellite

This will drive component selection going forward.

Transmission Protocol
The transmission protocol is the packeting and encoding of the data to be sent, which ensures that data can be verified for errors, and has a standardised method to interpret. This is discussed and selected in Section 12.5.1.

Modulation
The next parameter to select is modulation. The modulation technique is the method used to imprint data onto a radio wave for it to be transmitted. Notable techniques are Frequency, Amplitude, and Phase-keying, which vary the respective attribute of the carrier wave to represent data. A Gaussian filter can be applied to the selected technique to reduce sideband emissions (unwanted frequencies), at the cost of a small sensitivity reduction of the main signal. This is to be defined with the selection of an on-board transceiver that is compliant with OfCom's requirements for amateur frequency band usage.

The following are the most common options for modulation: 2FSK, 4FSK, 2GFSK, 4GFSK, OOK, GMSK. These can be explained as follows [71]:
Features

- 2 vs 4: This represents the number of bits per incident piece of information. The

default is 2. 4 means double the bits, so double the data rate can be achieved in the same bandwidth (better spectral efficiency). However, it does lead to worse sensitivity, degrading it by 2 dB

- OOK vs FSK: On-Off keying is where no wave signifies a 0, and a wave signifies a 1. It uses less power but is also worse in terms of its sensitivity than FSK (about 3dB worse), where 2 different frequencies mean 1 and 0 respectively
- FSK vs GFSK: G stands for Gaussian, and means a Gaussian filter is applied to the wave. This means the sidebands (resonant frequencies on side) drop dramatically, reducing emissions and increasing spectral efficiency. However, the desired wave also suffers a small drop of 0.5dB, slightly harming sensitivity
- FSK vs MSK: MSK is the minimum frequency you can use in FSK, but it may be out of allowed range for this application

From these attributes, a Pugh Matrix can be generated to rank the techniques. The parameters to optimise are:

1. Data rate: How fast data can be sent
2. Sensitivity: The power of the signal (how easily it can be read by the receiver)
3. Bandwidth: The frequency range used around the centre frequency
4. Emissions (sideband power): The amount of power in resonant sidelobes
5. Power consumption: The minimum power required to close the link budget

The most difficult challenges for the CubeSat are the lack of AOCS and the lack of deployable solar panels. As such, sensitivity, then Emissions will be prioritised to minimise power and maximise signal strength. Spectral efficiency will be considered least important. The Pugh matrix will compare the various characteristics of each modulation technique. It is assumed that all the minimum constraints above can be reached by each technique, but they have varying degrees of how well they do this. The most important criteria are ranked as 1, and the least as 3. The techniques are ranked from best to worst, 1 to 6. The technique with the lowest score will be chosen.

Criteria	Weight	Techniques											
		2FSK		4FSK		2GFSK		4GFSK		OOK		GMSK	
		Score	W. Score	Score	W. Score	Score	W. Score	Score	W. Score	Score	W. Score	Score	W/ Score
Spectral Efficiency	3	5	15	2	6	4	12	1	3	6	18	3	9
Sensitivity	1	1	1	4	4	2.5	2.5	5	5	6	6	2.5	2.5
Emissions	2	5	10	2	4	4	8	1	2	6	12	3	6
Total		11	**26**	8	**14**	10.5	**22.5**	7	**10**	18	**36**	8.5	**17.5**

Table 14.2: Pugh Matrix for the modulation techniques. Note W. Score is the Weighted Score for the criteria/technique.

Rank	Technique	Weighted Score
1	**4GFSK**	**10**
2	4FSK	14
3	GMSK	17.5
4	2GFSK	22.5
5	2FSK	26
6	OOK	36

Table 14.3: Results of Pugh Matrix analysis of Modulation Techniques

From the analysis, 4GFSK is the most optimal modulation technique. The other techniques have also been ranked, since certain transceivers do not have access to all techniques, As such, the best one available should be chosen.

14.2.4 Ground Segment

The Ground segment of the system is being developed by Warwick Aerospace Society, external to the project. As such, the components of this segment need to be parametrised to account for potential impact on the space segment. The confirmed data is that the ground segment will be located at the university, will aim to have a directional antenna, and maximum transmission power of 100W due to legal limitations. It has also been decided that a Software-Defined Radio ("SDR") will be used, allowing flexibility of encoding schemes. The estimated range is 157 degrees for the antenna pointing mechanism.

14.2.5 Link Segment

The link segment is defined primarily by the link budget itself. Last year's communications sub-team did extensive analysis on the parameters comprising of the link budget. Since the other components of the sub-system were underdeveloped, this academic year has focused on bringing these up to the same point. Due to time constraints and factors mentioned in the project management overview document a full simulation with the link budget was not possible, since some parameters are yet to be defined.

However, the outputs of this have been parameterized, using the System Budgets spreadsheet. The link budget values would be used in MATLAB to determine the ground station viewing angle, by analysing the signal strength along with the field-of-view of the satellite and ground station to calculate link closure times. The output would be the contact times of the two segments across the link.

Using these contact times, and the total data generated on board the satellite, the minimum data rate to comply with **W4-TTC-10** can be calculated as shown in the table

below, accounting for margins. This can be seen fully in the 'Data Budget' sheet of the 'System Budgets' spreadsheet.

Housekeeping	471082.3308
Margin	20%
Total	565298.797
Header Length (Bytes)	16
Packet Length (Bytes)	65536
Image Size (Bytes)	15728640
Compression Ratio	10
No. Packets Required	33
Contact Time per Orbit (mins)	4
Data Rate Required (kbps)	8.8

Table 14.4: Sources of data and the resultant required data rate. Header and Packet lengths taken from Section 12.5.1

Assuming an average contact time of 4 minutes per orbital pass across a 6 month mission, the data rate required would be 8.8kbps. The standard rate of 9.6kpbs can be chosen to transmit using this model, which is also the maximum allowed by OfCom for this frequency band.

It is important to note that this value is not final. The link budget analysis from last year must be completed, and modelled to finish the scenario in the MATLAB file provided, to determine accurate contact timings. From this, a more accurate data rate can be obtained.

14.3 Design

The component selection for this subsystem cannot be finalised until the completion of the link budget parameters, and simulations to discover the minimum required antenna gains and powers. The Endurosat UHF antenna and transceiver [72] that were suggested from last year's team would undoubtedly be sufficient, however these are costly solutions, and are over-engineered. It is important to complete the analysis to optimise the sub-system, and explore solutions that minimise expenditure while staying within the requirements.

14.4 Closing Remarks and Next Steps

This year the RF Communications sub-system underwent a full redefinition, with a significant focus on the underdeveloped parts of the sub-system in the space segment. Foundational work was undertaken with Warwick Aerospace Society to establish base constraints of the Ground Station, which can be developed further for more accurate models. The

budgets for the system have been parameterised, so outputs can evolve as analysis becomes more accurate. The recommended next steps are:

- Compute the access times to obtain a minimum data rate requirement.
  - Review the link budget section of last year's RF Comms subsection in the technical portfolio
  - Review the Satellite Communications toolbox in MATLAB, specifically the Scenario Viewer and Link Budget Analyser
  - Use these tools to simulate the link budget closure and obtain access times to the satellite
- Select an Antenna and Transceiver for the Space Segment
  - Using the link budget, select an Antenna with the required gain, and transceiver with the required modulation technique to close the link
- Work with Warwick Aerospace Society to develop the Ground Segment
- Draw up AIV and FMEA documents, ready for the qualification phase

15 Conclusion

After the work performed this year, a comparison of the development stages of the project is shown below:

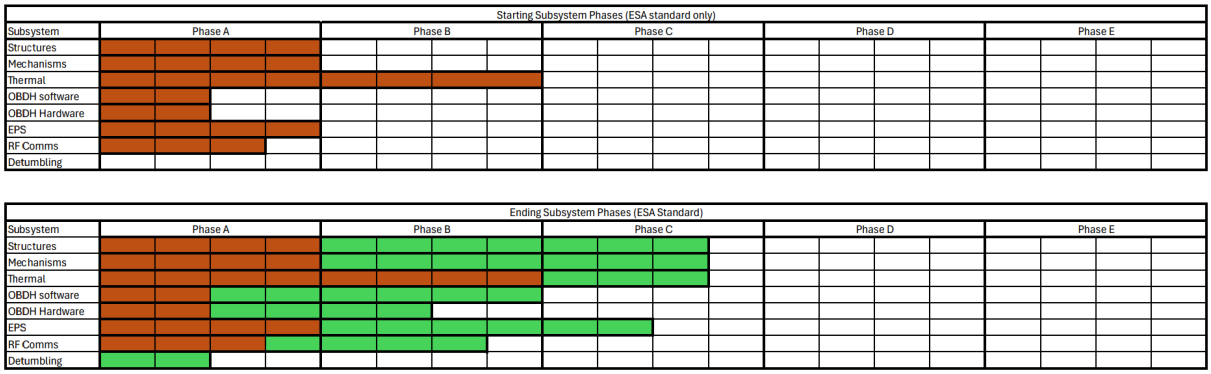

Figure 15.1: Comparison of start position (top) vs current progress (bottom)

Across the academic year, the 24/25 iteration of WUSAT has significantly progressed the preliminary definition and moved to detailed definition and model production of many sub-systems. On top of this, a project redefinition was undertaken, with members collaborating to create consistent documentation, and ensuring that all work was undertaken to ESA standards and requirements of the space industry. Technical progress was defined, open points and instructions developed for the future team, and a clean design freeze implemented by each sub-system to ensure a smooth handover

References

[1] J. Margolis, "How a tweet about the mars rover dying blew up on the internet and made people cry." https://laist.com/news/jpl-mars-rover-opportunity-battery-is-low-and-its-getting-dark, 2019. Accessed: 2025-03-05.

[2] L. Ward, H. Wise, A. Akram, M. Kho, J. Pittaway, J. Voong, S. Chandrakumar, and M. C. Pascual, "Portfolio of evidence." https://livewarwickac.sharepoint.com/:b:/s/WUSAT-4435/EV7cFnQFv0pHuUDFr2xoJacB-tXXQjG2oh2ke4yB2wHfJA?e=4Nuej9, 2024.

[3] Y. Zhang, J. Wu, X. Li, L. Zhang, and Y. Zhao, "Spacecan: A spaceflight bus network with high reliability and real-time performance," *Acta Astronautica*, vol. 162, pp. 344–353, 2019.

[4] N. Boskovic, "Electrical power system." ESA Power Systems, EMC and Space Environment Division, 2024.

[5] J. Samson, "Update on dependable multiprocessor cubesat technology development," in *Proceedings of the IEEE Aerospace Conference*, pp. 1–7, 2012.

[6] Consultative Committee for Space Data Systems, "Tm space data link protocol." https://public.ccsds.org/Pubs/132x0b3.pdf, 2021. Accessed: 2025-03-02.

[7] T. Bova and T. Krivoruchka, "Reliable udp protocol." https://datatracker.ietf.org/doc/html/draft-ietf-sigtran-reliable-udp-00/, 1999. Accessed: 2025-03-02.

[8] Skyrocket, "Equisat - satellite data." https://space.skyrocket.de/doc_sdat/equisat.htm, 2025.

[9] T. Instruments, "Tms320f2800132 microcontroller datasheet." https://www.ti.com/lit/ds/symlink/tms320f2800132.pdf?ts=1698682676194&ref_url=https%253A%252F%252Fwww.ti.com%252Fsitesearch%252Fen-us%252Fdocs%252Funiversalsearch.tsp%253FlangPref%253Den-US%2526searchTerm%253DF2800132RGZR%2526nr%253D5, 2023.

[10] E. S. A. (ESA), "Opened-out flatsat for cubesat testing." https://www.esa.int/Enabling_Support/Space_Engineering_Technology/Opened-out_FlatSat_for_CubeSat_testing, 2025.

[11] NASA, "Zarya module," Sep 2023.

[12] S. Ahmed khan, Y. Shiyou, A. Ali, M. Tahir, S. Fahad, and S. Rao, "Cubesats detumbling using only embedded asymmetric magnetorquers," *Advances in Space Research*, vol. 71, no. 5, pp. 2140–2154, 2023.

[13] M. Lovera, "Magnetic satellite detumbling: The b-dot algorithm revisited," in *2015 American Control Conference (ACC)*, pp. 1867–1872, 2015.

[14] echristhuraj, "Cubesat detumbling simulator." `https://github.com/echristhuraj/CubeSatDetumblingSimulator?tab=readme-ov-file`, 2022. Accessed: 2025-02-10.

[15] T. C. Program, "Cubesat design specification rev 14.1," *CubeSat Design Specification*, 2022.

[16] Ansys, "Granta edupack," *Al-6082 Material Properties*, 2024.

[17] S. Raviprasad and N. S. Nayak, "Dynamic analysis and verification of structurally optimized nano-satellite systems," *Jour. of Aerospace Science and Technology*, vol. 1, 4 2015.

[18] EnduroSat, "UHF Antenna III Datasheet," 2021.

[19] ECSS Requirements & Standards Division, *Space engineering Thermal analysis handbook ECSS Secretariat ESA-ESTEC Requirements & Standards Division Noordwijk, The Netherlands.*, vol. ECSS-E-HB-31-03A. ESA Requirements and Standards Division, 2016. Accessed 4th March 2025.

[20] D. Gilmore, *Spacecraft Thermal Control Handbook.*, vol. 1. Aerospace Press, 2002. Accessed 4th March 2025.

[21] A. Bowman, "State-of-the-art of small spacecraft technology." `https://www.nasa.gov/smallsat-institute/sst-soa/thermal-control/`, 2025. Accessed 4th March 2025.

[22] A. F. R. Laboratory, *Small Satellite Thermal Modeling Guide.* USSF, 2022. Accessed 4th March 2025.

[23] N. A. R. Center, "Biosentinel: Mission summary and lessons learned from the first deep space biology cubesat mission," 2023. Accessed 4th March 2025.

[24] A. B. Narimane Blanchete, "Thermal design, analysis and test: Framework for cubesat in low earth orbit," 2024. Accessed 4th March 2025.

[25] ECSS Requirements & Standards Division, *Thermal design handbook - Part 6: Thermal Control Surfaces.*, vol. ECSS-E-HB-31-01 Part 6A. ESA Requirements and Standards Division, 2011. Accessed 4th March 2025.

[26] ECSS Requirements & Standards Division, *Thermal design handbook – Part 7: Insulations.*, vol. ECSS-E-HB-31-01 Part 7A. ESA Requirements and Standards Division, 2011. Accessed 4th March 2025.

[27] ECSS Requirements & Standards Division, *Thermal design handbook - Part 9: Radiators.*, vol. ECSS-E-HB-31-01 Part 9A. ESA Requirements and Standards Division, 2011. Accessed 4th March 2025.

[28] Sierra Space Corporation, "Spaceflight hardware catalog," 2023. Accessed 4th March 2025.

[29] D. P. Kubdade S, Kulkarni S, *Transient Thermal Analysis of 1U Modular CubeSat Based on Passive Thermal Control System.* Arch Metall Mater, 2023. Accessed 4th March 2025.

[30] S. Tracking, "Iss zarya, satellite tracking and predictions." Accessed 4th March 2025.

[31] S. A. F. Company, *The Red Book.* Sheldahl Flexible Technologies, 2020. Accessed on 4th March 2025.

[32] M. J. Uddin, M. M. Rahman, and K. T. Mahmood, "A comprehensive review on cubesat electrical power system architectures," *ResearchGate*, 2021.

[33] S. R. V. Venkata and P. Rodriguez, "Comprehensive survey on energy storage systems for cubesat missions," *Advances in Space Research*, vol. 71, no. 1, pp. 1–20, 2022.

[34] I. S. I. Space, "Iceps2 datasheet," 2019. Accessed: March 5, 2025.

[35] D. Technology, "Dhv 3u cubesat solar panel datasheet," 2024. Accessed: March 5, 2025.

[36] P. Li, "Integration of mppt algorithms with spacecraft applications: Review, classification and future development outlook," *Elsevier*, vol. 308, 2024.

[37] S. Sanchez-Sanjuan, J. Gonzalez-Llorente, and R. Hurtado-Velasco, "Comparison of the incident solar energy and battery storage in a 3u cubesat satellite for different orientation scenarios," *Journal of Aerospace Technology and Management*, vol. 8, no. 1, pp. 91–102, 2016.

[38] ISISPACE, "Cubesat solar panels," 2024. Accessed: March 5, 2025.

[39] The Pi Hut, "ZeroCam - Camera for Raspberry Pi Zero." `https://thepihut.com/products/zerocam-camera-for-raspberry-pi-zero`. Accessed 26th February 2025.

[40] R. F. Haines, *The effects of video compression on acceptability of images for monitoring life sciences experiments*, vol. 3239. National Aeronautics and Space Administration, 1992.

[41] Texas Instruments, "CCSTUDIO IDE." `https://www.ti.com/tool/CCSTUDIO`, 2024. Accessed: 2025-03-04.

[42] M. Barr, *Programming embedded systems in C and C++.* " O'Reilly Media, Inc.", 1999.

[43] S. Kumar, S. Dalal, and V. Dixit, "The osi model: overview on the seven layers of computer networks," *International Journal of Computer Science and Information Technology Research*, vol. 2, no. 3, pp. 461–466, 2014.

[44] WUSAT-4, "obdh-sw." `https://github.com/WUSAT-4/obdh-sw`, 2025. Accessed: 2025-03-04.

[45] Consultative Committee for Space Data Systems, "Space packet protocols." `https://public.ccsds.org/Pubs/130x3g1.pdf`, 2023. Accessed 5th March 2025.

[46] J. Kurose, *Computer networking: a top-down approach.* Harlow: Pearson Education, Limited, global;8th; ed., 2021.

[47] Mathworks, "Discrete cosine transform." `https://uk.mathworks.com/help/images/discrete-cosine-transform.html#f21-16137`, 2024. Accessed: 2025-03-02.

[48] librespacefoundation, "Open space data link protocol." `https://gitlab.com/librespacefoundation/osdlp`, 2019. Accessed: 2025-03-06.

[49] Perforce, "Nasa's 10 rules for developing safety-critical code." `https://www.perforce.com/blog/kw/NASA-rules-for-developing-safety-critical-code`, 2024. Accessed: 2025-03-03.

[50] D. Ross, "Fdspp instrument: Power and communication details, v1.a," 2024.

[51] XCAM, "Camera system subassemblies." `https://xcam.co.uk/products`.

[52] G. Richardson, K. Schmitt, M. Covert, and C. Rogers, "Small satellite trends 2009-2013," in *Proceedings of the 29th Annual AIAA/USU Conference on Small Satellites*, 2015.

[53] P. Fortescue, G. Swinerd, and J. Stark, *Spacecraft Systems Engineering.* Wiley, fourth ed., 2011.

[54] V. L. Pisacane and R. C. Moore, *Fundamentals of Space Systems.* New York: Oxford University Press, 1994.

[55] ESA, "Esarad – esa thermal analysis tool," 2025. Accessed: 2025-03-04.

[56] B. Klofas, J. Anderson, and K. Hedman, "Dsp implementation of integrated store-and-forward aprs payload and obdh subsystems for low-cost small satellite," *Acta Astronautica*, vol. 61, no. 1-6, pp. 313–323, 2007.

[57] T. Szewczyk, "Data-handling subsystem," 2024. Lecture presented at FYS Design Booster – Training Week, ESA.

[58] A. Cratere, L. Gagliardi, G. A. Sanca, F. Golmar, and A. Dell'Olio, "On-board computer for cubesats: State-of-the-art and future trends," *IEEE Aerospace and Electronic Systems Magazine*, vol. 39, no. 5, pp. 537–551, 2024.

[59] H. J. Kramer, "Chapter 10 - small satellites," in *Space Science and Technologies* (H.-P. Roeser, ed.), pp. 217–286, Elsevier, 2020.

[60] E. Dubrova, *Fault-Tolerant Design*. Springer eBooks, Springer, 2013.

[61] ESA, "Introduction to savoir." `https://indico.esa.int/event/53/contributions/2644/attachments/2138/2486/01_-_Introduction_to_SAVOIR_27.10.2014_v1.1.pdf`, 2014. Accessed: 2025-03-04.

[62] N. Cornejo, J. Bouwmeester, and G. Gaydadjiev, "Implementation of a reliable data bus for the delfi nanosatellite programme," in *Proceedings of the 3rd International Conference on Recent Advances in Space Technologies (RAST)*, pp. 591–596, 2009.

[63] A. Designer, "Serial communications protocols - can and lin." `https://resources.altium.com/p/serial-communications-protocols-can-and-lin`. Accessed: 2025-03-05.

[64] M. Noca, F. Jordan, N. Steiner, T. Choueiri, F. George, G. Roethlisberger, N. Scheidegger, H. Peter-Contesse, M. Borgeaud, R. Krpoun, and H. Shea, "Lessons learned from the first swiss pico-satellite: Swisscube," in *Proceedings of the 23rd Annual AIAA/USU Conference on Small Satellites*, 2009.

[65] WUSAT-4, "Obdh-hw-wiring." `https://github.com/WUSAT-4/OBDH-hw-wiring`, 2025. Accessed: 2025-03-04.

[66] EnduroSat, "Onboard computer." `https://www.endurosat.com/products/onboard-computer/`.

[67] B. University, "Cubesat will study earth's atmosphere." `https://www.brown.edu/news/2017-03-23/cubesat`, 2017.

[68] W. contributors, "Equisat." `https://en.wikipedia.org/wiki/EQUiSat`, 2025.

[69] OfCom, "The united kingdom frequency allocation table," Mar 2023.

[70] M. Williamson, "Understanding the difference between uhf and vhf two way radios," Sep 2024.

[71] Silicon Labs, "Community - silicon labs," Jul 2021.

[72] "Uhf transceiver ii," Jan 2022.

A Final Chassis Engineering Drawings

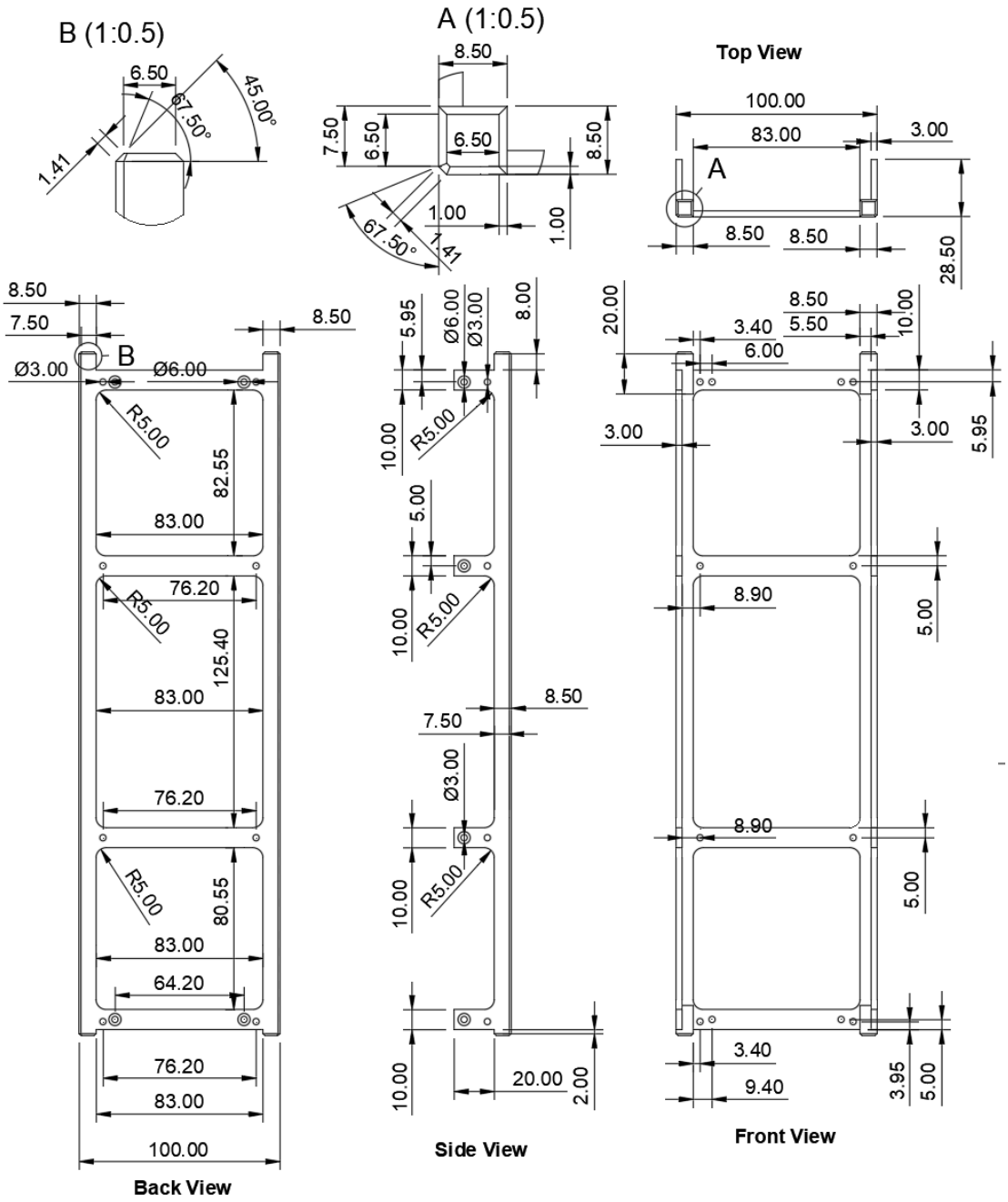

Figure A.1: 3U Rail Engineering Drawing

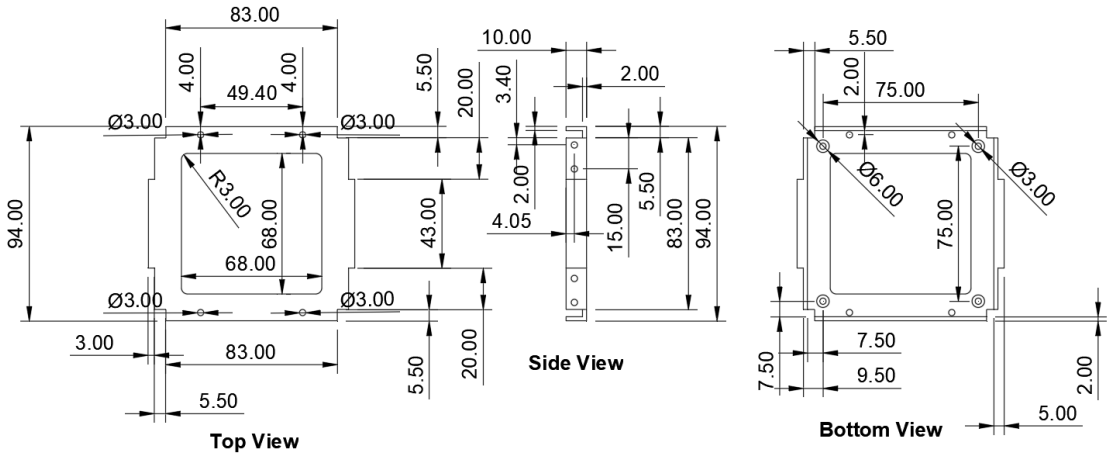

Figure A.2: 1U Top Member Engineering Drawing

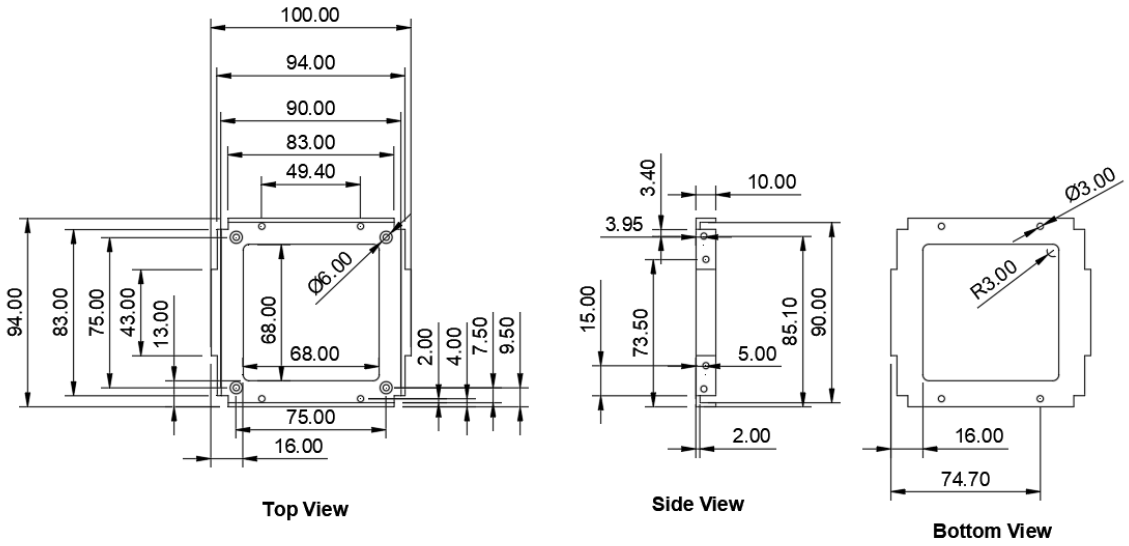

Figure A.3: 1U Bottom Member Engineering Drawing

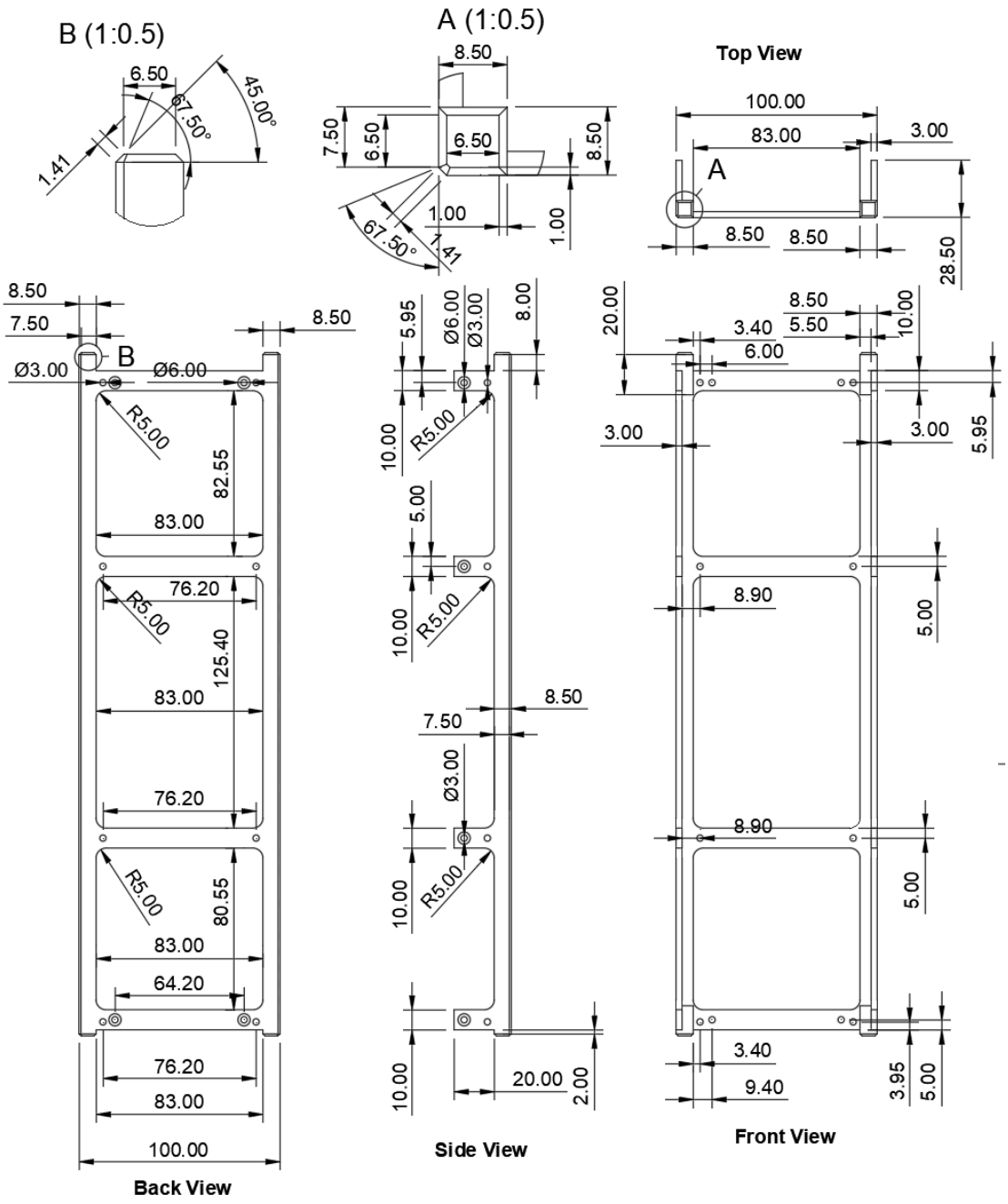

Figure A.4: Crossmembers Engineering Drawing

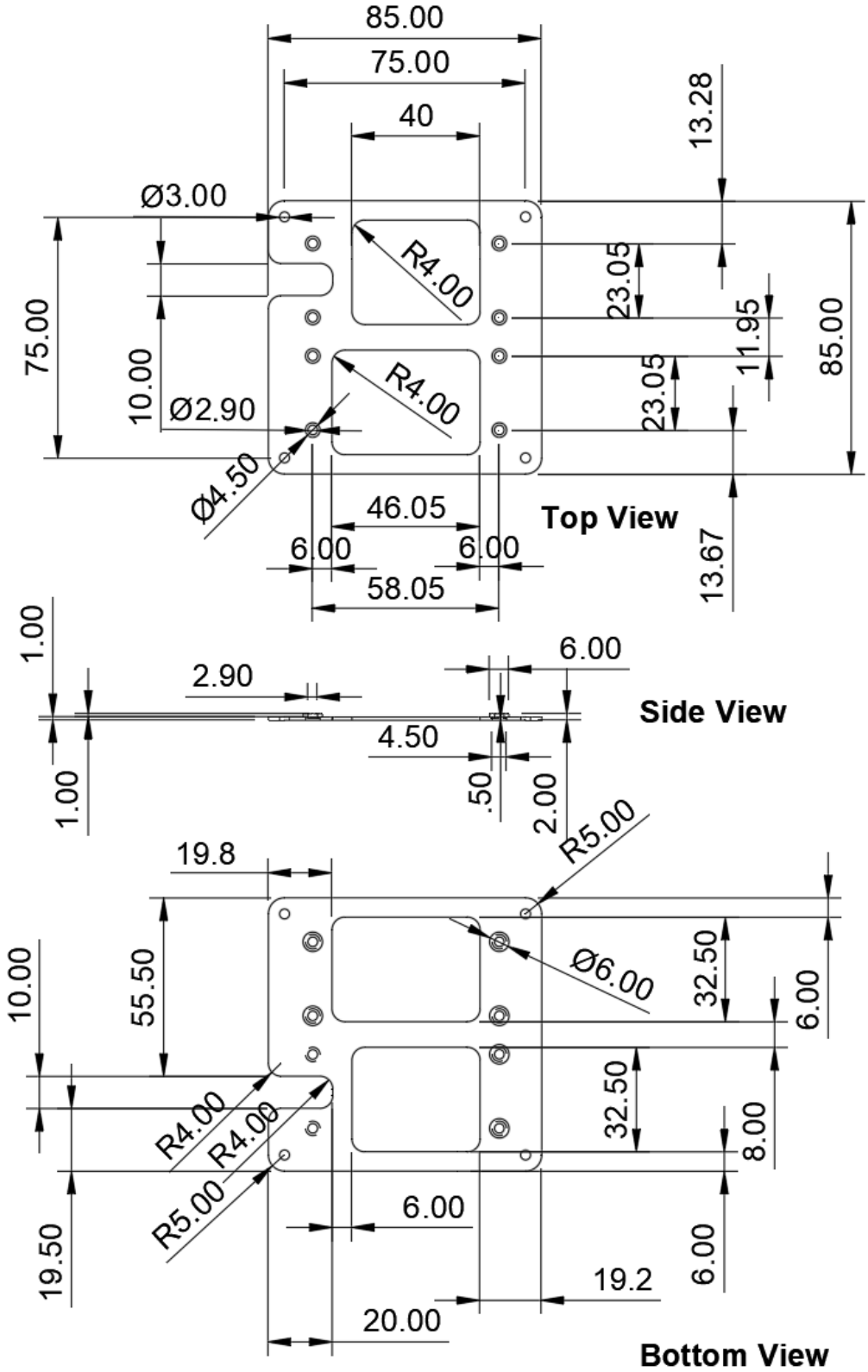

Figure A.5: FDSPP Top Mount Engineering Drawing

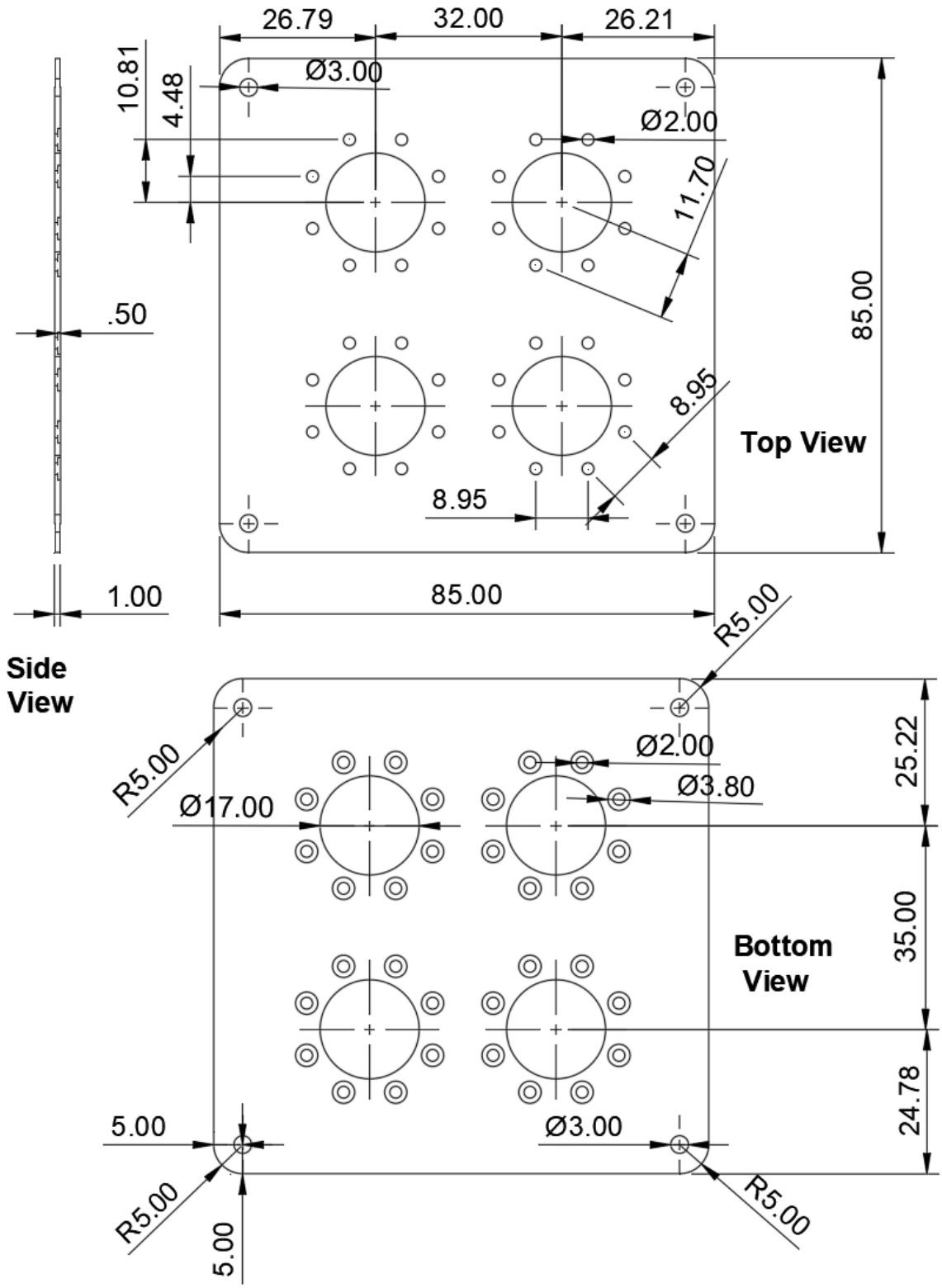

Figure A.6: FDSPP Bottom Mount Engineering Drawing

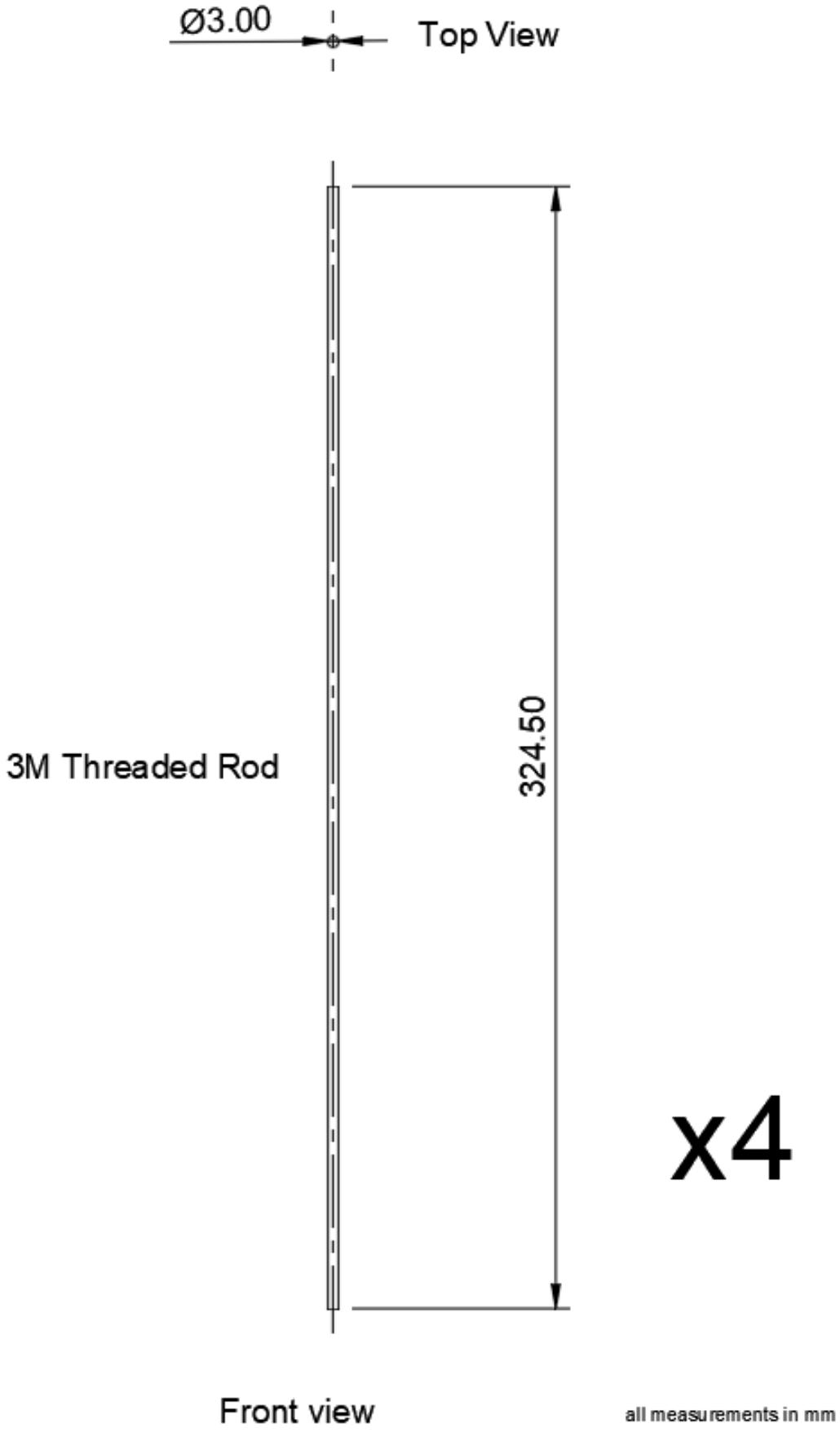

Figure A.7: M3 Threaded Rod Engineering Drawing

B DHV Solar Panel Engineering Drawings

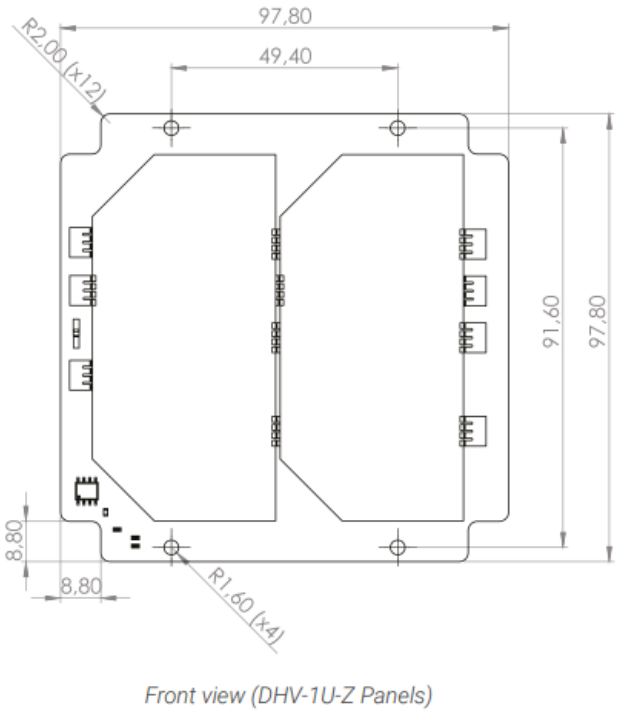

Figure B.1: DHV-1U-Z Solar Panel Front View Engineering Drawing

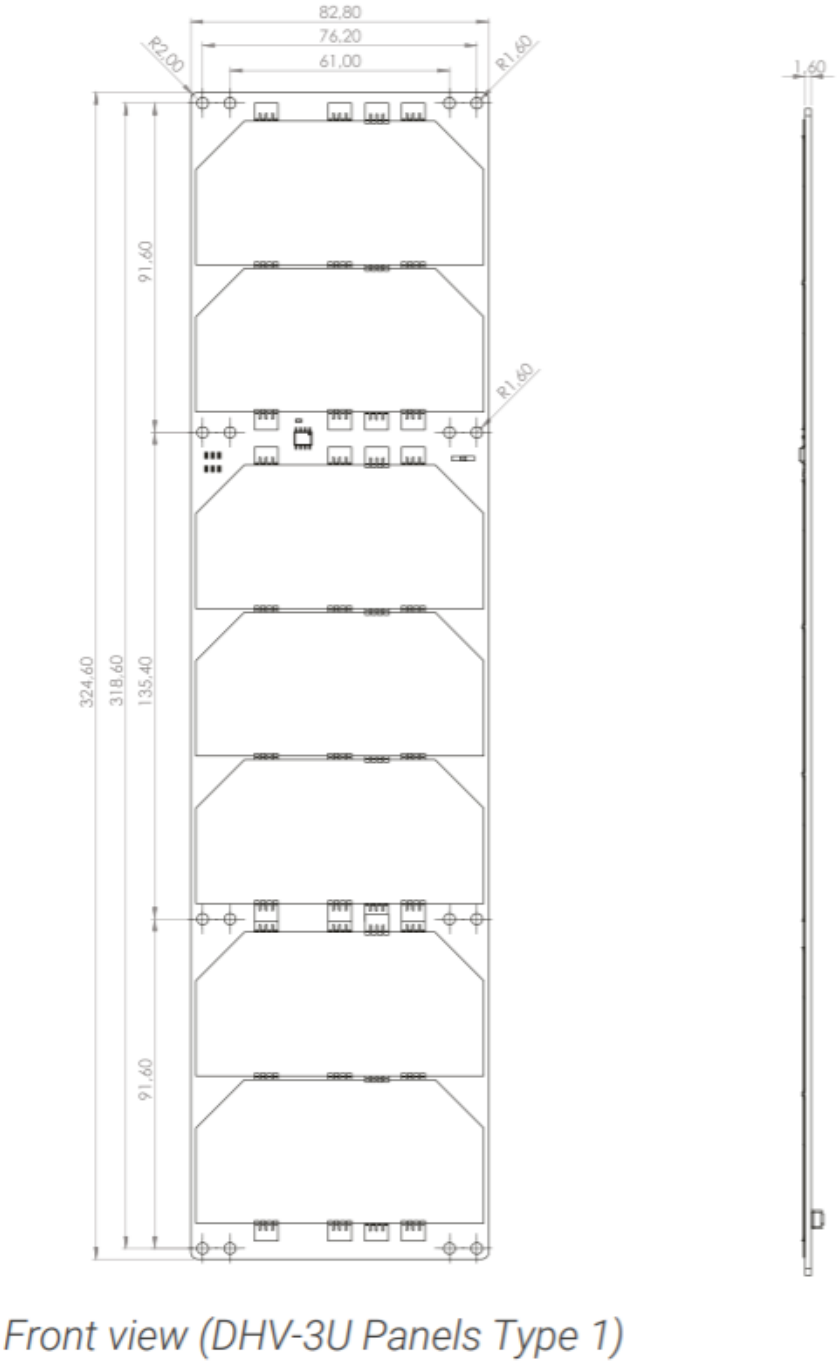

Figure B.2: DHV-3U-Z Solar Panel Type 1 Front View Engineering Drawing

C EnduroSat UHF II Engineering Drawing

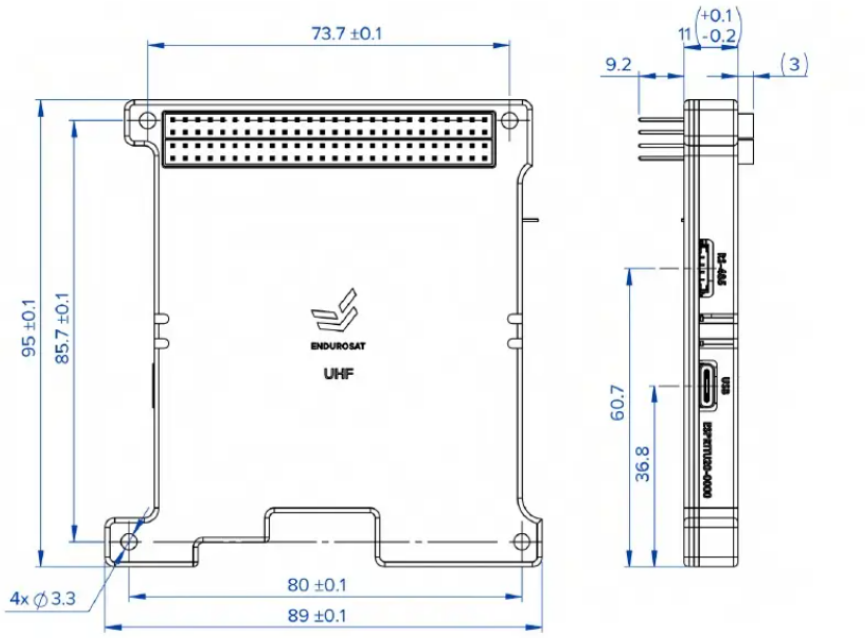

Figure C.1: EnduroSat UHF II Engineering Drawing

D FDSPP Primary Pod Assembly 1U

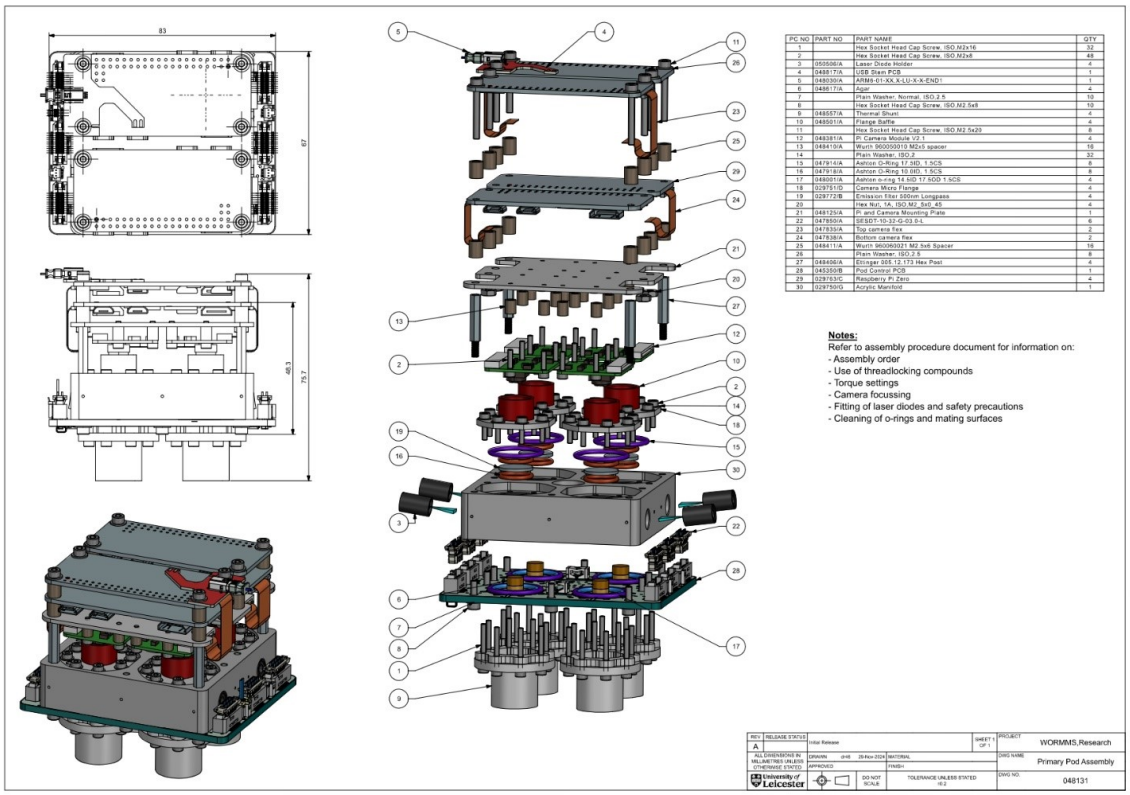

Figure D.1: FDSPP Primary Pod Assembly 1U

E Packet Formation Flowchart

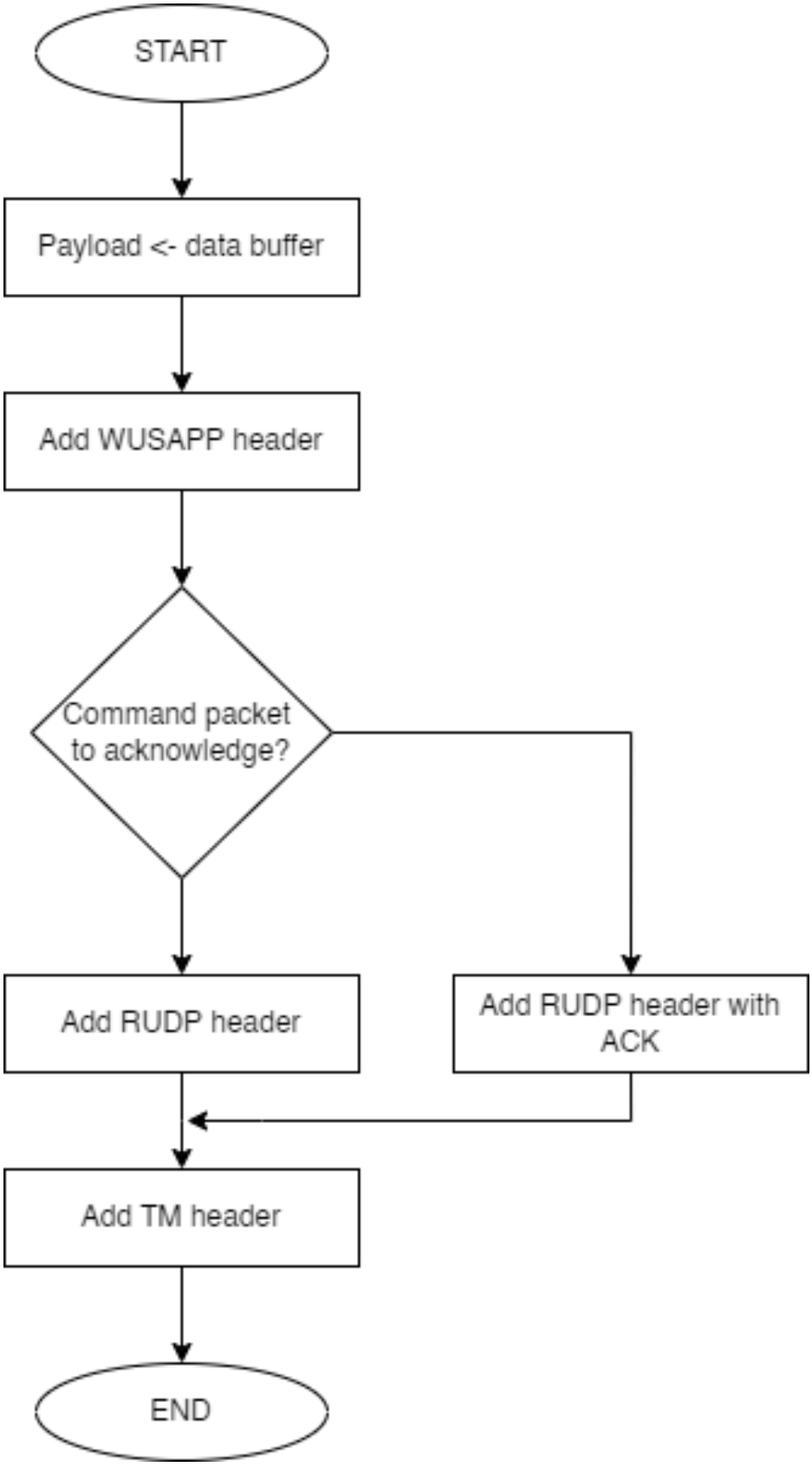

Figure E.1: Packet formation

F Data Transmission Flowchart

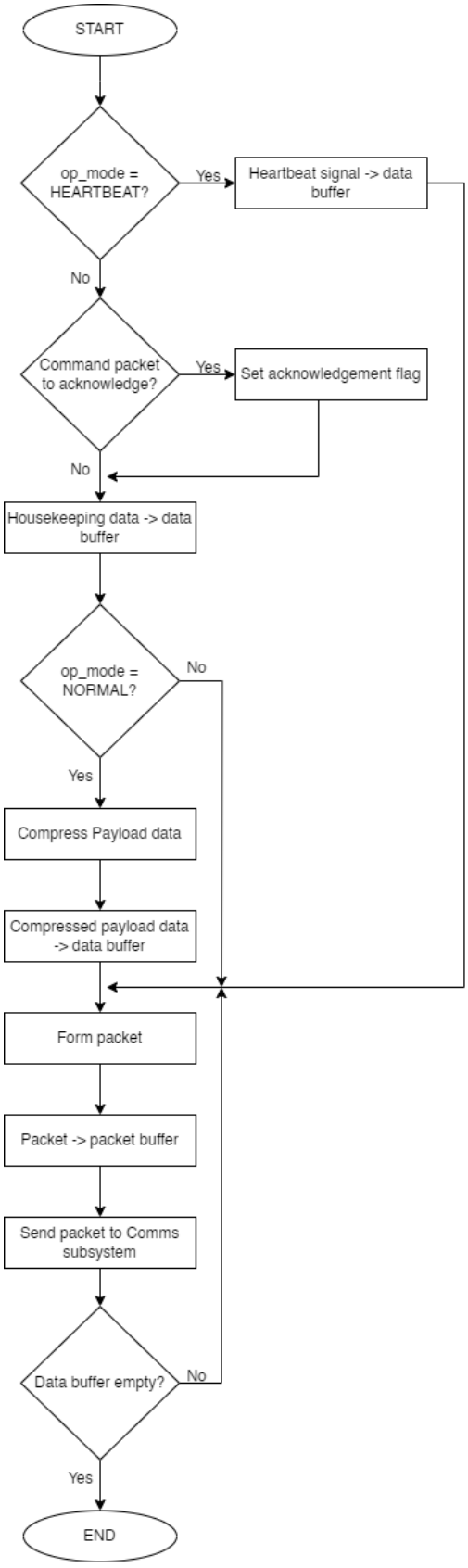

Figure F.1: Data transmission

G Software Functionality Flowchart

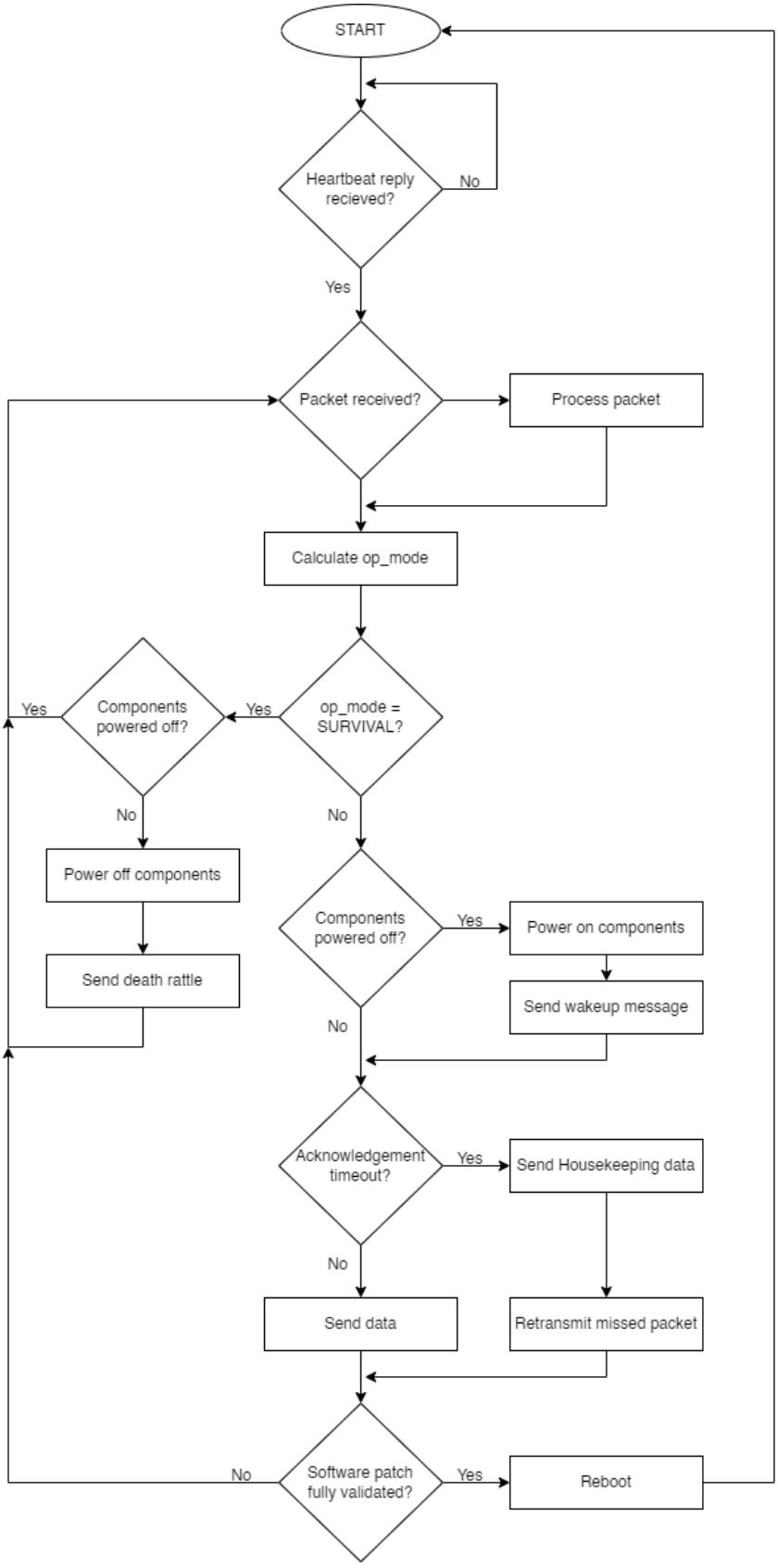

Figure G.1: Overview of software

H FDSPP Power Budget

Component	Part	Function	Voltage	Boot (mA)	Boot (W)	Standby (mA)	Standby (W)	Run (mA)	Run (W)
U1	LPS22HB	P/T sensor	3.3	0.012	3.96E-05	0.012	0.0000396	0.012	0.0000396
U2	LPS22HB	P/T sensor	3.3	0.012	3.96E-05	0.012	0.0000396	0.012	0.0000396
U3	LPS22HB	P/T sensor	3.3	0.012	3.96E-05	0.012	0.0000396	0.012	0.0000396
U4	LPS22HB	P/T sensor	3.3	0.012	3.96E-05	0.012	0.0000396	0.012	0.0000396
U6	LPS22HB	P/T sensor	3.3	0.012	3.96E-05	0.012	0.0000396	0.012	0.0000396
R4	3K resistor	Heater	28	0	0	0	0	9	0.252
R5	3K resistor	Heater	28	0	0	0	0	9	0.252
R8	3K resistor	Heater	28	0	0	0	0	9	0.252
R9	3K resistor	Heater	28	0	0	0	0	9	0.252
U11	FAN5622SX	LED driver	5	0.001	0.000005	0.001	0.000005	21	0.105
U12	FAN5622SX	LED driver	5	0.001	0.000005	0.001	0.000005	0	0
U13	FAN5622SX	LED driver	5	0.001	0.000005	0.001	0.000005	0	0
U14	FAN5622SX	LED driver	5	0.001	0.000005	0.001	0.000005	0	0
U7	iC-WKM	Laser driver	12	0	0	1	0.012	100	1.2
U8	iC-WKM	Laser driver	12	0	0	1	0.012	0	0
U9	iC-WKM	Laser driver	12	0	0	1	0.012	0	0
U10	iC-WKM	Laser driver	12	0	0	1	0.012	0	0
	Control								
Pi Zero 2W+cam		Main Pi	5	550	2.75	200	1	350	1.75
Pi Zero 2W+cam		Sub Pi	5	200	1	200	1	200	1
Pi Zero 2W+cam		Sub Pi	5	200	1	200	1	200	1
Pi Zero 2W+cam		Sub Pi	5	200	1	200	1	200	1
	Total Watts			Boot:	5.75	Standby:	4.05	Run:	7.06

Figure H.1: FDSPP Power Budget